International

WOCE

Newsletter

Number 30 ISSN 1029-1725 March 1998

IN THIS ISSUE

Published by the WOCE International Project Office at Southampton Oceanography Centre, UK

Technology Developments (Don't take them for Granted!)

W. John Gould, Director, WOCE IPO

This issue of the Newsletter concentrates on some of the many technical advances that have been made in areas of interest to WOCE. We often tend to take such things for granted - today's students assume that positional information will be available from GPS to a few tens of metres accuracy 24 hours a day. As most of us know it has not always been so!

Technological innovation is moving very fast but that means that it is often poorly documented in the literature. The articles in this issue are an excellent testament to, and a record of, the progress we've made in some areas that were critical to the success of WOCE.

The WOCE Science Plan published in 1986 highlighted that the programme was dependent on the timely launch of the satellites (since achieved) and on some modest advances in in-situ measurement capabilities that at that time could not be guaranteed. We have for the most part met and often greatly exceeded these earlier expectations.

We now take as routine the many products from satellite sensors outlined in Victor Zlotnicki's summary. Despite occasional hardware failures the satellite missions have been remarkably successful, much progress has been made in data distribution and continuation of key missions seems assured. The quality of TOPEX/POSEIDON data is outstanding and this and many other satellite products are now being used by a wide range of modellers and in situ observationalists to complement, and to aid interpretation of, sparser in situ data sets.

We also highlight in this issue some striking examples of progress in in-situ measurements that have gone far beyond what was required or hoped for. The ALACE floats and their later profiling derivatives were barely beyond the conceptual stage when WOCE was planned. They are now a reality that can provide a directly-measured subsurface flow field across an entire ocean basin together with upper ocean temperature and salinity profiles from areas rarely visited by ships. These floats seem set to be a key element of future observing systems.

Surface drifters were already used in large numbers when WOCE was planned. However their ability to represent upper ocean currents unambiguously and to survive for multi-year missions was poor. Developments to meet TOGA and WOCE requirements have resulted in lower cost and improved data quality and quantity.

The advances in navigational accuracy (position and ships' heading) reported in WOCE Newsletter 26 have made ADCP measurements from ships both routine and valuable. Here we now report the increasing use of ADCPs from lowered packages. We also present an example of the use of data capsules that could in future obviate the need for ships to visit remote mooring locations.

Less obvious, but equally vital, have been the developments in tracer chemistry that have allowed the use of small volume samples in place of the huge Gerard barrels and that have extended analysis to a wider range of CFCs. These advances made significant reductions in both the ship time required to complete the WOCE global survey and in the seagoing support required.

Not all developments have been quite so successful or have yet "caught on" - a streamlined multisampler, a free-fall CTD profiler, expendable current meter moorings, acoustic correlation current profilers for example. However some or all of these may eventually become parts of the armoury with which we will explore and understand the oceans.

Some generic problems still remain despite considerable investment of money and effort. Outstanding among these is the need for salinity sensors capable of retaining their calibrations through multi-year deployments in both the upper ocean and deep sea. Salinity measurements are seen as vital in new programmes such as CLIVAR, GODAE and GOOS. Increased data transmission rates between in-situ sensors and satellites will surely come, as will autonomous moored profilers and other elements needed for operational ocean observations. Few research observations are yet routinely entered onto the Global Telecommunications System (GTS), this must change.

The truth is that progress in technology innovation comes from a partnership between inventiveness, willingness to embrace new ideas and, above all, critical evaluation of data from new instruments.

Who knows what the next decade will bring but what is clear is that, in some senses, WOCE ocean observations have made the first steps that will enable a truly global operational observing system to be possible.

And finally…

The WOCE Conference

We have been very pleased with the response to the call for posters for the WOCE Conference. We will have about 300 on display and we look forward to seeing large numbers of scientists meeting in Halifax in May to assess what WOCE has achieved and to plan future co-operative analysis and interpretation of data and model results.

Register now - it promises to be a great event!

Autonomous Floats in WOCE

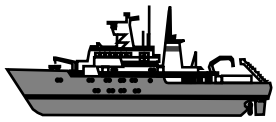

Russ E. Davis, Scripps Institution of Oceanography, UCSD, La Jolla, CA 92093, USA. rdavis@ucsd.edu.

The way we observe the ocean has changed dramatically during the WOCE field period. There have been tremendous advances in how well we can measure things (e.g. water properties, microstructure) and in what we can measure (e.g. purposeful tracers). These developments may have, however, been overshadowed by the revolutionary expansion of the spatial coverage with which we can continuously observe dynamically important ocean variables. Satellite observations of surface winds and sea surface height provide global time series of perhaps the two most important measures of ocean forcing and response, respectively. Repeated surface meteorological observations from volunteer ships and moorings make possible useful surface flux analyses. New sampling strategies for expendable temperature and salinity probes and instruments like Acoustic Doppler Current Profilers allow commercial shipping routes to yield time series of section data that approach research sections in utility. Surface drifters provide near-global coverage of SST, surface atmospheric pressure and upper-level currents while below the ocean surface autonomous neutrally buoyant floats observe subsurface currents and regularly report profile data over basin scales.

This new ability to observe the ocean globally, coupled with new methods of blending models and data, promises to rapidly change the way we study the ocean. A majority of the needed observations may come from satellites but there will be a continued need for in situ observations to keep remote measurements accurate, to extend these observations into the deep ocean, and to observe things that remote sensors cannot see (e.g. salinity, velocity, subsurface structure). Because autonomous vehicles provide a feasible way to support global observations of the deep ocean, a summary of recent developments and a status report on present capabilities is provided here.

ALACE

The first autonomous (not requiring an acoustic network for positioning) neutrally buoyant float was the Autonomous Lagrangian Circulation Explorer (ALACE) originally developed to provide economical long-term measurements of subsurface currents. The goal of this development was to reduce observational costs so that we could feasibly deploy enough floats to determine mean absolute velocity in the presence of energetic variability, thereby providing a level of known motion to reference the geostrophic shear climatologies that would be available at the end of WOCE. The central elements in ALACE achieving this economy were (a) a small hydraulic pump used to change float volume, allowing it to periodically cycle from depth to the surface where it could be located by, and relay data to, Argos satellites, and (b) long operational life, which required efficient use of onboard energy and effective corrosion control (see Davis et al., 1991, for details of ALACE).

Between 1990 and 1996 a total of 303 ALACEs were deployed as part of WOCE to map the absolute circulation of the tropical and South Pacific at 900 m depth. Only preliminary results from this campaign are available now because over half the floats, which can live six years or more, are still operating. While the full value of these observations will be known only when they are rationally combined with the hydrographic data they were designed to complement, the preliminary results provide the first opportunity to test the utility of velocity mapping using autonomous floats. Characteristics of the South Pacific data are described in Table 1 and a more complete description and analysis are given by Davis (1997).

The primary challenge in establishing the mean (say over the WOCE decade) absolute velocity field is eliminating the effects of variability. It was initially believed that mesoscale eddies would contribute most of the variability and that, based on the current estimates of characteristic scales, approximately 5 years of data would be required to produce a useful average. Most of the 25-day ALACE observations obtained so far are, as anticipated, essentially serially uncorrelated and confirm the 5-year estimate for usefulness. In the tropics, however, zonal variability with time scales of several months makes it more difficult to determine the mean zonal velocity.

Since methods for analysing large Lagrangian data

Table 1. Typical sampling in the WOCE South Pacific ALACE array

Depth: 850-950 m. Submerged duration: 25 days. Surfacing: 1 hour to surface.			Measurements: submerged temperature and depth. Surface duration: 24 hours. Diving: 3 hours to within 100 m of target.			
Year	1991	1992	1993	1994	1995	1996
Deployed	46	108	50	74	11	14
Alive mid 1997	12	24	29	48	10	13

sets are evolving, it may be useful to discuss how the South Pacific ALACE data has been treated. For practical reasons, the analysis has been divided into two steps: space-time averaging and objective mapping. Hoping to reduce sampling error by reducing variation of the true mean flow within averaging areas, 'nearby' samples were aggregated using a 'distance' based on the barotropic potential vorticity, f/H. In this way, data that were averaged are clustered along isobaths where topography varies rapidly and are clustered along longitude lines in the tropics. Averages over ellipses with area equal to that of a 400 km radius circle are shown in Fig. 1 (see page 24). Signal-to-noise ratios for these averages cluster between 0.5 and 2.

Space-time averages were used as data for an objective analysis. This allows averages with different sampling errors to be efficiently combined, accomplishes additional filtering of sampling noise without excessive loss of spatial resolution, and allows the anticipated constraint of geostrophic non-divergence, $\nabla \cdot (fU_H) = 0$, to be used to filter out highly divergent sampling noise. The geostrophic constraint also allows results of velocity mapping to be portrayed as dynamic height fields. In the objective analysis, noise statistics come directly from the space-time averaging while the scales of the signal are effectively adjustable parameters that are set to be consistent with the resulting mapped signal. Ideally the signal covariance would come from a large ensemble of model runs that span the range of plausible mean flows. In the meantime, various forms for signal dynamic-height covariance were examined in which the spatial scale decreased across rapidly varying lines of f/H. So long as the adjustable scales were set to be consistent with the resultant map the covariance's form had little impact on the results. In order to preserve the characteristics of the data themselves, no constraint was applied to keep the mapped velocity from flowing through the boundaries.

Fig. 2 is an example of the mean dynamic topography deduced from the data collected through mid-1997. A number of expected features appear in this map including an Antarctic Circumpolar Current with peak velocities of 2 to 3 cm/s and an East Australian Current (EAC) with peak speeds of O(1 cm/s). The EAC broadens as it passes through the Tasman Sea and apparently feeds both a westward flow south of Australia and the polar limb of the subtropical gyre to the east. Perhaps less anticipated is what might be called the South Equatorial Current (SEC) that serves as the tropical limb of the subtropical gyre and the polar limb of a confused tropical gyre. This current is strongest west of 120°W while its eastern parts, like the tropical gyre itself, appears to be broken up by the East Pacific Rise. The tropical circulation north of the equator is confused and not well determined by the data.

Because the mapping procedure does not prohibit flow through the boundaries and because boundary currents are often narrow and not well described at the 600 km resolution of the mapping procedure, coherent currents can appear to flow across continental boundaries. Most obvious is how the SEC appears to flow into Australia and then reappear as the EAC. Similarly, at its eastern boundary the SEC seems to flow out of Chile.

Completion of this preliminary analysis makes clear the strengths and weaknesses of autonomous floats for measuring large-scale ocean velocity. The foremost advantage is the feasibility of gathering numerous, long records of absolute velocity. Absence of tracking networks, deployment from cooperating research cruises of opportunity and simplicity of tracking make possible a complete cost of about $2000 per record year. The penalties are a random tracking error associated with movement during ascent/descent (generally less than 0.3 mm/s and never significant) and ignorance of small scale flow structures that distort submerged trajectories between descent and ascent. This reduced resolution is a factor only in strong currents near topography (such as in Drake Passage) and will be greatly reduced in the future when two-way communication is established with the floats so their cycle time can be changed on command. A more serious resolution problem is fundamental to the long-term Lagrangian approach. Because the sampling array diffuses toward a uniform concentration, it is impossible to maintain a high

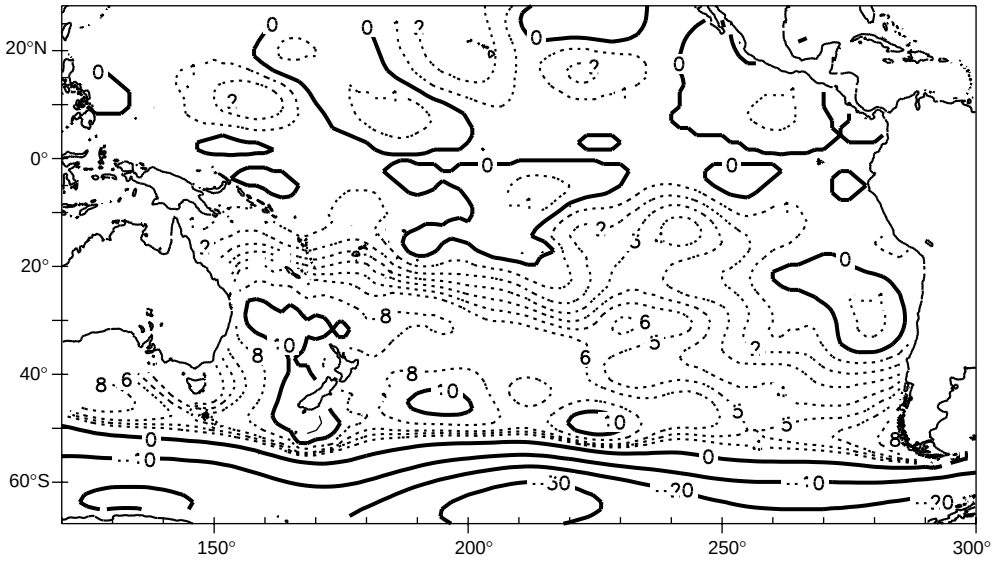

Figure 2. Objective map of mean dynamic height (in cm) at 900 m deduced from ALACE observations. Solid contours are separated by 10 cm. Dashed contours are drawn at -1, 1, 2, 3, 4, 5, 6, 8 although many are deleted in the Southern Ocean. Contours are plotted only where the expected error exceeds half the signal variance.

sampling density in places, like boundary currents, where extra resolution is needed.

PALACE

While deploying the South Pacific array, work began to develop a Profiling ALACE (PALACE) that could report temperature and salinity profiles whenever the float surfaced or dove. The new technical challenges were a data encoding scheme to permit full profiles to be transmitted through Argos and a salinity sensor that would be stable for years of operation. For both temperature-only and CTD PALACEs the instrument size was increased about 20% to house the doubled battery pack needed to support increased Argos transmissions while maintaining a 150-cycle power-limited life.

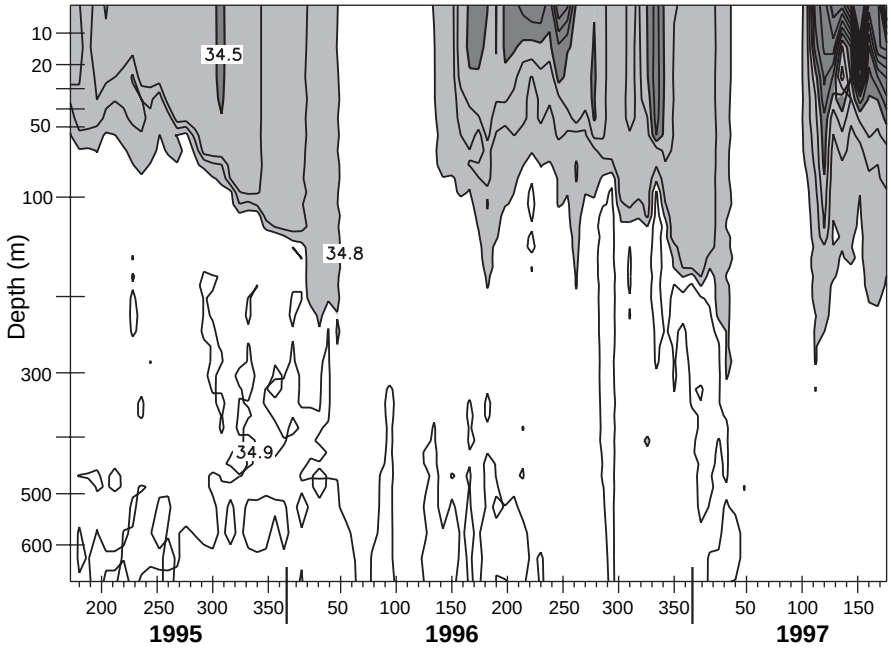

Figure 3. Time series of salinity profiles from PALACE float 392 operating in the central and western Labrador Sea. Time series shows complete destruction of upper-ocean salinity stratification during the convection season followed by very abrupt restratification of the upper 100–200 m.

After trying others, the adopted data compression scheme involves sending each profile in blocks of depths. Values are scaled by the extremes in each block and sent with 8 bit resolution for temperature and 6 bits for the departure of conductivity from a prescribed function of temperature. Using a single Argos ID we send 104 depths of a temperature profile or 56 depths of both T and S using 4 unique messages. In most places explored all messages are received 98% of the time when 24 hours are used for transmission. Argos channel capacity, not instrumental factors, limits the resolution of the transmitted profiles. This will improve with new satellite systems. No data correction scheme is employed because tests show that most Argos errors occur in long strings that are not feasible to correct.

A titanium housed thermistor provides a 2 sec time constant (0.5 m length constant at typical rise/fall rates) with 5-year drifts of about 0.01°C. The requirement of low instrument cost forced compromises in pressure and salinity sensor capabilities. The strain-gauge pressure sensor suffers drift and hysteresis (probably a result of temperature changes) of O(10 db) which require special data treatment when profiles are measured during ascent. To date an inductive conductivity sensor made by Falmouth Scientific has been used. It is small, easily mounted, uses little power compared with pumped sensors and has good short-term (month) stability. Long term results, however, show two kinds of error. Long-term bio-fouling causes drift in the sense of a false freshening. A PALACE probe recovered by Howard Freeland (IOS, Canada) after one year operation near Station P exhibited such fouling. The thickness of the fouling compared well with that required to cause drift of the observed magnitude. Anti-fouling attempts have so far been unsuccessful and some have accelerated drift as the physical properties of the anti-fouling agent change with time. Errors of a second kind are sudden shifts of O(0.1 psu) of either sign. We have been unsuccessful in identifying the cause of these errors. While drift caused by fouling can be reasonably well corrected if the profile extends into water with a stable T/S relation, jumps make the conductivity data useless.

The strengths and weaknesses of autonomous floats for measuring temperature are similar to those for measuring velocity. They return profiles spanning depths up to 1700 m with accuracy slightly superior to, and depth resolution slightly inferior to, XBTs. Even if the value of the associated velocity measurements is ignored, the total cost of an archived temperature profile is about $75, comparable to the total cost of XBT records. A relatively long life (150 profiles) makes them useful in monitoring remote locations using occasional research vessel of opportunity or even prevailing currents to access infrequently visited areas. The primary weakness of today's autonomous profilers is the relatively low temperature and depth resolution with which profiles can be transmitted through Argos.

Autonomous CTD profilers are now delivering time series of salinity that are particularly useful in the upper ocean where salinity changes are large enough that salinity uncertainties of O(0.03 psu) do not cloud the picture. An example of this is the 2-year record of salinity profiles in Fig. 3 from PALACE 392 in the interior of the Labrador Sea, not far from Weather Station B (53°W, 57°N). This is the site of deep winter convection and the associated formation of Labrador Sea Water. Driven by surface heat loss, convection must overcome a strongly stabilising salinity distribution that results from melt of ice and fresh water

input from the West Greenland Current and Davis Strait. Dynamical models of the convection process suggest that the downward mass transport driven by convection occurs mainly when convective chimneys collapse and are capped over by low density fluid from their surroundings. Thus the restratification following the cooling season is not only important in setting the stage for the next year but also in allowing the newly formed water to escape its source region. Temperature and salinity profiles from floats like 392 show that during early 1996 and 1997 convection reached at least 1200 m and that the subsequent restratification over the upper 100 m or more occurred quite abruptly.

While today's autonomous CTD profilers are providing a window on processes that have previously been difficult to observe, they are less successful than their temperature counterparts because of the problems with instability of the conductivity sensor calibration. These cause the typical useful life of a conductivity sensor to be only a year or two and even at a relatively fast cycle time of O(15 days) this leads to a total operational cost of nearly $400 per profile. Development of a long-term salinity sensor will tremendously increase the information to be gained from autonomous floats, long-term moorings and unattended shipboard salinographs.

One characteristic of autonomous float sampling pertains to both velocity and profile observations. Because time and space changes cannot be separated along a single float trajectory, successful analysis of variability from float data depends critically on either having floats remain in one ocean region or having a high enough sampling density to determine both space and time structure. In regions with significant flow across spatial structure a few Eulerian measurements (like moorings) are vastly more effective in determining temporal variability than are a similar number of floats. On the other hand, the wandering nature of float trajectories eliminates the topographic biases that can confuse moored observations.

The future

ALACE floats have been significantly less reliable than hoped for. In the laboratory, failures of the reciprocating pump were found to be caused by very small amounts of contamination or unavoidable dissolved gases in the hydraulic fluid. This has increased the manpower spent in preparation and, as Table 1 shows, caused many floats not to reach their power-limited lifetime. Furthermore, the ALACE hydraulic system is not capable of allowing a float to decrease its volume to increase its depth after it has submerged. To provide improved reliability and increase operational flexibility, we have developed a second generation autonomous float called the Sounding Oceanographic Lagrangian Observer (SOLO). It uses a single-stroke high-pressure hydraulic pump augmented by an air pump to generate extra buoyancy at the surface and is easier and less expensive to build than a ALACE. SOLOs have recently been deployed in the subpolar North Atlantic and are proving both more reliable and easier to work with than their predecessor.

The possibility of fitting buoyancy changing floats with wings to produce a simple gliding autonomous underwater vehicle was recognised early by Henry Stommel in his concept of the thermally-powered Slocum glider. Both C. Eriksen of the University of Washington and a partnership of B. Owens of Woods Hole Oceanographic Institution and the author are pursuing adaptation of autonomous float technology to develop simple electric-powered underwater vehicles. Wings are used to efficiently convert buoyancy into forward motion of the O(30 cm/s) as the vehicle cycles between shallow and deep levels. The forward motion is envisioned as allowing a vehicle to either hold station while gathering a time series of profiles (a virtual mooring) or to autonomously sample a section of substantial length. Both the UW and WHOI/SIO vehicles are roughly twice the size of an ALACE and have design operating ranges of the O(3000 km). Testing of both vehicles has only just begun, so their utility can only be guessed, but it is hoped they will give observers a powerful new low-cost options for observing the ocean over large time and space scales.

References

Davis, R. E., D. C. Webb, L. A. Regier, and J. Dufour, 1991. The Autonomous Lagrangian Circulation Explorer (ALACE). J. Atmosph. Oceanic Tech., 9, 264–285.

Davis, R.E., 1997. Preliminary results from directly measuring mid-depth circulation in the tropical and South Pacific. Submitted to J. Geophys. Res.

Advances in Drifting Buoy Technology

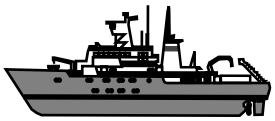

Sean C. Kennan, Pearn P. Niiler, and Andrew Sybrandy, Scripps Institution of Oceanography, La Jolla, CA 92093, USA. kennan@ucsd.edu

The WOCE/TOGA/CLIVAR Surface Velocity Program (SVP) has facilitated development and deployment of Lagrangian drifting buoys to sample the global upper ocean circulation on time scales of days to years. This initiative, now known as the Global Drifter Program (GDP) of the Data Buoy Cooperation Panel of the WMO and IOC, constitutes a major component of the effort to operationally monitor ocean currents. Over 17 countries and 41 principal investigators have contributed data and resources to the GDP. As of the beginning of 1997, over 750 SVP drifters that routinely measure sea surface temperature (SST) were being tracked globally. Of these, subsets have been successfully equipped with additional instrumentation to measure mixed layer temperature and salinity, barometric pressure, winds, and ocean colour. In this note we present a brief overview of the evolution of the SVP drifter and its state-of-the-art upper ocean measurements.

Drifter design

The basic SVP drifter design consists of a surface float for satellite telemetry of data and a subsurface drogue for approximating water parcel motion at depth. The drogue and float designs have evolved from the ancestral window shade drogue drifter with a spar buoy, to the TRISTAR drogue with surface and subsurface floats, into the present day holey sock drogue (Fig. 1). The present design combines desired water following characteristics with affordability, durability, and ease of deployment.

Hydrodynamics

Since winds cause drifters to slip through the water, it is desirable to have subsurface drogues to follow the motion representative of near surface circulation. However, a surface float, which is inevitably subject to the extremes of wind stress, seas, and swell, is required so that the drifter can telemeter its observations. Furthermore, vertical shear of the near surface currents and wave forces induce variable slip along the length of the drogue (Niiler et al., 1987). Consequently, upper ocean drifters are not perfect Lagrangian parcels.

The SVP design minimises the direct effects of wind and waves at the surface with partially submerged floats (Fig. 2, see page 24). In addition, wave effects on the drogue have been addressed with a subsurface float; low tension in the tether connecting the surface and subsurface floats allows the former to move in three dimensions with the sea surface while the latter is relatively unaffected by wind waves (Niiler et al., 1987; Niiler et al., 1995).

Meanwhile, the vector slip (U_s) of drifters may be successfully modelled as a linear function of wind speed at 10 m (W), vertical shear of horizontal currents across the length of the drogue (DU), drag area ratio (R), and the angles relative to the wind and shear directions (a and b), respectively:

$$U_s = (ae^{i\alpha}W + be^{i\beta}\delta U) / R \qquad (1)$$

where R is the ratio of the drogue drag area to the sum of the drag areas of the floats and tethers (drag area is the product of the drag coefficient and area). The slip and vertical shear have been measured by vector measuring current meters (VMCMs) at the top and bottom of drogues. Over 84% of the variance in the slip of both drogue types can be accounted for by linear fits to the four coefficients (a, b, a, and b), giving the result that R must be greater than 40 to achieve less than 1 cm/s slip in 10 m/s winds (performance in stronger winds is unknown) (Niiler et al., 1995). At the same time, it follows that knowledge of the winds can be used to correct drifter motions for slip.

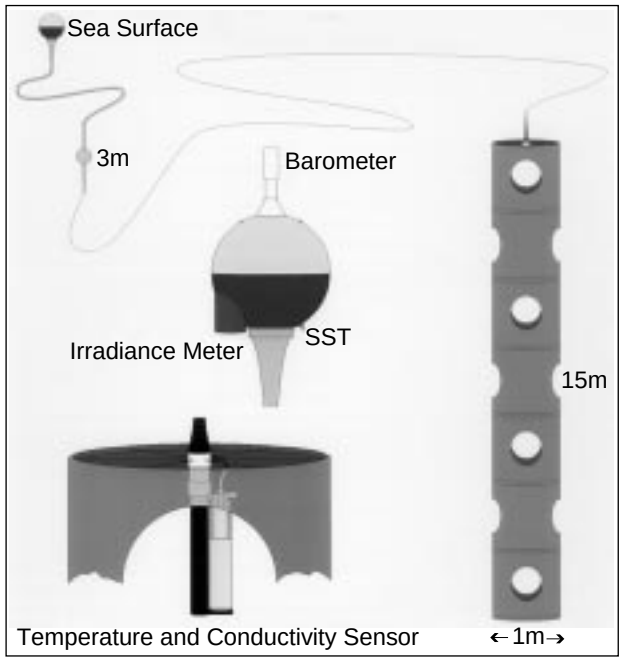

Figure 1. Schematic of the SVP drifter and various instrument configurations: the basic layout of surface buoy, tether, and holey sock drogue; barometer, submergence sensors, SST probe, and irradiance meter, mounted on the surface float; and SeaCat at the joining of the tether and drogue.

Global deployment

While both the TRISTAR and holey sock drogues minimise slip induced by vertical shear in the currents, the holey sock has been used because it is lightweight and durable, making it inexpensive to manufacture and easy to deploy. Over the past decade the cost of the standard SVP has dropped from $3,200 to $2,200, while the mean half life has more than doubled to 500 days. These improvements are direct consequences of the three way collaboration between academia, industry, and government in the development and deployment of the SVP drifter.

Drifter deployment may take place from ships or even aircraft; once in the water, the drifter packaging dissolves and the drogue unfolds itself under the influence of gravity. The drifters telemeter their identifiers and measured parameters to polar orbiting satellites from which Service Argos produces a raw data set of buoy fixes. These data are then routinely processed, archived, and distributed by the Global Drifter Data Center at NOAA Atlantic Oceanography and Meteorology Laboratory (AOML), which also aids in the global deployment of drifters. Over 17 countries and 41 principal investigators have contributed data and resources to the GDP.

Instrumentation

Velocity and SST

SVP drifters routinely provide in-situ data on mixed layer currents and sea surface temperature (SST). The SST is measured by a temperature probe located in a stainless steel housing on the underside of the surface float, where it is not subject to radiative heating (Fig. 1). Velocity is derived from satellite fixes of drifter position over time.

Most drifters operate for 1 out every 3 days, as this is adequate to sample global ocean currents (Hansen and Herman, 1989), but may be programmed with up to four different, consecutive sampling periods. When a drifter is on, NOAA polar orbiting satellites passing over pick up its transmissions. Service Argos determines drifter positions and transfers data to requesting principal investigators and the Drifter Data Center at NOAA AOML, which in turn provides raw (Argos), edited (bad data removed), and krigged (interpolated) data sets.

The krigging interpolation assumes a temporal covariance structure for the sampled fields and provides data at 6 hour intervals. As can be seen in Fig. 3a, the 3 day burst sampling is adequate for obtaining smooth positions as a function of time – the decorrelation time scale for velocity in the subtropics and tropics is approximately 6 days (Hansen and Herman, 1989). Interpolation of SST is also performed, but the diurnal cycle portion of the SST structure function is not resolved by drifters on the 1 day on, 2 days off cycle (Fig. 3b).

Drogue loss

Also standard for all SVP drifters are submergence sensors on the surface float. A properly drogued drifter spends a significant fraction of time completely submerged as surface waves break and swell pass by. Thus, a marked decrease in submergence is a robust indicator of drogue loss. This information is used to quality control drifter data by AOML. Knowledge of when drogue loss occurs is also being used to study the behaviour of free drifting surface floats. This will provide additional information on wind forcing and increase the total useful data base beyond that of only drogued drifters (Pazan, 1996).

Salinity

Thermistors and conductivity cells have been attached to SVP drifters at 11 metres depth to determine mixed layer temperature and salinity (Fig. 1). SeaCats were purchased from and calibrated by SeaBird and modified for a neutrally

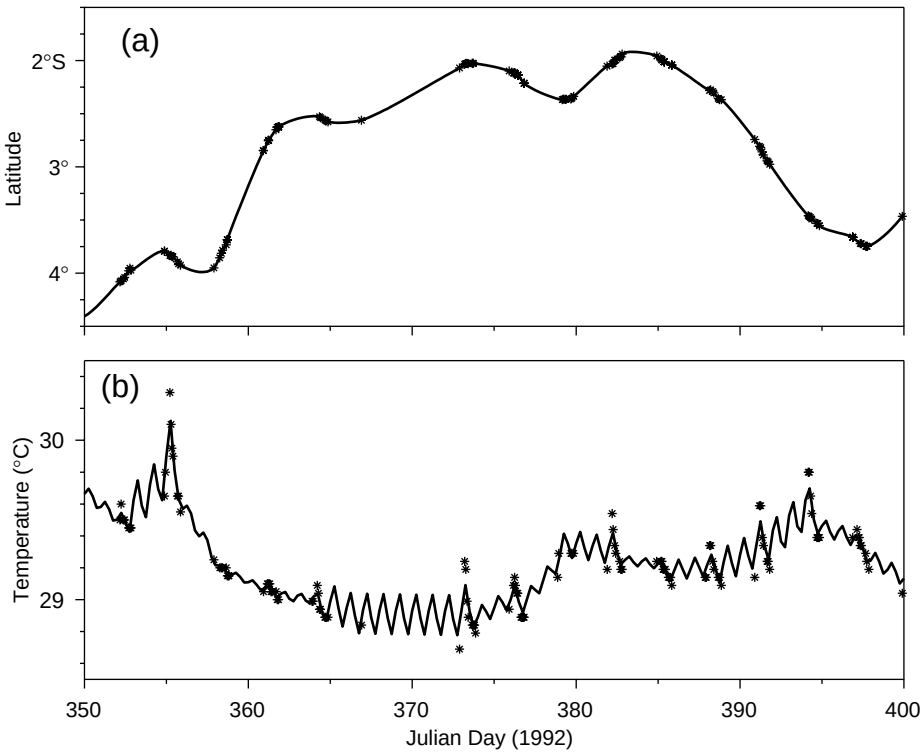

Figure 3. Comparisons of raw (asterisks) and interpolated (lines) drifter data as a function of time for (a) latitude and (b) sea surface temperature for drifter 15390.

buoyant, streamlined housing.

Seventy-two SVP SeaCat drifters were deployed in the western equatorial Pacific Ocean in 1992 and 1993. Several of these passed within 6 nautical miles of TOGA COARE moorings equipped with SeaCats in the mixed layer, allowing a comparison of the sensors. An example is shown in Fig. 4, which depicts drifter fixes as large bullets on top of a SeaCat mooring time series from 2°N, 156°E. In other instances where similar comparisons could be made, the drifters usually agreed with the moorings, or showed large gradients in salinity nearby to the moorings. The results not only confirm the stability of the SeaCat sensors on the drifters, but also the veracity of large temporal salinity gradients, associated with spatially patchy convection in the region.

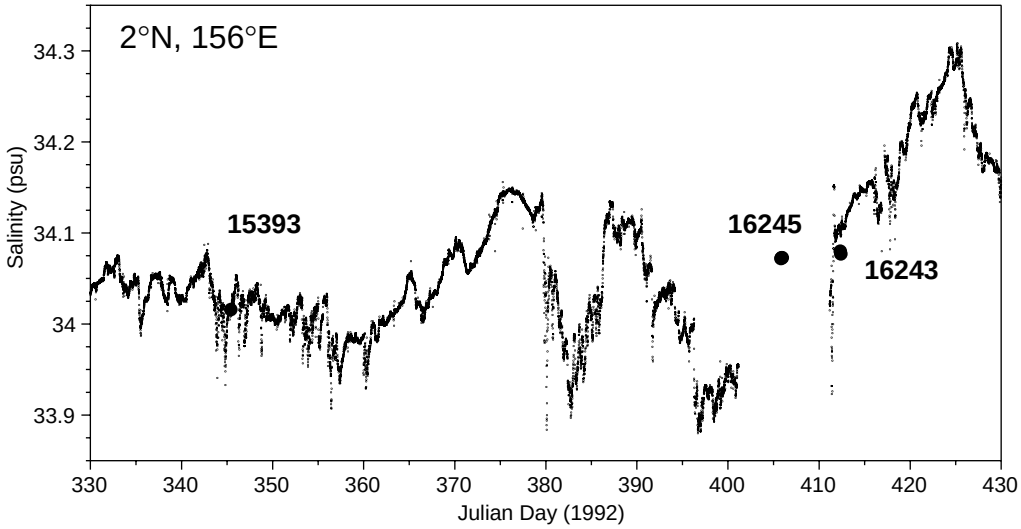

Figure 4. Comparison of salinity at 15 m depth as measured by a SeaCat moored at 2°N, 156°E and drifters (dots) that passed within 6 nautical miles. (Mooring data courtesy of R. Lukas).

Atmospheric Pressure

Barometers have been placed on the surface float of SVP drifters to measure the atmospheric pressure at the sea surface (Fig. 1). The barometer port extends vertically out of the top of the float with a pressure sensor located inside with the electronics and battery pack. The barometers are calibrated prior to drifter assembly, and have a half life of about a half year. The major obstacle to accurate SVPB drifters results from submergence of the barometer port in seas, giving erroneously high pressures. Thus, the data are quality controlled by taking the median of only the lowest 1/16 measurements. SVPB drifters cost approximately $3,400.

Winds

While the SVPB drifter augments global ship monitoring of atmospheric pressure at sea level, the Minimet represents a conceptual leap in Lagrangian ocean measurements by providing the wind stress condition following water parcels. The Minimet is a SVPB drifter, modified to carry a wind vane on the top of the surface float and a WOTAN hydrophone at 11 metres depth (Fig. 5). A compass composed of a 3-axis magnetometer and a 2-axis tilt sensor are housed within the surface float, which is rotationally decoupled from the subsurface motions via a swivel in the tether.

Comparisons at sea with anemometers mounted on a ship bow have shown that the Minimet vanes can measure

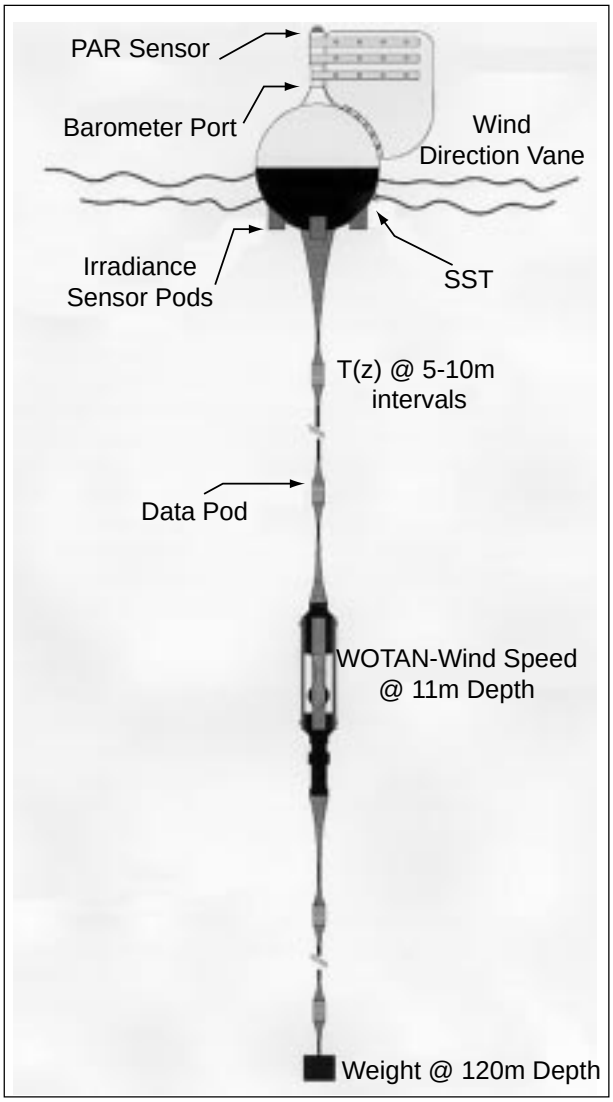

Figure 5. Schematic of a hybrid Minimet/ADOS drifter: a SVP drifter equipped with a wind vane, radiance (PAR) sensor, irradiance sensors, SST probe, thermistor chain, and WOTAN hydrophone.

wind direction to within 8° in winds up to 3 m/s, and to within 6° in higher winds up to 8 m/s. The wind speed measurements from the ship anemometers are being used to calibrate the hydrophones.

Future innovations

A wide variety of sensors may be attached to the SVP drifter so long as the casing is neutrally buoyant and does not significantly alter the drag area ratio. To date, SVP drifters have been fitted with SeaCats, barometers, hydrophones, and wind vanes as already described. They have also been equipped with radiometers to measure radiance and irradiance for biological productivity assessment, as well as thermistor chains at various depth intervals down to as much as 120 metres (Fig. 5). Many other parameters of physical, chemical, and biological interest can be imagined.

Currently, the SIO development laboratory is engaged in calibrating the wind speed measurements of the Minimet and improving confidence in quality control. Another recent development is an attempt to increase the lifetime of the tether through elimination of the subsurface buoy from the original SVP design. Although the subsurface buoy is effective at decoupling wave motions from TRISTAR drogues, holey socks have been observed to twist and fold in three dimensions regardless of its presence (Niiler et al., 1995). This advance will sacrifice minimal hydrodynamic advantage for substantial reductions in cost and drogue failure.

From sporadic use of various drifter designs in the past, to the present day global array of standard SVP drifters, obtaining accurate Lagrangian measurements in the upper ocean has become an affordable, reliable, and predictable endeavour. With the advent of globally inferred sea surface winds and ocean colour from satellite scatterometers and radiometers, SVP drifters further present the opportunity to directly test models of wind forced currents and biological influences in the Lagrangian frame. This can be attempted with unprecedented confidence because unlike its predecessors, the SVP exhibits easily modelled behaviour under various wind conditions.

Acknowledgements

Our gratitude to Roger Lukas for providing the SeaCat mooring observations and to Mayra Pazos for assistance in obtaining processed drifter data.

References

Hansen, D. V., and A. Herman, 1989: Temporal sampling requirements for surface drifting buoys in the tropical Pacific. J. Atmos. Oceanogr. Tech., 6:599–607.

Niiler, P. P., R. E. Davis, and H. J. White, 1987: Water-following characteristics of a mixed-layer drifter. Deep-Sea Res., 34(11):1867–1881.

Niiler, P. P., A. S. Sybrandy, K. Bi, P. M. Poulain, and D. Bitterman, 1995: Measurements of the water-following capability of holey-sock and TRISTAR drifters. Deep-Sea Res., 42(11/12):1951–1964.

Pazan, S. E., 1996: Intercomparison of drogued and undrogued drift buoys. In Oceans '96 MTS/IEEE: Prospects for the 21st Century: Conf. Proc., 23–26 September 1996, Fort Lauderdale, FL, pp. 864-872. Marine Tech. Soc., OES, IEEE.

Lowered ADCP Development and Use in WOCE

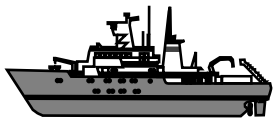

Eric Firing, SOEST, University of Hawaii, USA. efiring@soest.hawaii.edu

During the past eight years of WOCE field work, the lowered acoustic Doppler current profiler (LADCP) has evolved from an experimental instrument used only on selected stations to a standard tool of the WOCE Hydrographic Programme (WHP). The first LADCP velocity profile was made in 1989 on a WOCE project: the Hawaii Ocean Time series. The first WHP Pacific cruise with an LADCP was the P17 section on 135°W in 1991. The LADCP was used only within 3.5° of the equator, where direct velocity measurements were deemed most important. Use became increasingly common on later Pacific cruises. By the start of the one-time Indian Ocean WHP survey on the RV Knorr, near the end of 1994, the LADCP was securely strapped into the rosette frame for the duration, to be used on all CTD stations.

How the LADCP works

An LADCP is a self-contained ADCP that is lowered and retrieved with a hydro wire, usually as part of a CTD/rosette package. The ADCP pings as fast as possible, typically about once per second, yielding a large number of overlapping velocity profiles, each with a range of 100–200 m from the instrument, and each relative to the unknown velocity of the instrument. These unknown velocities are removed by differentiating the profiles in the vertical. The resulting overlapping shear profiles are then interpolated to a uniform depth grid and averaged to give a composite shear profile. Integrating this shear profile in depth gives a velocity profile relative to a single unknown constant of integration. If the vertical mean of the relative velocity

profile is subtracted out, then the constant that remains to be determined is just the depth-averaged velocity. This can be calculated by a method closely analogous to that used in shipboard ADCP work (Fischer and Visbeck, 1993). The depth-averaged absolute water velocity is the time-average of the velocity of the water relative to the instrument, plus the time-average of the ship velocity as calculated from the position difference between the start and end of the cast, minus a small correction (usually less than 1 cm/s), calculated from the time-integral of the relative velocity profile. If the vertical velocity were a constant during the downcast, and another constant during the upcast, then the time-integral would be equivalent to a depth-integral – which is of course zero for the de-meaned relative velocity profile. Hence the calculation of the depth-averaged velocity is very insensitive to the accuracy of the relative velocity profile.

What is it good for?

The most obvious "WOCE-type" information that one may wish to derive from LADCP measurements is a picture of the large-scale geostrophic circulation and transports. The primary strength of the LADCP for this purpose is probably its ability to accurately measure the depth-averaged velocity. Weaknesses of the LADCP are its inclusion of ageostrophic as well as geostrophic velocities, and its point-sampling in space and time. Unlike geostrophic calculations, there is no along-track averaging inherent in LADCP measurements,

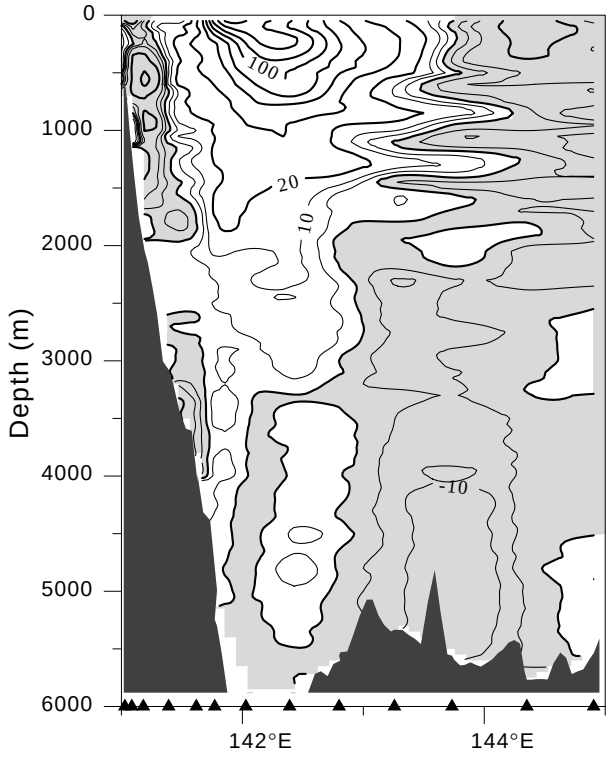

Figure 1. Eastward velocity component from LADCP measurements on the WHP P10 line near Japan in November 1993. Westward flow is shaded.

so transports estimated from LADCP profiles alone are limited in accuracy by the degree to which horizontal current structures are resolved by the sample spacing, and by a random-walk accumulation of errors that are, at best, independent from one profile to the next. Horizontal resolution is also a critical factor when using the point LADCP measurements, vertically-averaged, to reference geostrophic currents averaged between stations. Particularly at high latitudes, an entire current jet sometimes fits between a pair of stations, so that it is missed by the LADCP. Despite these limitations, LADCP profiles have proven useful in identifying locations of strong abyssal currents and indicating their circulation patterns. An example is the extensive deep westward flow just offshore of the Kuroshio on the WHP P10 line (Fig. 1; Wijffels et al., 1998).

A particular concern when trying to use vertically-averaged LADCP currents for geostrophic referencing is the amplitude of the barotropic tide. Measurements of open-ocean barotropic tidal currents are rare; depth-averaged LADCP measurements provide a means of checking tide models, which may in turn be useful in estimating the tidal component in LADCP datasets. In Fig. 2, an example from the Indian Ocean shows unusually large tidal currents in the LADCP data (P. Hacker, personal communication) but indicates that they are systematically overestimated by the tide model of Egbert et al. (1994). It remains to be determined from additional LADCP-model comparisons whether the overestimation is specific to this time and place or is more widespread.

The LADCP's lack of inherent horizontal averaging can be an advantage rather than a liability. Consider, for example, the submesoscale feature sampled at 62°S, 103°W, on the WHP P18S line. The 30 cm/s westward jet at 3000 m in Fig. 3 is much faster than indicated by geostrophic calculations (G. Johnson, personal communication). Similar but weaker features have appeared in LADCP profiles from at least two other Southern Ocean sections.

High vertical resolution, and the ability to measure ageostrophic as well as geostrophic currents, makes the LADCP good for measuring near-equatorial currents – an important part of the original motivation for its development – and also for looking at internal waves. Polzin and Firing (1997) show how LADCP profiles may provide information about the geographical distribution of diapycnal mixing. In addition to this statistical approach, one may study particular examples of energetic small-scale structure such as the packet of wiggles between 500 and 2000 m in Fig. 1, on the south-east flank of the Kuroshio.

How well does it work?

Several factors control LADCP profile accuracy. It is important to distinguish between the accuracy of the relative velocity profile as a function of vertical wavenumber, and the accuracy of the depth-averaged velocity. One must also distinguish instrumental errors, caused by the fundamental limitations of the hardware and software, from errors or shortcomings associated with the way the LADCP samples

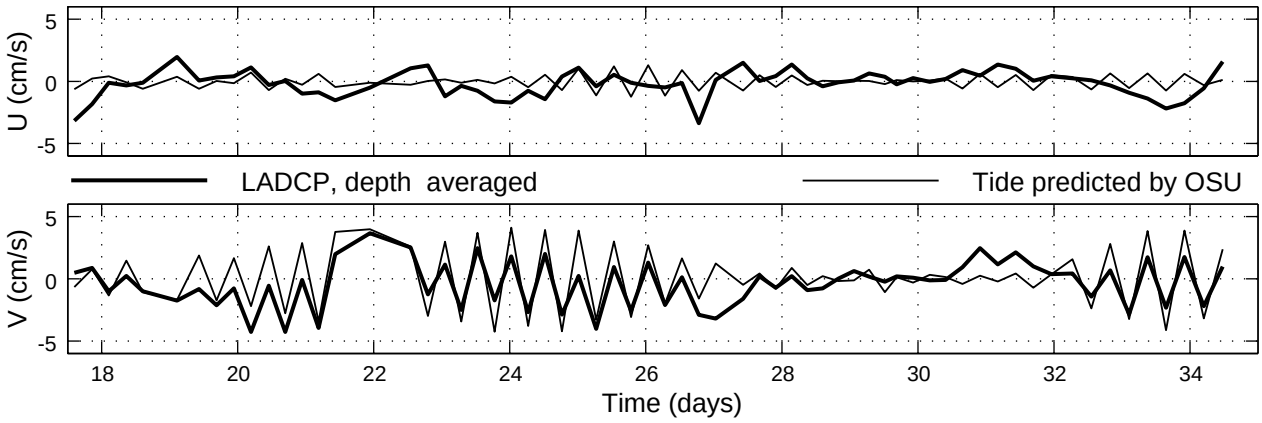

Figure 2. Depth-averaged currents (east component in the top panel, north below) from the LADCP on the second half of the WHP Indian Ocean I9 line, compared to the prediction of the OSU TOPEX/POSEIDON crossover global inverse solution version 3.0 (Egbert et al., 1994), averaged over the duration of each station. Time is in days from the first station of the cruise.

the ocean.

Because the relative velocity profile is calculated as the depth-integral of a composite shear profile, relative velocity errors between two depths tend to grow as the square root of the separation, as in a random walk. The velocity error wavenumber spectrum is red for scales larger than the depth range of each individual ADCP profile (from a single ping), and white for smaller scales (Firing and Gordon, 1990). The magnitude of the error increases with uncertainty in the raw ADCP velocity estimates, and decreases with increasing range of the individual profiles and with increasing numbers of profiles. This analysis assumes unbiased ADCP profiles. Unfortunately, the relative velocity profile is extremely sensitive to small shear biases in the individual profiles; however, such bias has been dominant only in a small fraction of the profiles that have been made. The reason for these occasional episodes of bias, which cause the downcast and upcast profiles to cross in a characteristic "X" on plots of velocity versus depth, has not yet been determined. The problem can often be reduced by rejecting data from more distant bins in each of the single-ping profiles.

Because the relative velocity profile accuracy depends on the accuracy and the range of the single-ping ADCP profiles, it decreases with reduced acoustic backscattering strength. Backscattering at the 150–300 kHz frequencies typical of LADCPs varies widely with depth and location. It generally decreases from the upper ocean to the abyss, often with a sharp change near 1000 m. Typical differences exceed 20 db. At all depths, scattering tends to be weak in the tropics and subtropics, increasing slightly at the equator (particularly in the eastern Pacific) and increasing greatly in subpolar regions. Consequently, it tends to be easiest to get good LADCP profiles at high latitudes; and in some low latitude regions, the relative velocity profiles have been rendered useless below about 1000 m.

Until recently, relative velocity profiles were subject to major interference from sound reflected from the ocean bottom. For each individual ping in the affected depth range, the bottom reflection of the previous ping overwhelms the signal scattered from the water. With a 1-Hz ping rate, for example, the interference would be centred at about 650 m off the bottom, and could contaminate a depth band up to 200 m thick. The velocity signature of this interference depends on the velocity of the package over the ground. When the velocity is small, the bottom-contaminated velocity estimates are similar to the surrounding uncontaminated estimates, and the interference is not visually evident in the calculated velocity profile. When the package velocity is larger than 10 cm/s or so, the interference shows up as velocity spike and/or offset in the processed LADCP profile, if no special editing is done. Editing out the contaminated depth range leaves a gap in the composite shear profile and therefore an uncertain offset between the parts of the velocity profile on either side of the gap. The problem can be avoided entirely by using a staggered ping sequence, so that the interference appears in two non-overlapping depth ranges on alternate pings. Editing out the interference then leaves no gap in the composite shear profile. The use of two ADCPs, one looking up and the other down (Visbeck, 1997), also solves the problem; the upward-looking profiler's data remains uncontaminated.

The accuracy of the depth-averaged velocity depends almost entirely on the accuracy of the position fixes at the start and end of the cast, and on the accuracy of the time-integrated velocity of the water relative to the package. Fix accuracy is not a major concern, now that military GPS accuracy is widely available on US ships, and differential GPS (real-time or post-processed) and GLONASS receivers can provided similar accuracy on non-US ships. Even civilian GPS contributes an error less than 1.6 cm/s to 95% of all casts lasting 2.5 hours or longer. Of greater concern is the velocity integral, for which there are two types of error: that of the velocity measurement itself, and that due to gaps in the sampling. Long gaps, as opposed to occasional ping dropouts and the normal interval between pings, are caused primarily by interference from sound reflecting off the ocean bottom instead of the water. Although such gaps can last several minutes, this interval is short compared to

the entire profile, and can be filled by interpolating a low-pass filtered time series of the water velocity relative to the package. Even if the interpolated velocity is in error by 10 cm/s on average, and the gap is 5 minutes, the contribution to the depth-averaged velocity error will be only 0.3 cm/s for a 2.5-hour profile. Therefore the most worrisome type of error is that which contributes a bias to the velocity measurement. Of the possible causes, I will discuss only one here: compass error.

Compass error affects both the relative velocity profile and the depth-averaged velocity calculation. The LADCP is much less sensitive to compass error than a shipboard ADCP because the magnitude of the velocity error is proportional to the magnitude of the velocity relative to the instrument, which is usually smaller for the LADCP by a factor of 10 or more. For example, if the velocity of the water relative to the LADCP is 20 cm/s, a 5° compass error will cause a 1.7 cm/s velocity error perpendicular to the mean velocity. Compass accuracy will vary with geographic position and instrument tilt, becoming increasingly problematic near the magnetic poles. Nevertheless, LADCPs seem to have performed well in such adverse locations as the Iceland basin, and the Southern Ocean south of Australia and New Zealand. Apart from one recent episode of major compass failure, compass errors have not been immediately obvious from inspection of the velocity profiles.

This brings up an important question: how do we evaluate LADCP performance in practice? And, how good or bad is it? There have been only a few comparisons between LADCP profiles and independent velocity profile measurements. Fischer and Visbeck (1993) showed the result of comparison with Pegasus profiles: rms differences of about 5 cm/s in each component, up to a factor of two larger than the rms difference between Pegasus up and down casts. Hacker et al. (1996) made a similar comparison, but compared only the depth-averaged velocity estimates from the two methods. Rms differences of the depth-averages were about 1.5 cm/s on a cruise in 1992, and under 1 cm/s on a 1993 cruise using a better LADCP. On the November 1997 cruise of RV Knorr, 18 XCP profiles were made during LADCP casts in collaboration with Eric Kunze and Kurt Polzin. The results are not yet available.

Given that direct comparisons between LADCP and other profiling methods are rare, and clouded by uncertainties in the alternative methods and by spatial and temporal differences in sampling, we are led to rely on other consistency checks. The most general one is the comparison between up and down casts. As noted above, this comparison sometimes shows obvious problems. A second useful comparison is between the top of the LADCP profile and simultaneous shipboard ADCP data. This comparison is made separately for LADCP up and downcasts; temporal differences are often substantial, as verified by on-station shipboard ADCP time series. Similarly, Send (1994) has shown that Pegasus up-down differences are roughly consistent with a Garrett-Munk type internal wave spectrum. A third type of comparison is between the bottom of the LADCP profile and the near-bottom velocity calculated by tracking the bottom in addition to the water. Cunningham et al. (1997) have shown cases where this method together with the shipboard ADCP comparison reveal a disturbing lack of consistency; the cause of the error is not yet clear.

As this discussion of error sources suggests, there is no good easy answer to the question, "What is the error in an LADCP profile?" A reasonable but vague answer would be, "A few cm/s, except when backscattering is very low, or something else goes wrong." A better answer would point out that accuracy tends to be highest for the depth average, but lowest for the lowest non-zero vertical wavenumbers; that relative velocity profile errors are larger for deep profiles than for shallow ones, but the reverse may be true for the depth-averaged velocity; etc. More precisely quantifying the errors in existing LADCP profiles, and finding ways of reducing errors in future profiles, is an ongoing project.

Although far from perfect, the LADCP has made a substantial contribution to WOCE. Interest in the technique

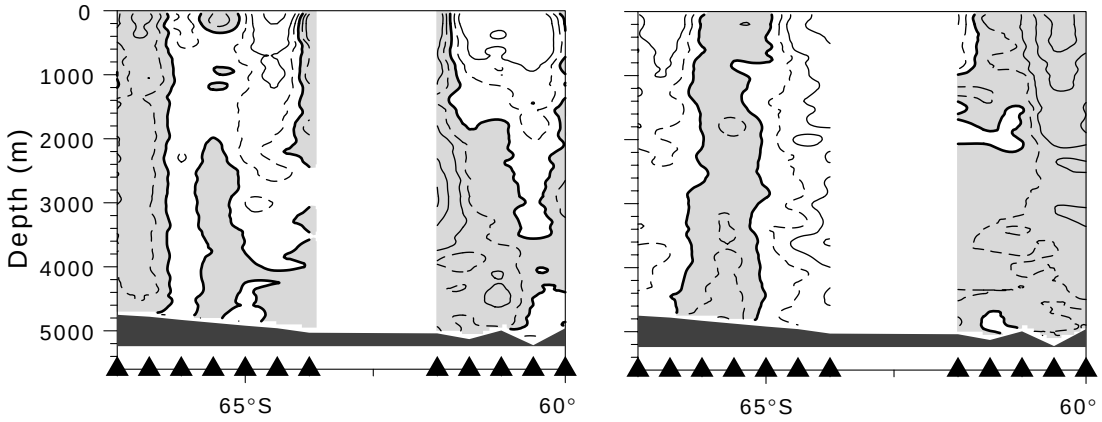

Figure 3. LADCP zonal (left) and meridional (right) velocity components from WHP line P18. Solid contours are at 10 cm/s intervals, negative components are shaded. Note the 30-cm/s westward jet at 3000 m, 62°S, in the left panel.

continues to grow, along with improvements and innovations such as Visbeck's (1997) dual upward and downward-looking system based on RD Instruments' compact "Workhorse" ADCP, and a new Sontek dual system with a high ping rate and other optimisations.

References

Cunningham, S. A., M. J. Griffiths, and B. A. King, 1997: Comparison of bottom-tracking and profiling LADCP data in a section across the ACC at Drake Passage. International WOCE Newsletter, 26, 39–40.

Egbert, G. D., A. F. Bennett, and M. G. G. Foreman, 1994: TOPEX/POSEIDON tides estimated using a global inverse model. J. Geophys. Res., 99, 24,821–24,852.

Firing, E. and R. Gordon, 1990: Deep ocean acoustic Doppler current profiling. Proc. IEEE Fourth Working Conf. on Current Measurements, Clinton, MD, Current Measurement Technology Committee of the Oceanic Engineering Society, 192–201.

Fischer, J., and M. Visbeck, 1993: Deep velocity profiling with self-contained ADCPs. J. Atmos. and Oceanic Technol., 10, 764–773.

Hacker, P., E. Firing, W. D. Wilson, and R. Molinari, 1996: Direct observations of the current structure east of the Bahamas. Geophys. Res. Ltrs., 23, 1127–1130.

Polzin, K., and E. Firing, 1997: Estimates of diapycnal mixing using LADCP and CTD data from I8S. International WOCE Newsletter, 29, 39–42.

Send, U., 1994: Accuracy of current profile measurements: Effect of tropical and midlatitude internal waves. J. Geophys. Res., 99, 16,229–16,236.

Visbeck, M., 1997: Lowered Acoustic Doppler Current Profiler. http://www.ldeo.columbia.edu/~visbeck/ladcp/.

Wijffels, S., M. Hall, T. Joyce, D. J. Torres, P. Hacker, and E. Firing, 1998: The multiple gyres of the western North Pacific: a WOCE section along 149°E. J. Geophys. Res., submitted.

Bottom Pressure Measurements across the Drake Passage Choke Point

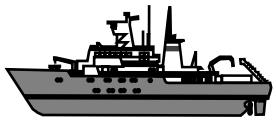

J. M. Vassie, R. Spencer and P. R. Foden, Proudman Oceanographic Laboratory, Birkenhead, UK. imv@pol.ac.uk

Long-term measurements of sea level or the equivalent pressure variations at the sea bed have proved their value to the scientific community for the study of climate change. Sea level and its possible trends are of direct interest and its variations can be related to internal processes such as changes in ocean circulation. Sea level is at present measured by instruments in-situ or on a global scale by altimetric satellites such as ERS-1, ERS-2 and TOPEX/POSEIDON. The WOCE tide gauge network recently provided a basis from which long term drift in the TOPEX/POSEIDON altimeter was detected which was finally ascribed to a software error. In-situ sea level measurements have shown themselves to be complementary to altimetry and between the two we now have global measurements of ocean dynamics at the sea surface. Measurements of bottom pressure to study dynamics associated with deep flows and the thermohaline circulation are less widespread. They have been concentrated in areas of particular interest. One such area is the Southern Ocean which plays an important role in the global climate balance through the interchange of water masses between the major ocean basins.

ACCLAIM

A programme of measurements was started in the late 1980s in the South Atlantic and the Southern Ocean which became known as ACCLAIM, (Antarctic Circumpolar Current Levels from Altimetry and Island Measurements, Spencer et al., 1993), an acronym which omits the important contribution from Bottom Pressure Recorder (BPR) measurements to the programme. The programme was oriented towards a study of the circulation of the Antarctic Circumpolar Current (ACC) as one of the UK contributions to WOCE.

The principal objective was to study variations in the ACC over a range of time scales and to resolve the spatial scales of the variability. BPRs were positioned across the main filaments of the ACC to measure transport fluctuations in the region of the Drake Passage 'choke point'. A parallel investigation using altimeter data was undertaken (Woodworth et al., 1996b). The first BPR array was installed in 1988 in the Scotia Sea. In 1992 the work was relocated to concentrate on measuring across the Drake Passage between Burdwood Bank and Elephant Island where it has remained. The instruments were replaced annually to produce a long term data set.

POL sea level stations were installed on islands and at Antarctic mainland sites (Fig. 1), the latter through collaborative work with the British Antarctic Survey. With the development of improved instrumentation and modern microprocessor technology it became possible to construct autonomous sea level stations in remote areas and to have them run continuously (Woodworth et al., 1996a). The desire to obtain data in quasi real time and to monitor the operation of the stations led to daily transmission of the data through a telemetry link. Operational stations have been installed at Ascension, St Helena, Tristan da Cunha, Port Stanley (Falkland Islands), Signy Island (South Orkney), Faraday (now Vernadsky) and Rothera. These stations record sub-surface pressure, sea temperature, air temperature and barometric pressure from which sea level variations can be derived. Goal 2 of WOCE, which is to measure the long-term representativeness of any short term measurements, is satisfied to an extent by our BPR array and the sea

level stations.

Qualitative comparisons have been made between the BPR data which were placed in the Drake Passage and earlier measurements made during the ISOS programme of the 1970s (Whitworth and Peterson, 1985). In general the standard deviation of the ACC transport derived from cross passage slopes is lower in the ACCLAIM data than was seen during the ISOS period (8 Sv compared to 10 Sv) but not significantly different when compared to the inter-annual variability. However there were two occasions when the transport changed by 40% in the ISOS data which has not been seen during the ACCLAIM period. This suggests the ACC as well as undergoing interannual changes may alter on long time scales.

The bottom pressure measurements from these sites were inter-compared and shown to be related to wind stress (Meredith et al., 1996). At the south side of the Drake Passage the ACC transport is most correlated with the zonally averaged eastward wind stress. The similarity with wind stress curl in latitude bands adjacent to the ACC is felt to be coincidental rather than causal. Large spatial scale coherence in the low frequency components of the signals was shown to exist between the BPRs on the south side of the passage and sea level stations along the Antarctic coast over a region of several hundred kilometres. The coherent signals over such large distances are also seen in FRAM. The instruments on the north side were less coherent due to the effect of steric changes in the surface layers. A full set of comparisons will be made between the Drake Passage data and similar measurements made by Tom Whitworth of Texas A&M University at the African and Australian 'choke points' of the ACC. This will provide a measure of the extent of the large-scale coherence in bottom pressures in the Southern Ocean.

At some of the Drake Passage BPR positions, Inverted

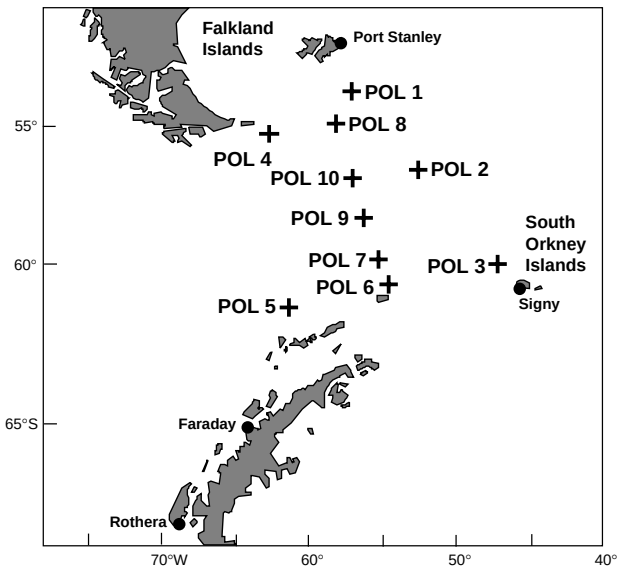

Figure 1. ACCLAIM deployment sites in the Scotia Sea and Drake Passage where bottom pressure measurements have been made between 1988 and 1997.

Echo Sounders provide additional information on the variations in the internal structure of the water column. The instruments were positioned to make it possible to examine aspects of the meridional structure of the ACC in the area of the Scotia Sea and Drake Passage that is known to have the strongest flow in filaments constrained by the Sub-Antarctic and Polar Fronts.

MYRTLE

Most long term pelagic measurements, away from continents or islands, are made by replacing BPRs annually. To create a long data set the end points of each record have to be matched in some manner which can create difficulties in the interpretation of results. The use of instruments capable of continuous long term operation was considered at POL and MYRTLE (Multi Year Return Tide Level Equipment) was developed to meet this requirement (Spencer et al., 1994). This BPR (Fig. 2, see page 24) is capable of continuous operation for 5 years on the sea bed. At predetermined times, which are normally one year apart, a capsule containing the measured data is released to the surface (Foden and Spencer, 1995).

So far one such instrument has been constructed and was deployed in November 1992 from the RRS Bransfield at position 59°44'S 55°30'W on the WOCE hydrographic section SR1 in the Drake Passage. This is shown as POL7 in Fig. 1. Because it was felt important to obtain data for WOCE from this area MYRTLE was deployed before the development of the satellite telemetry link for the capsules was completed. As a result the capsules were released by acoustic command from a surface ship and then recovered in the conventional manner. It is planned to make the capsules self release and transmit the data through an ARGOS satellite to the UK. A high degree of data security is ensured by storing all the data in each capsule and in a data logger on the main frame. In November 1996 the one remaining capsule and the complete instrument were recovered using the RRS James Clark Ross providing us with four years of sea bed pressure.

The availability of this continuous data provided the opportunity to study the measured tides and low frequency sea level signal in detail. From an instrumental viewpoint the results have an important consequence. The tides are the main component of the signal and are coherent. When the data set was analysed the amplitudes of the harmonic constituents of the tide were found to remain substantially constant for the four year period. This suggests that the calibration of the pressure sensor is not changing with time which is important for long-term monitoring as an ocean observing system inevitably prevents the sensors from being returned to the laboratory for calibration.

Tides are important as they are by far the most energetic signal in sea level and may be important in driving circulation in enclosed areas. There is a need for tidal information under ice shelves where little is known of their characteristics. In-situ measurements are difficult and satellite altimetry is not applicable. Numerical models of

the tides under ice shelves only give acceptable values if bottom friction is increased to an unreasonably high value. Hence more tidal measurements are required to validate hydrodynamic models (Smithson et al., 1996). A spectrum derived from the four years of pressure data recorded by MYRTLE shows evidence of non-linear tides which must emanate from the Weddell Sea. The tides in the Weddell are being investigated at the present time with a series of BPRs deployed along the ice front.

The low frequency signal showed some coherence with the BPR to the south of MYRTLE, POL6 in Fig. 1, but it contained a component of larger amplitude which was caused by the existence of a quasi-stationary eddy which existed locally. The bottom temperature showed evidence of cooling for a period of 10 months during 1995 after which it recovered to its original value. The decrease in temperature of 0.1°C appeared to be widespread and is being investigated by a student at the University of East Anglia.

The large scale coherence which is seen to exist in the Southern Ocean is being investigated and measured on a basin scale by placing several BPR around the South Atlantic. Most of these are already in place and are to be recovered in early 1999. The instruments used are a development from the MYRTLE technology but are smaller and less expensive containing only one pressure device. Many of the questions related to the large scale features of the ocean circulation could be addressed by arrays of BPRs deployed in the appropriate places. Satellite gravity missions, which have been approved for the year 2001, have the potential to improve our knowledge of ocean circulation but will require ground truth to improve the spatial resolution in particular areas, a role which can be filled with an array of BPRs.

Data Availability

The data sets discussed in this paper can be obtained via Anonymous FTP from POL. FTP to "bisag.nbi.ac.uk/pub/woce/acclaim/bprs" and consult the file "INVENTORY".

References

Foden, P. R., and R. Spencer, 1995: A releasable data capsule for the deep ocean. In: Oceans95, MTS/IEEE: Challenges of our changing global environment, October 9–12, 1995, San Diego (Calif.) Proceedings, Volume 2, The Marine Technology Society, pp.1240–1246.

Meredith, M. P., Heywood, K. J, Spencer, R., and J. M. Vassie, 1996: On the temporal variability in the transport through Drake Passage. J. Geophys. Res., 101(C10), 22485–22494. (Correction published in Vol. 102, C2, 3501)

Smithson, M. J., Robinson, A. V., and R. A. Flather, 1996: Ocean tides under the Filchner-Ronne Ice Shelf, Antarctica. Annals of Glaciology, 23, 217–225.

Spencer, R., Foden, P. R., and J. M. Vassie, 1994: Development of a multi-year deep sea bottom pressure recorder. In: Sixth International Conference on Electronic Engineering in Oceanography, 19–21 July 1994, Cambridge, B.S. McCartney, et al., eds., Institution of Electrical Engineers, pp. 175–180.

Spencer, R., Foden, P. R., McGarry, C., Harrison, A. J., Vassie, J. M., Baker, T. F., Smithson, M. J., Harangozo, S. A., and P. L. Woodworth, 1993: The ACCLAIM Programme in the South Atlantic and Southern Oceans. International Hydrographic Review, 70(1), 7–21.

Whitworth, T., and Peterson, R.G., 1985: The volume transport of the Antarctic Circumpolar Current from bottom pressure measurements. J. Phys. Oceanogr., 15,810–816.

Woodworth, P. L., Vassie, J. M., Spencer, R., and D. E. Smith, 1996a: Precise datum control for pressure tide gauges. Marine Geodesy, 19(1), 1–20.

Woodworth, P. L., Vassie, J. M., Hughes, C. W., and M. P. Meredith, 1996b: A test of the ability of TOPEX/POSEIDON to monitor flows through the Drake Passage. J. Geophys. Res., 101(C5), 11935–11947.

In-situ Temperature Calibration: A Remark on Instruments and Methods

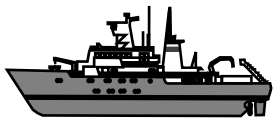

G. Budeus and W. Schneider, Alfred-Wegener-Institut für Polar- und Meeresforschung, Bremerhaven, Germany. gbudeus@awi-bremerhaven.de

Traditionally, reversing thermometers are utilised for in-situ temperature comparisons with CTDs. The most accurate mercury reversing thermometers are those with expanded scales ('Polar scale', -2° to +3°C), alternatively electronic reversing thermometers (SIS) are frequently in use. Here we describe our experience with a relatively new electronic reference thermometer with internal memory (SBE-35) which is triggered by the electric bottle release signal.

Problems of in-situ temperature calibration mainly include employed methods and suitable reference instruments. To start with the latter, basic demands for a reference instrument are its better stability, accuracy and precision compared with the instrument to be controlled and the data quality requested. With a demanded accuracy of 1 mK, available reversing thermometers do not serve as reference instruments in the above sense. None of them is specified to this accuracy, and their actual design limits accuracy enhancements by user specific methods (e.g. use and storage in a confined temperature range). The mercury thermometers restrict reading accuracy to about 2 mK, while the SIS electronic reversing thermometers are specified to 2 mK and can be read to 1 mK.

The possibility of using duplicate sensors on modern CTDs is undoubtedly a big advantage which allows detection of a rapid drift or inconsistent calibrations. But according to the identical design of duplicate sensors, unwanted sensitivity to other parameters (like pressure or movement induced bending) may also be similar, and not

be detectable by a comparison between them. Thus, if working well, the SBE-35 would be a most welcome reference.

Its specified accuracy is better than 1 mK, the drift per year is specified to be smaller than 1 mK. The instrument stores 156 samples internally. An advantage is that it can be mounted close to the CTD sensors, but it requires accessibility for memory readout after a number of casts. We utilised this instrument (S/N 003) during a cruise to Fram Strait and Greenland Sea in summer 1997. The instrument was used for about 150 profiles and its samples are compared to those of a CTD with duplicate temperature sensors (SBE-3, S/N 1338 and 1491). The duration of the campaign was 15.8–20.9.97, with most casts extending to a range between 3000 and 4000 dbar. The SBE-35 was mounted in the water sampler at the same height as the CTD sensors, but in a distance of roughly 30 cm. The CTD and the SBE-35 have both been adjusted to sample for 1 second after a bottle release.

Great care has been taken to use appropriate methods for a comparison. As the ocean is not as homogeneous as a stirred calibration bath, the most important aspect is to avoid intercomparisons at locations where this is prohibited. Generally, values stemming from pressure levels shallower than 2000 dbar have been discarded from the data set because of too large temperature gradients. But also deeper than this level, in-situ calibration is not automatically allowed, as Fig. 1 exemplarily shows. Depicted are vertical temperature gradients from the CTD cast (1 dbar means)

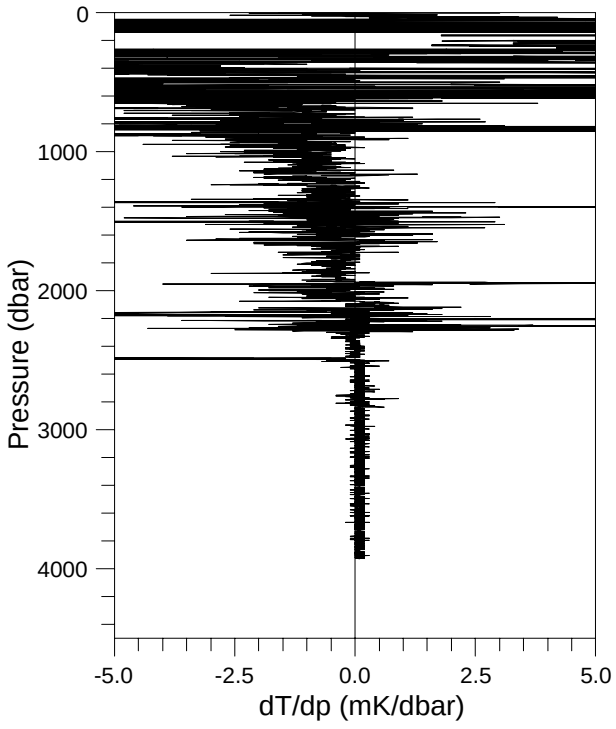

Figure 1. Profile of the vertical temperature gradient for a station in north-western Fram Strait from CTD measurements. At this station we allow for in-situ calibrations only at pressures higher than 2500 dbar.

from the presumably thermally very quiet deep regions of the Nordic Seas. The position of the station is at about 82°N, 5°W, i.e. in the north-western part of Fram Strait. We request temperature gradients, somewhat arbitrarily, below 1 mK/dbar for calibration points to be valid. Greater gradients would certainly inhibit a comparison to the required accuracy between a CTD at the bottom of a rosette and a reversing thermometer attached to a sampling bottle 1 m above, particularly with a moving (rolling) ship and differing sampling intervals or time constants, so this is not an unduly constraint for us. At every sample it has been checked whether temperature gradients are small enough to allow for an in-situ calibration.

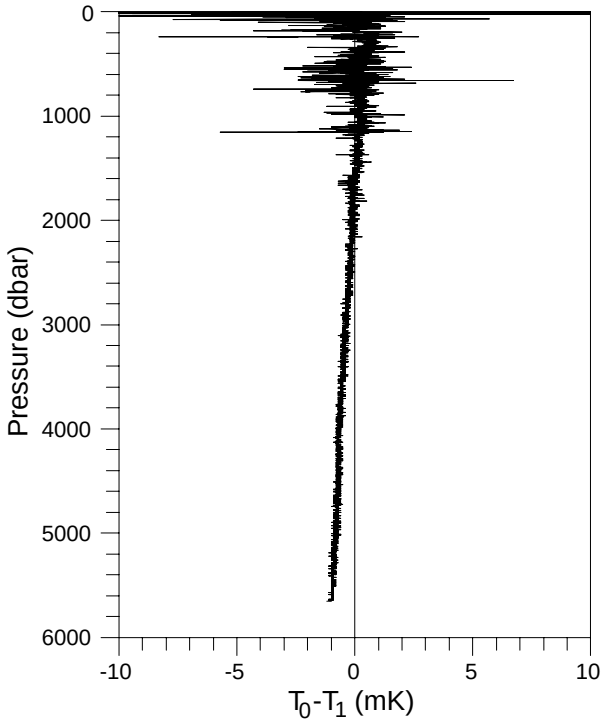

Figure 2. Difference between two CTD temperature sensors (SBE-3, S/N 1491 and 1338) at a Fram Strait station (Molloy Deep). By means of reversing thermometers it was impossible to decide which sensor shows a pressure sensitivity.

The comparison between the two SBE-3 sensors (Fig. 2) reveals that one of them shows a small pressure sensitivity, or alternatively that they possess different pressure sensitivities. This behaviour was already known from previous cruises, but because of the small deviations it was impossible to decide for one of these alternatives by means of reversing thermometers. The comparison with the SBE-35 (Fig. 3) now shows, that sensor 1338 exhibits a slight pressure dependence (about 1 mK/4000 dbar), while sensor 1491 is not pressure sensitive. This can be seen best at stations 10, 13, 21 because valid measurements are available over a pressure range of 2000 dbar there (compare Fig. 3d). The deviations between the latter sensor and the SBE-35 are below 0.5 mK over the entire cruise and

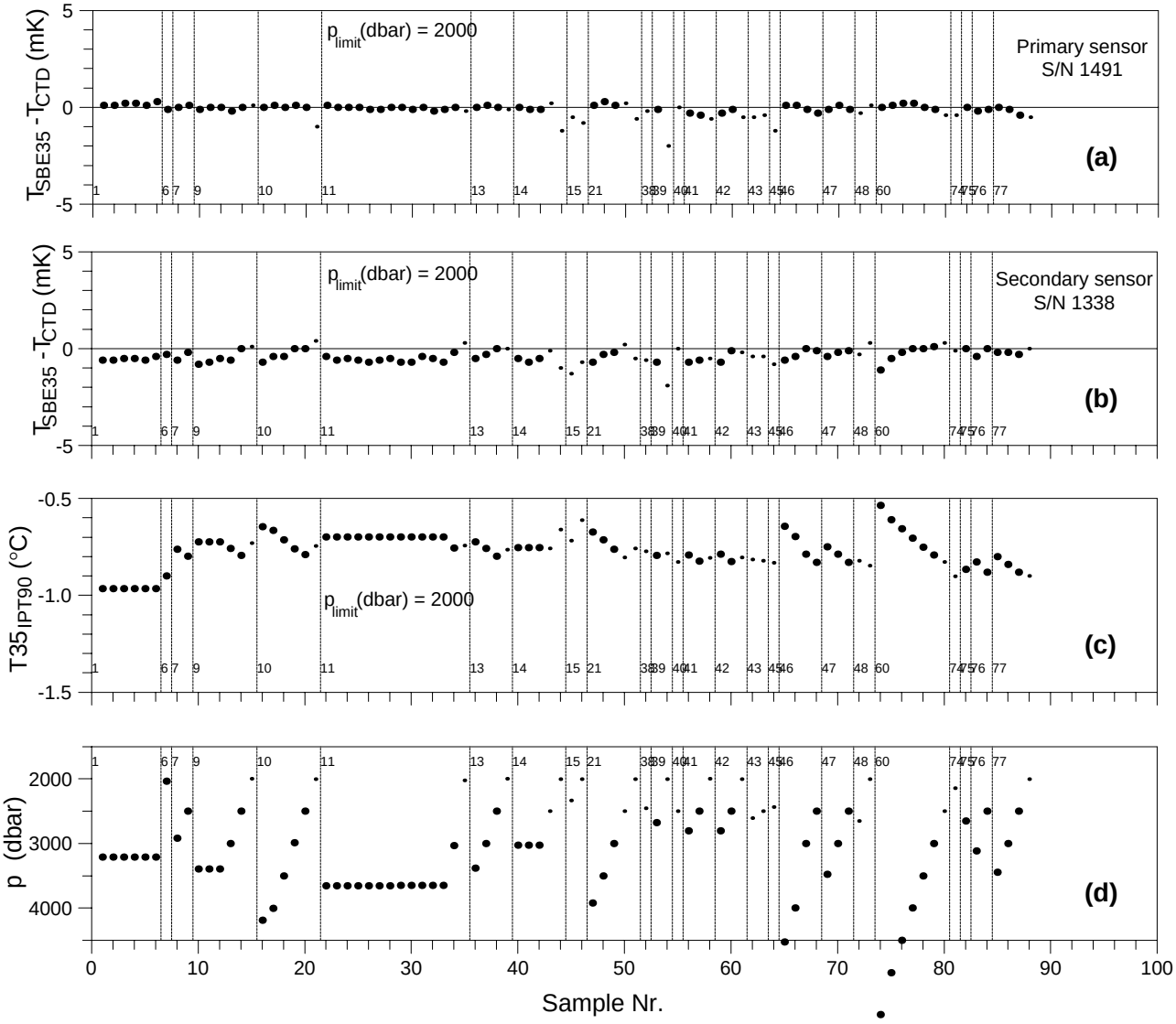

Figure 3. (a) Difference between temperatures measured by an SBE-35 (S/N 003) and an SBE-3 sensor for about half of the complete data set. Big dots represent valid calibration points, smaller dots invalid calibration points (see text). The vertical lines separate different stations which are given by the small annotated numbers. (b) Same as (a) for a second sensor. (c) Temperatures at the calibration points. (d) Pressures at the calibration points. Note that frequently in-situ comparison is not allowed (small dots) despite the considerable depth of the sample's location.

range of application (see Fig. 3a). Please note that with the exception of station Nr. 60 (Molloy Deep, 5600 m) our data set would not show deviations exceeding 1 mK for sensor 1338 (see Fig. 3b). Due to their different mechanical design it is most unlikely that the two thermometer types SBE-3 and SBE-35 show a similar sensitivity to other parameters, but this can only be excluded explicitly to the accuracy reversing thermometers provide.

It is evident from Fig. 3c that the temperatures of the in-situ calibrations are restricted to a narrow range (-0.5 to -1.0°C), as is typical for field campaigns. In order to check the sensor's accuracy outside of this range, laboratory calibrations are necessary. Therefore all mentioned sensors have been calibrated before and after the cruise by the manufacturer. After 11.5 months and the described utilisation in the field the SBE-35 showed a deviation of about 0.1 mK from the previous calibration. Over the entire range of our interest (T<5°C) both SBE-3 sensors show a time drift below 0.1 mK between the pre-cruise and post-cruise calibration (5 months).

This means that with appropriate care and suitable instrumentation temperature accuracies of 1 mK can operationally be achieved in field measurements, and that with the SBE-35 a true reference instrument is available for temperature. A further advantage is the fact that it can be checked in a triple point cell. It has to be kept in mind, however, that field calibrations without checking and specifying the in-situ conditions are likely to be of limited value.

Technology Revolutionises Tracer Oceanography During WOCE

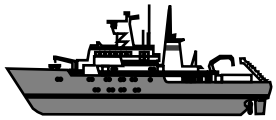

Robert M. Key, Ocean Tracer Laboratory, Department of Geosciences, Princeton University, Princeton, NJ; and Ann McNichol, National Ocean Sciences Accelerator Mass Spectrometry Facility, Woods Hole Oceanographic Institute, Woods Hole, MA. key@geo.princeton.edu.

Results from the GEOSECS, TTO and SAVE programmes demonstrated the value of several chemical tracer measurements for the determination of the long-term-mean large-scale ocean circulation, thermocline ventilation, upwelling rates, and air-sea gas exchange. During those programmes, these "exotic" tracers included radiocarbon ($\Delta^{14}C$), tritium (^{3}H), members of the uranium-thorium decay chain (^{222}Rn, ^{226}Ra, ^{228}Ra). and radioactive noble gases (^{39}A and ^{85}Kr). Difficulties of one type or another existed with each of these measurements. $\Delta^{14}C$ measurements required large sample volume (~200 litres), significant at-sea processing, additional laboratory processing, and extended counting time on low-background equipment. ^{3}H measurements by nuclear counting were becoming more difficult with time simply because of decay of the bomb-produced spike and natural dilution of the signal by mixing. The radon and radium isotopes required intermediate to large water volumes (30–200 litres), were extremely labour intensive, and required extraordinary effort to consistently maintain data quality. ^{85}Kr and ^{39}A required large to very large sample volumes (200–1200 litres) and in the case of ^{39}A extremely low background counting equipment and very long counting times.

Given the scope of the WOCE programme, none of these measurements would have been practical without significant technological advances. In the case of radium and radon isotopes and ^{39}A sufficient advances were not made and these tracers were not measured to any large extent during WOCE – the cost to benefit ratio was insufficient. ^{85}Kr measurements were, for all practical purposes, replaced by the much less expensive and nearly routine measurement of CFCs. Both $\Delta^{14}C$ and ^{3}H were measured throughout the WOCE programme. In the case of ^{3}H, the measurement technique was changed from nuclear counting to mass spectrometry. In addition to increasing both sensitivity and precision, this change also allowed the addition of ^{3}H measurements, effectively extending the useful life of this tracer. Additionally, during the latter portion of the WOCE field work, sample extractions were carried out at sea in a specially constructed van. This not only increased sample throughput, but also provided an environment less prone to sample contamination. The greatest technological advances, however, occurred for $\Delta^{14}C$. By switching from nuclear counting to accelerator mass spectrometry, the sample size was reduced by three orders of magnitude to 0.25 litres, shipboard processing was totally eliminated, laboratory processing could be automated, and the per sample analytical cost was reduced, not to mention elimination of the ship cost required to collect the large volume samples. The remainder of this note outlines the technological advances in the measurement of $\Delta^{14}C$ and then briefly demonstrates the resulting potential for scientific information.

Discussion

Prior to WOCE a routine radiocarbon station required two hydro casts of 9 Gerard barrels each and a minimum of 7 hours ship time with at least 2–3 hours between the casts. Maintaining the barrels and their piggyback Niskin bottles was more of an art form than a science (Key et al., 1991) and relatively calm seas and a large ship were required to assure reasonable reliability. A minimum of 3 deck technicians, a crane operator and a winch operator were required to deploy and retrieve the casts. Salinity and frequently nutrient analyses were required from both the Gerard and Niskin to assure sample integrity and frequently, these nutrient results (especially phosphate) were unreliable due to contamination. On deck the samples were transferred to plastic drums, acidified, then gas extracted for up to 5 hours each. The extraction equipment was bulky, extremely fragile and annoyingly loud due to the number of air pumps used. The extracted CO_2 was collected in extremely pure (and expensive) NaOH solution in glass bottles. These solutions were carefully shipped to the laboratory (as hazardous material) where a demanding separation procedure was necessary prior to nuclear b counting. In spite of all, the precision and accuracy of the results were maintained at 2–4‰ over long time periods due to extraordinary diligence at the two primary analytical labs (G. Östlund at U. Miami and M. Stuiver at U. Washington). The greatest hindrance to use of $\Delta^{14}C$ as an oceanographic tracer was that the station separation could not be decreased below ~300 km due to the time, cost and effort involved in sample collection and analysis.

During the mid 1970's accelerator mass spectrometry was demonstrated to be a viable technique for analysing seawater radiocarbon. During the WOCE planning phase (and before) the effort of G. Östlund and others convinced NSF to support the development of a national lab dedicated to oceanographic radiocarbon analysis. Glenn Jones at Woods Hole Oceanographic Institution won the grant competition. Construction of the National Ocean Sciences Accelerator Mass Spectrometry Facility (NOSAMS) began in 1989 and the first WOCE samples were run in 1992 at a precision of ~15-20‰. Reported precision improved dramatically over the next 2 years to an average less than 3‰. At the same time sample throughput increased from a few hundred samples/year to more than 2000/year. Analysis of replicate samples indicates that the overall precision of

the AMS technique is ~4‰. This is within the precision range reported for the large volume b counting technique. To date results of approximately 6200 analyses at 344 stations in the Pacific have been reported to the various principal investigators by NOSAMS and many of these published (Key, 1996; Key et al., 1996). The remainder of the Pacific results will be completed within a year and the Indian and Atlantic Ocean samples approximately 2 years after that. Schematic diagrams, pictures, and explanations of procedural details and equipment used at NOSAMS are all available via the NOSAMS web site (http://ams245.whoi.edu/nosams.html).

During the US Pacific WOCE field work, both large volume and AMS samples were collected. Large volume samples were collected in lower thermocline, deep and bottom waters with an average station spacing of 300 km along many of the WOCE sections. On most cruises AMS samples were collected in surface and upper thermocline waters with an average 100 km station spacing. On a few Pacific cruises and all Indian and Atlantic Ocean cruises sampling was by AMS for the entire water column. In terms of science the real effect of the technological advance in $\Delta^{14}C$ analysis is that it is now possible to collect a significantly higher density data set. This point is clearly demonstrated by the work of Wunsch (1984 and the preceding papers by Broecker et al, 1978) in which he used GEOSECS radiocarbon results in the Atlantic to place constraints on the estimated Equatorial upwelling rate. In Wunsch's words,

> "The major uncertainty in the radiocarbon calculations derives from the sparsity of sampling so that very great extrapolations are required to estimate the zonal mean $\Delta^{14}C$ concentrations and the time histories between the prebomb period and 1972."

Relative to standard hydrographic measurements, the $\Delta^{14}C$ data set will still be sparse even when all of the WOCE measurements are complete, however, Figs. 1 and 2 (see page 25) give some indication of the new potential. Fig. 1 shows a full depth $\Delta^{14}C$ section from WOCE line P17 in the tropical Pacific (cruises P17C and P16S17S). Sampling density along this section is fairly typical for meridional WOCE lines in the Pacific and Indian Oceans. Data from 27 stations was used to make Fig. 1. In the Wunsch analysis, only 8 GEOSECS stations were available for the same latitude range in the entire Atlantic. The solid black dots (primarily in the upper half of the image) indicate samples analysed by the AMS technique while the white squares (primarily in the lower half) were large volume samples. The large volume sample density along this section is roughly the same as during GEOSECS (7 stations) while the AMS density (27 stations) is approximately 4 times higher. The increase in information content provided by the AMS samples is obvious (though not quantified here) in Fig. 1 by the detailed structure in the contours.

Fig. 2 shows an objective map of the $\Delta^{14}C$ distribution at 200 metres for most of the tropical Pacific. The latitude range is the same as in Fig. 1. It would have been fruitless to even attempt making such a map prior to WOCE AMS sampling. Furthermore additional details can be added to such maps when the sample analyses are complete – results from P10, P18 and part of P19 are not final and consequently were not included.

This note has been limited to a very brief description of recent technological changes in the sampling and analysis of $\Delta^{14}C$ and to a very simple graphical illustration of how the science which uses these results will be improved. Key (1997) gave a few other similar examples. The first quantitative applications of the new data set are just now emerging (c.f. Sonnerup et al., 1994; Key et al., 1996b; Ortiz et al., 1997; Peng et al., 1997; Orr et al., 1997; Toggweiler et al., 1997)

Acknowledgements

The success of the US WOCE radiocarbon programme has been dependent upon many people including the PI's P.D. Quay and P. Schlosser, the analytical labs including G. Östlund and staff, M. Stuiver and staff and all of the members of NOSAMS. This work was funded by numerous grants to the authors and all of the those mentioned above by both NSF and NOAA.

References

Broecker, W. S., T.-H. Peng, and M. Stuiver, 1978: An estimate of the upwelling rate of in the equatorial Atlantic based on the distribution of bomb radiocarbon. J. Geophys. Res., 83, 6179–6186.

Key, R. M., D. Muus and J. Wells, 1991: Zen and the art of Gerard barrel maintenance, WOCE Hydrographic Program Office Technical Report.

Key, R.M., 1996: WOCE Pacific Ocean radiocarbon program. Radiocarbon, 38(3), 415–423.

Key, R. M., P. D. Quay, G. A. Jones, A. P. McNichol, K. F. Von Reden and R. J. Schneider, 1996: WOCE AMS Radiocarbon, I: Pacific Ocean results; P6, P16 & P17, Radiocarbon, 38(3), 425–518.

Key, R. M., C. Rooth, G. Östlund and M. Stuiver, 1996b: Ventilation of the Deep Pacific Ocean, AGU/ASLO 1996 Ocean Sciences Meeting, San Diego, CA.

Key, R. M., 1997: Changes in the Pacific Ocean distribution of radiocarbon since GEOSECS. 1997 US WOCE Report, US WOCE Implementation Rep. No. 9, US WOCE Office, College Station, TX.

Orr, J. C., J. L. Sarmiento, E. Maier-Reimer, U. Mikolajewicz, P. Monfray, J. R. Palmer, J. R. Toggweiler, R. M. Key, C. L. Sabine, and N. Gruber, 1997: Anthropogenic CO_2 in the ocean: 3-D models vs. reality. 5th International CO_2 Conference, Cairns.

Ortiz, J. D., A. C. Mix, P. Wheeler and R. M. Key, 1997: An estimate of the anthropogenic offset of oceanic d13CDIC based on the ventilation of the California Current at 42°N. Global Biogeochem. Cycles, submitted.

Peng, T.-H., R. M. Key and H. G. Östlund, 1997: Temporal variations of bomb radiocarbon inventory in the Pacific Ocean. Marine Chem., in press.

Sonnerup, R. E., P. D. Quay, J. L. Bullister, R. M. Key, A. P. McNichol, and G. A. Jones, 1994: Thermocline ventilation rates in the North Pacific. Am. Geophys. Union Conf., San Francisco, CA.

Toggweiler, J. R., B. Samuels, and R. M. Key, 1997: Why is the deep water around Antarctica so old?, in Ewing Symposium Monograph, Tucson, AZ, submitted.

Wunsch, C., 1984: An estimate of the upwelling rate in the Equatorial Atlantic based on the distribution of bomb radiocarbon and quasi-geostrophic dynamics. J. Geophys. Res., 89, 7971–7978.

Advances in Tracer Measurement

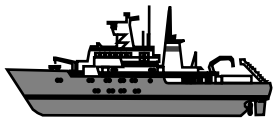

Wolfgang Roether, Alfred Putzka, Klaus Bulsiewicz, Gerd Fraas, Olaf Klatt, Wilfried Plep, Christine Rüth, and Bjoern Schlenker, Universität Bremen, Germany. crueth@physik.uni-bremen.de

Among the various technical developments that accompanied our routine tracer measurements during WOCE (CFCs, helium isotopes/neon, tritium), we here report on CFC measurement and on a novel way to collect helium samples.

CFC measurement

Our early CFC measurements used the packed-column gas chromatographic technique of Bullister and Weiss (1988), but in 1992 we embarked upon capillary-column chromatography. The status reached by 1996 will be published shortly (Bulsiewicz et al., 1998). Features of our system are (i) a full automation, (ii) a small and well temperature-controlled trap that at the same time serves to separate low-volatility components so that no pre-column is needed, (iii) a combination of two columns to effect a separation of the critical peaks, and (iv) a replacement of the glass syringes commonly used for water transfer from the sampling bottles by flow-through glass ampoules. The ampoules are easier to handle, and can alternatively be flame-sealed for sample storage. In upcoming field work with Polarstern (ANT XV/4, 1998), however, a different column combination (DB-VRX 0.45 mm/GasPro 0.32 mm) will be used.

Moreover we have recently developed a microtrap (ca. 1/1000 ml packing only, and allowing a temperature rise rate > 40 degrees/s for injection). Placed at the front end of the column, it effects a cryotrapping, enabling us to accommodate columns narrower than used in CFC work so far, with a corresponding gain in resolution. As an example, Fig. 1 shows a chromatogram for a seawater sample using a DB-VRX column of 0.25 mm diameter. The half-height peak widths are near 0.05 min only. For operational use with this system, a combination with a second column is envisaged, like in our present seagoing system.

Note that the chromatogram of Fig. 1 was obtained on a stored Weddell Sea sample collected in 1996 on Polarstern (ANT XIII/4), which demonstrates that we obtain decent chromatograms also for stored samples. In fact, we have begun to collect samples for laboratory CFC measurement routinely. A systematic comparison of ship-borne and laboratory measurements is planned for the mentioned forthcoming Polarstern cruise. This will show whether the compounds of interest are sufficiently stable during storage, which for CCl_4 at the moment looks questionable.

Helium sampling

The classical procedure to obtain helium samples uses storage in copper tubing, sealed by the popular "bang-bang-bang" clamp-off method or by John Lupton's crimper. Before the sample can be admitted into the mass spectrometer, however, a sample preparation step in the laboratory is necessary, which is labour intensive and moreover forces a substantial delay in the actual measurement. To avoid the latter, seagoing sample processing has been developed, and has been employed on various recent WOCE cruises [Lott and Jenkins, this issue]. We had built a somewhat similar seagoing system which was also quite successful. More recently however it occurred to us that it was sufficient to provide a water sample with an appropriate head space. In view of the low helium solubility in water, virtually all the helium collects in the head space, from which it is easily transferred into the mass spectrometer. This consideration led us to search for a way to draw helium samples from the sampling bottles directly into containers providing such a headspace.

The resulting device is sketched in Fig. 2. An evacuated, sealed glass ampoule is attached to a vacuum valve, which was previously connected to the sampling bottle and flushed with the water sample. Now the ampoule seal is broken and the valve is opened to fill the ampoule halfway, whereafter the ampoule is flame-sealed; at this point it is ready to be attached to the mass spectrometer. Ampoules are evacuated prior to a cruise by entering a small amount of water and pumping on the vapour with a rotary pump, which yields non-detectable helium within a few minutes. The end tubing of the ampoules (3 mm or

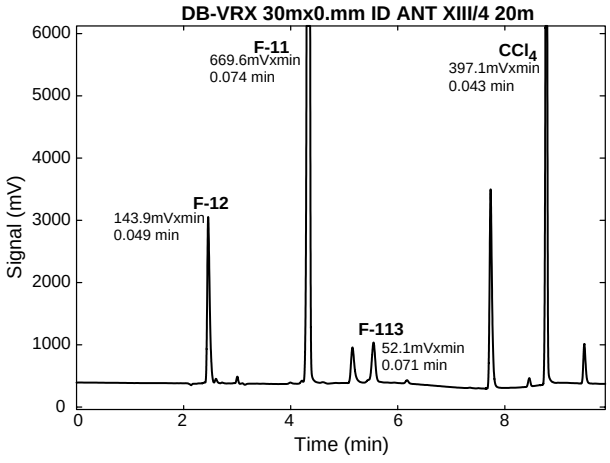

Figure 1. Chromatogram of a stored sample (Weddell Sea cruise ANT XIII/4 of Polarstern, 1996, 20 m depth) measured recently in the laboratory with a system similar to that described by Bulsiewicz et al. (1998), but using a DB-VRX column, 30 m x 0.25 mm diameter, and two-stage trapping (see text). Time is from heating the second trap for injection; due to a severe detector overload, the F-11 peak appears as too broad.

1/8" o.d.) is inserted into two O-ring sealed fittings with off-centre bores (Fig. 2), such that turning the outer fitting breaks the tubing. The volume between ampoule and valve seal is small (0.1 ml), and shaped to avert trapping of air. Soda glass is used for low helium permeability and the ampoules are pre-treated to minimise helium in the glass. Blank samples serve to check for any helium remaining from the evacuation step, or gained prior to measurement thereafter.

Perhaps surprisingly, it has turned out that the ampoules are quite safe to handle also under rough field conditions despite their narrow end tubing. For routine use, the number of ampoule-carrying devices available should match the number of helium samples to be taken from a rosette cast. The new method is less straightforward to apply than the copper procedure(s), but definitely easier than a seagoing extraction, with which is shares the feature of allowing helium measurements to begin as soon as the samples have been received in the laboratory.

Table 1 summarises results from our most recent field test (Meteor M39/3, 1997). Pairs of samples have been taken in clamped-off copper containers and in glass ampoules. Table 1 shows that the blank of the two procedures

Table 1. Comparison between pairs of regular samples ("copper") and ones obtained by the new technique ("vacuum"; 40 pairs total).

	^4He[a]	^4He / Ne[a]	$^3He/^4Ne$[b]
	reproducibility [%][c]		
copper	0.253	0.064	0.210
vacuum	1.190	0.202	0.160
	blank [%][d]		
copper	0.092		
vacuum	0.097		
	difference [%]		
mean difference[e]	-0.386	-0.206	-0.009
standard deviation[f]	0.809	0.205	0.291

a 30 pairs out of 40 (75%)
b 35 pairs out of 40 (88%)
c duplicates and one set of four
d relative to the mean signal of the corresponding water samples
e (cu-va)/cu [%]
f of the differences

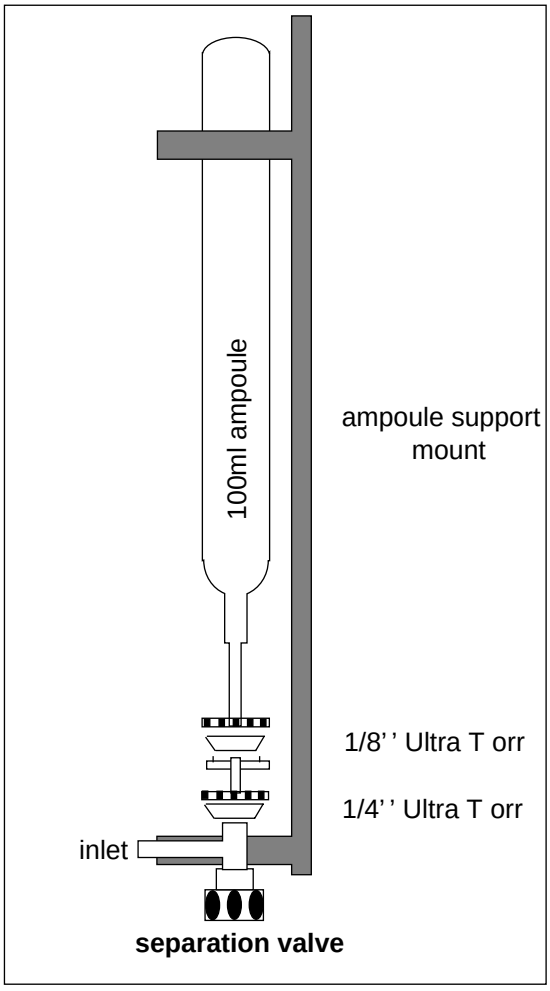

Figure 2. Ampoule-carrying device for helium sampling.

is indistinguishable, and that in the helium isotope and helium to neon ratios (columns 3 and 2) there is virtually no offset and the reproducibilities are similar. Since our interpretation of helium data rests primarily on these two ratios (Roether et al., submitted), we conclude that the new method is capable of giving good data. However, a certain air contamination still exists, which shows up as an offset and a lesser reproducibility in helium concentration for the ampoule samples (Table 1, column 1), even though 25% of the pairs, which showed a large such contamination, were excluded. We have taken measures which we hope will straighten this out.

We plan to use the new technique in a semi-routine fashion during the mentioned forthcoming Polarstern cruise. A final remark is that we are willing to let our gear to helium laboratories interested in the new method.

Acknowledgement

Our WOCE work is supported by the BMBF and the DFG, both Bonn-Bad Godesberg, Germany.

References

Bullister, J. L., and R. F. Weiss, 1988: Determination of CCl_3F and CCl_2F_2 in water and seawater. Deep-Sea Res., 35, 839-853.

Bulsiewicz, K., H. Rose, O. Klatt, A. Putzka, and W. Roether, 1998: A capillary-column chromatographic system for efficient chlorofluorocarbon measurement in ocean waters. J. Geophys. Res. (to be published).

Lott, D. E. and W. J. Jenkins, 1998: Advances in shipboard processing of tritium and helium isotope samples. WOCE Int. Newsletter No. 30.

Roether, W., R. Well, A. Putzka, and C. Rüth, 1998: Component separation of oceanic helium. J. Geophys. Res., submitted.

Exploring WOCE Hydrographic Data with OCEAN-DATA-VIEW

Reiner Schlitzer
Alfred Wegener Institute for Polar and Marine Research
Columbusstrasse, D-27568 Bremerhaven, Germany
(e-mail: rschlitzer@awi-bremerhaven.de)

Summary

OCEAN-DATA-VIEW (ODV) is a software package for the exploration and visualization of oceanographic data on computers running or emulating Windows 95 or Windows NT. ODV together with the currently available WOCE bottle data in ODV format are now available at:

http://www.awi-bremerhaven.de/GPH/ODV/

ODV Features:

- Produces cruise maps, property/property plots, scatter plots, color sections and color surface plots
- Fast data access and dense storage format
- Easy import of new data (WOCE, NODC SD2 & WOA94 formats accepted)
- Automatic calculation of derived quantities (pre-coded or user macros)
- Hardcopy output on any printer; GIF and PostScript output supported

Cruise maps

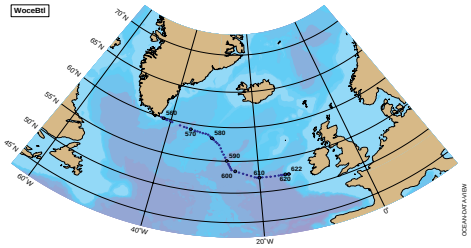

Property/property plots of selected stations

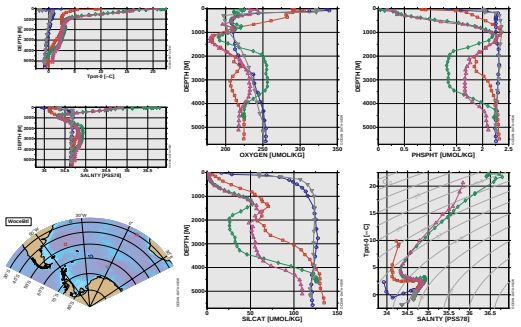

Scatter plots of all stations

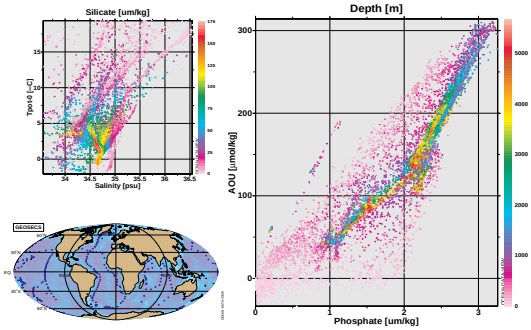

Property sections along arbitrary cruise tracks

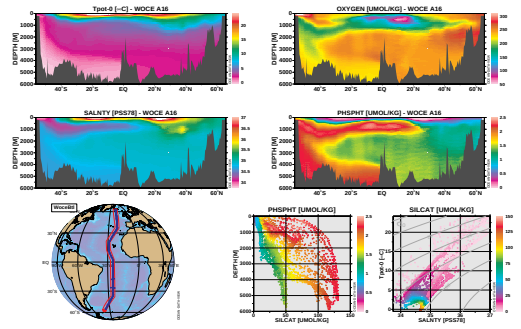

Property distributions on iso-surfaces

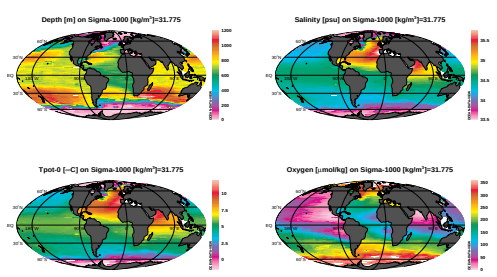

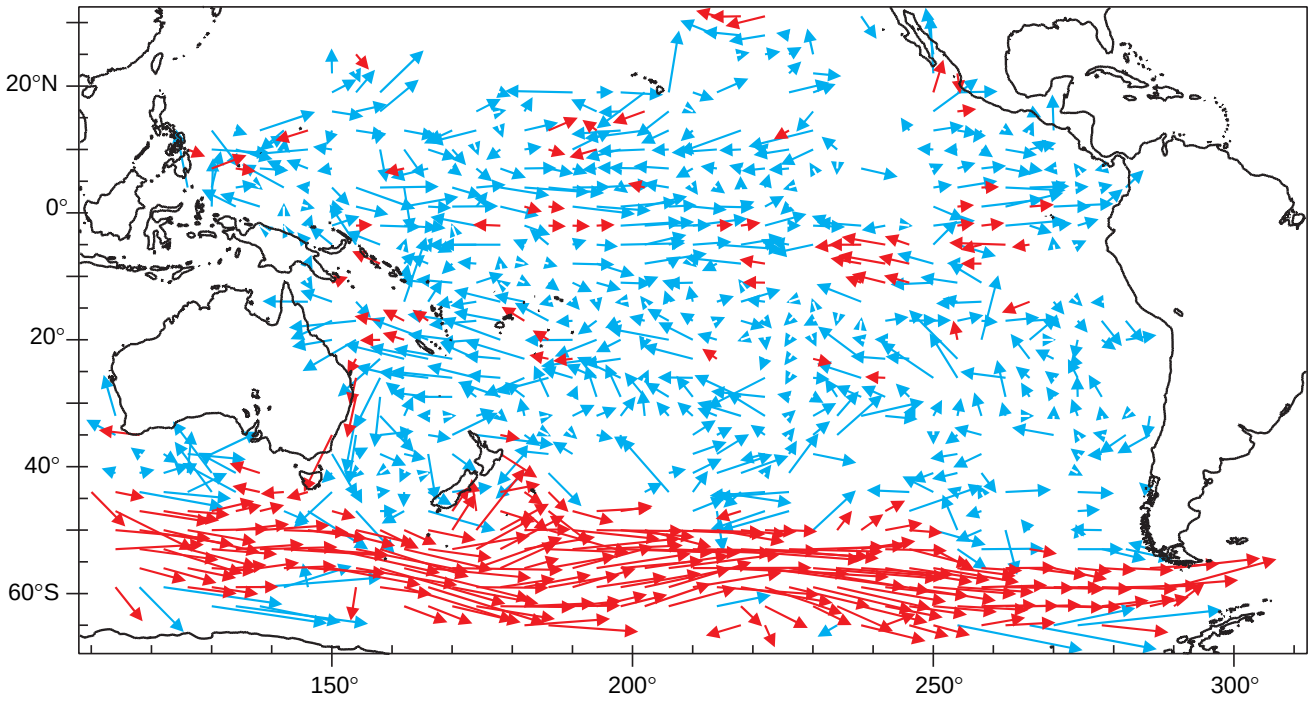

Davis, page 3, *Figure 1. Space-time average velocities at 900 m deduced from 760 float years of ALACE observations. Average velocities are plotted as displacements over specified time periods. Blue arrows show displacement a float would experience over 800 days moving at the mean velocity. Red arrows describe mean velocities with magnitudes greater than 1.5 km/day as displacements over 200 days moving with the mean velocity.*

Kennan, et al., page 7, *Figure 2. Photograph of the SVP surface float deployed in calm seas. The upward protrusion is a barometer port; the pair of raised circles on the facing side of the float are submergence sensors.*

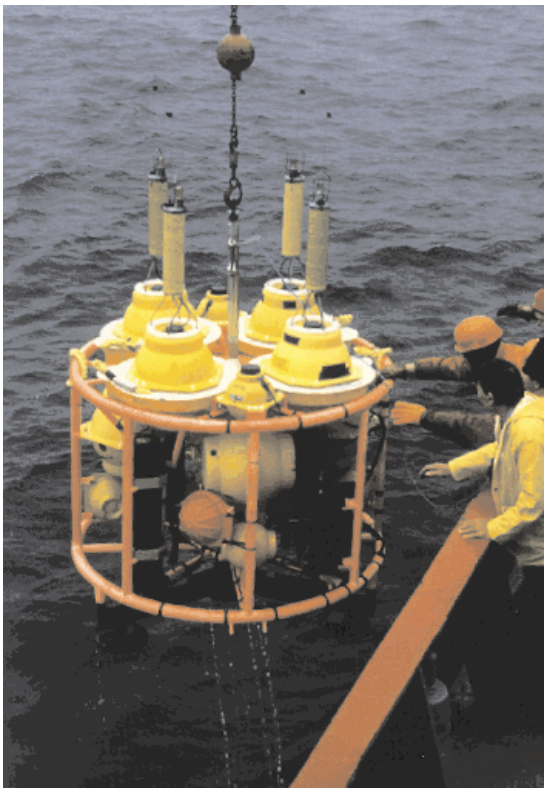

Vassie et al., page 14, *Figure 2. MYRTLE (Multi Year Return Tide Level Equipment). This instrument is capable of 5 years continuous operation at depths to 6000 m. The measured pressure variations near the sea bed are returned by releasable data capsules annually.*

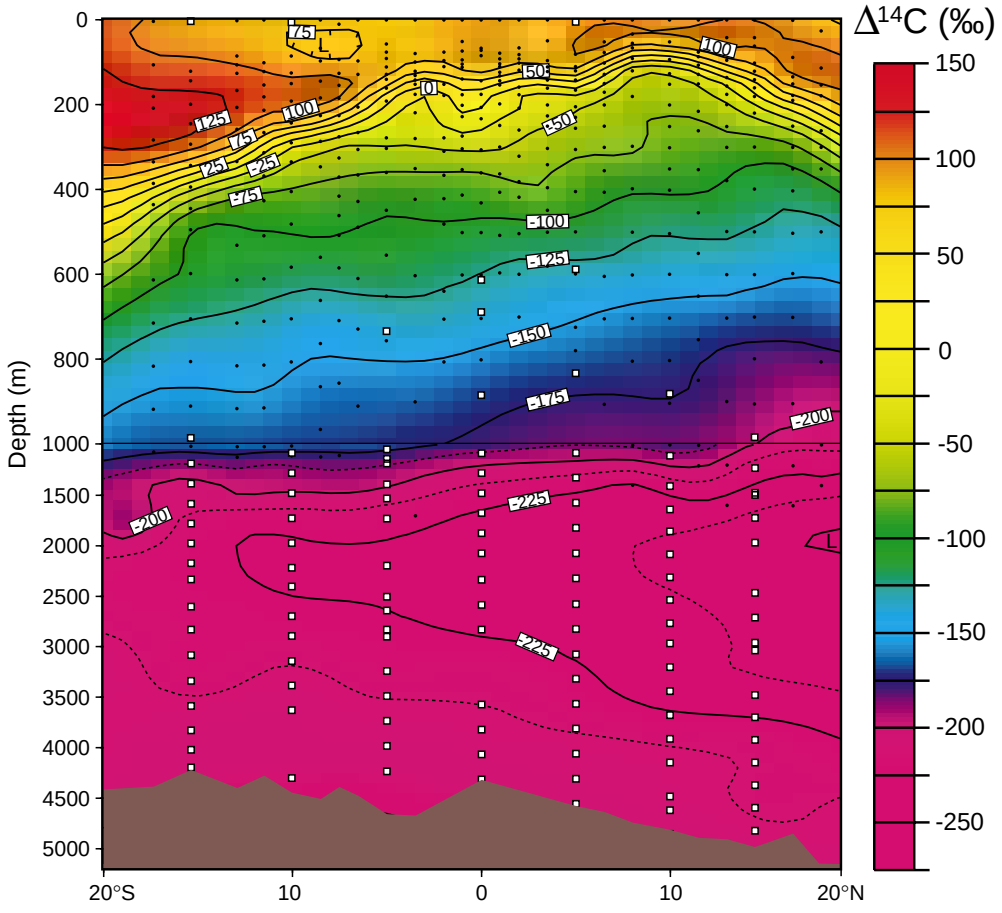

Key, et al., page 19, *Figure 1. Full depth section of* $\Delta^{14}C$ *along 135°W (WOCE section P17) in the tropical Pacific. The solid dots indicate samples that were analyzed by the AMS technique and the white squares large volume samples analyzed by the traditional* b *counting technique. The contour lines and colours carry the same information.*

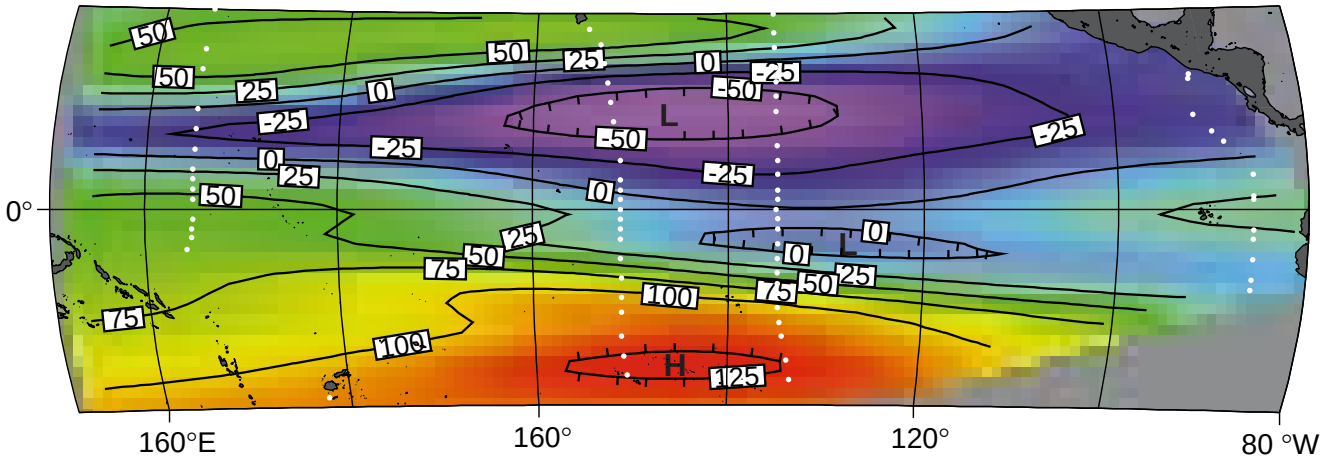

Key, et al., page 19, *Figure 2. Objective map of the* $\Delta^{14}C$ *distribution at 200 metres in the tropical Pacific. The 75 stations used for this map are from WOCE sections P13, P16, P17 and P19. Additional results will soon be available from sections P10, P18 and P19. Once those data are available we will be able to generate maps with significantly less smoothing than shown here (shorter correlation length scales in the x dimension).*

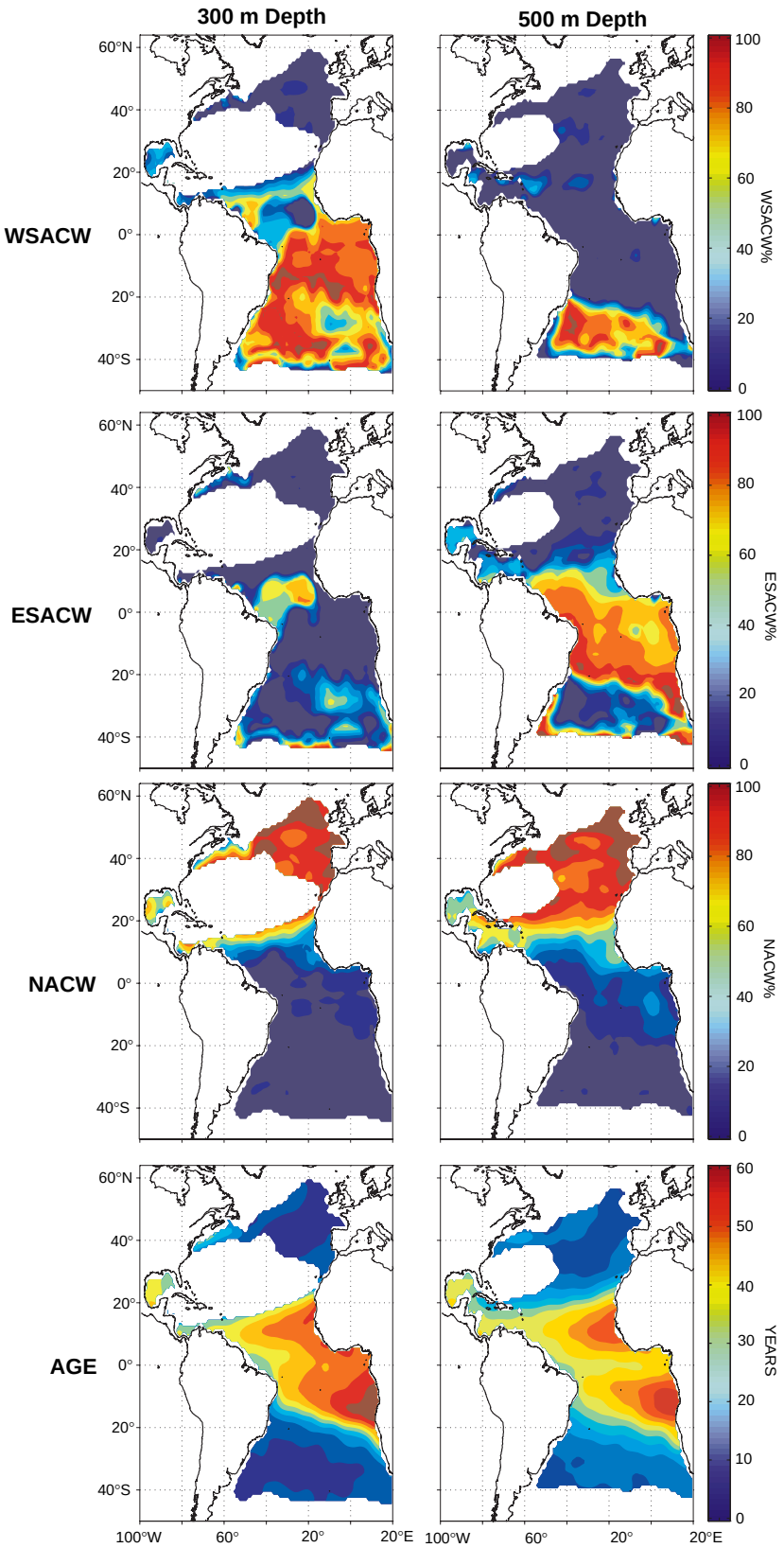

Tomczak, page 43, Figure 1. *The distribution of water masses in the Atlantic Ocean at 300 m (left) and 500 m (right), derived from optimum multiparameter analysis. WSACW: Western South Atlantic Central Water, ESACW: Eastern South Atlantic Central Water, NACW: North Atlantic Central Water, Age: uncalibrated pseudo-age identifying "shadow zones" of old water and well ventilated regions. Southern and northern limits are defined by the subtropical fronts. The solution conserves mass within 5% everywhere except in the uncoloured region in the northern hemisphere where no results are shown.*

Advances in Analysis and Shipboard Processing of Tritium and Helium Samples

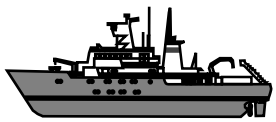

D.E. Lott, III, and W. J. Jenkins, Woods Hole Oceanographic Institution, Woods Hole, USA. wjenkins@whoi.edu

The World Ocean Circulation Experiment (WOCE) one-time hydrographic survey was aimed at the characterisation of the global distributions of properties for the purposes of describing and quantifying the large scale mean circulation and ventilation of the world's oceans. Our role in WOCE was to determine distributions of tritium, ^{3}He and the light noble gases (He and Ne). The large number of samples demanded a substantial increase in analytical capability, which is limited by both measurement throughput and sample handling capacity. Advances in automation and cryogenic techniques (e.g., Lott and Jenkins, 1984) have dramatically improved the former, but the latter had not changed substantially since the days of GEOSECS, nearly a quarter of a century before.

It immediately became clear that at-sea sample processing would be required. Once a water sample is obtained from a Niskin bottle, the gases must be extracted from the water and stored in aluminosilicate glass ampoules in preparation for mass spectrometric analysis of helium isotopes and neon. Additionally, water must be degassed and stored in aluminosilicate glass flasks for incubation and measurement of tritium by ^{3}He regrowth (e.g., see Clarke et al., 1976). Prior to WOCE, water samples were stored in clamped copper-tube samplers for He-Ne analysis, and argon-filled glass bottles for tritium analysis, both of which were shipped back for shore-based processing. For this programme, we developed a system which enabled the ship-board extraction of helium and neon from sea water samples, and the degassing of samples for ^{3}He regrowth measurement of tritium. This reduced the risk of contamination and sample loss, while speeding up the sample processing programme, reducing the amount of shore-based effort, and advancing the initiation of the tritium incubation period. The net result was more efficient processing and more reliable, better quality results.

The at-sea sample processing system

The sample processing system consisted of a self-contained 20 ft × 8 ft laboratory van which was shipped to the port of departure and mounted on the ship's deck. The van contained two vacuum systems, attendant instrumentation and computer control systems, a sink, drawers, cabinets and bench-top work-space. It required a single phase electrical source, compressed air, and fresh water supply, all of which were supplied through a common interface panel. In addition, a modest amount of crushed ice was required for sample extraction. No additional cryogens were required.

Separate water samples were drawn for tritium and helium from Niskin bottles through tygon tubing into valved, stainless steel sampling cylinders. On return to the van, the sample details were entered into a computer data base for tracking purposes. The sample cylinders were attached to their respective processing lines. There were two lines, a degassing line for tritium samples and an extraction line for helium/neon samples. These systems are described in more detail below. The samples are processed on the vacuum systems under computer control, and bar-code labels are automatically generated for glass ampoules or flasks containing the processed gas or water samples.

Helium and neon extraction

Sample cylinders were constructed from lengths of type 316 stainless steel tubing welded to custom-made diameter reducers and o-ring sealed plug valves on either end (see Fig. 1). The plug valves (Nupro SS-4P4T-3571) were modified by drilling a 0.094 in hole through the plug into the "bore" to permit cleaning and pumping out the bore while the sample was isolated within the cylinder. After connecting to the Niskin bottle with tygon tubing, the cylinder was flushed with several volumes of sample water from the Niskin, while the valves were repeatedly rotated to release air trapped in the valve bores and pump-out holes. Also, the cylinder was rapped sharply with a wooden "bat" to loosen any adhered bubbles during transfer. Once a bubble-free water stream was achieved, the cylinders were closed and disconnected from the Niskin and tubing. The salt water was immediately shaken out of the cylinder ends, and the ends were then flushed with fresh water and rinsed with isopropynol and allowed to air-dry.

The system consisted of eight identical extraction sections (Fig. 1, eight samples were processed at a time) attached to a pumping manifold which was evacuated through a cryogenic trap using first a rotary mechanical pump (Varian SD-200) and ultimately using an oil-based diffusion pump (Varian HS-2). The diffusion pump was backed by another rotary mechanical pump, and cooled using a closed-system water + ethylene glycol recirculation loop (Neslab CFT-33). The cryogenic trap was held at roughly -130°C using a PolyCold (P-75) refrigeration system. Vacuum pressure was measured by convection and ion gauges which were monitored by computer. The cryotrap was routinely warmed up and accumulated water removed after 25-50 extractions.

When an adequate vacuum pressure was achieved (less than 3×10^{-7} torr), indicating the lack of significant vacuum leaks, beakers of water with crushed ice were mounted to cool the glass ampoules. Then the sections were isolated from the pumping manifold and the water was allowed to drain into the reservoirs by opening the cylinder valves. 100 watt heaters, which were clamped to the bottom

of the reservoirs, were then turned on. After a few minutes, when the water temperature rose above a critical value, water transfer to the ampoule commenced. Boiling of the water sample, aided by stainless steel "boiling chips" effectively stripped dissolved gases from the water sample, and the water vapour transfer quantitatively swept the gases into the ampoule. The constant vapour stream prevented back-streaming of accumulated gas through the capillary back into the system. Over the course of the extraction, several grammes of water would be transferred, and a significant water transfer rate was observable by the downward deflection of the accumulating water's surface. After 10 minutes (from the time the heater was turned on) the sample was sealed off by applying a glass blowing torch to the capillary. The samples were subsequently labelled and stored, and the vacuum sections removed, rinsed with fresh water and isopropynol and dried using a compressed air flow. With care, and barring significant problems, extractions could be done at a rate of approximately one every two hours.

Through extensive experimentation, using prototype systems attached directly to a mass spectrometer, we established that quantitative (>99.8%) extraction was achieved with this procedure. One consideration, however, was the potential for compromise of the water sample due to diffusion through the polymer seals during storage in the sample cylinder. We performed a series of tests by storing degassed water in these sample cylinders for various periods

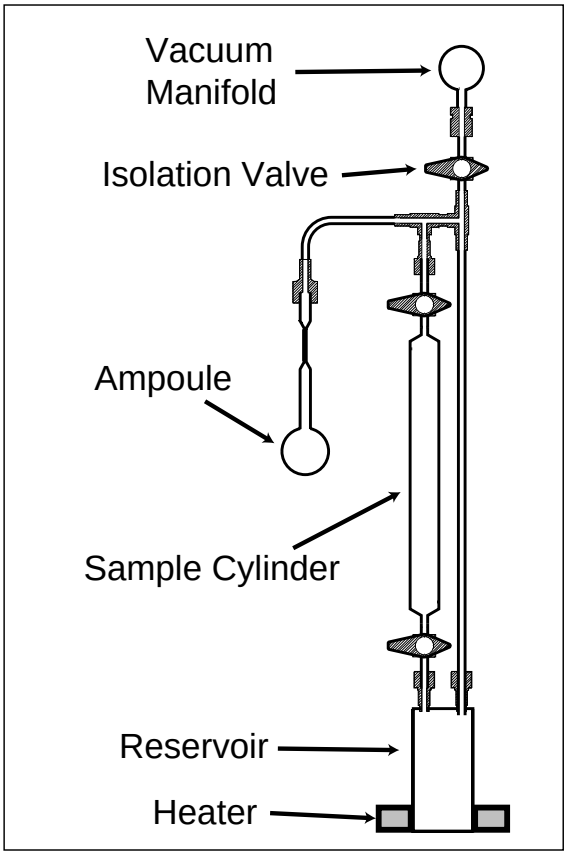

Figure 1. Extraction line section schematic.

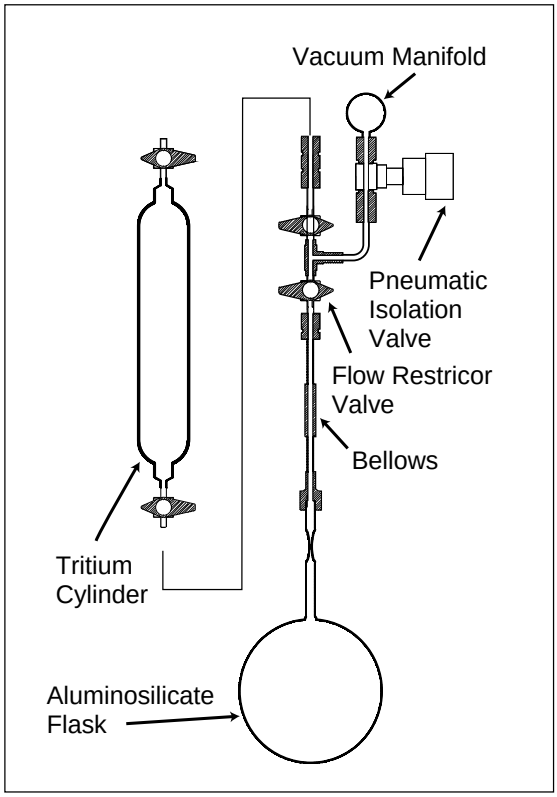

Figure 2. Degassing line section schematic.

of time. The observed rate of He increase in the cylinders was 0.019 0.003% per hour. Thus a sample of Pacific deep water, with a helium isotope ratio anomaly of 30%, stored for about 12 hours (typically the maximum that we stored samples at sea) would have its isotope ratio lowered by only about one half our analytical uncertainty, and could in principle be corrected since we tracked sample acquisition and processing times. For neon, the rate of contamination was much lower, being 0.004 0.002% per hour. Inasmuch as dissolved neon concentrations rarely departed from equilibrium more than a few percent, the corresponding errors were infinitesimal.

Tritium sample degassing

Prior to drawing water samples from the Niskin bottle, the tritium (500 cc) cylinders were dried and filled to a slight positive pressure with dry argon. Immediately prior to connecting the tygon tubing to the Niskin, the lower valve was opened, venting the argon through the tubing to displace ambient air. The cylinders were flushed with about two volumes of sample water, while the valves were actuated and the cylinder was rapped to remove adhering bubbles. After disconnecting, the cylinder ends were rinsed and dried prior to attaching to the degassing line. During this process the exposure of the water sample to ambient water vapour was minimised due to the risk of contamination. In particular, extreme care was used to avoid contact with devices (e.g., luminous dial watches) containing tritiated materials.

The degassing line (Fig. 2) consisted of six sections

which are evacuated by a vacuum manifold virtually identical to that of the extraction system. The cryotrap was "cleaned" much more frequently, usually after every third degassing because water accumulation was much greater for degassings. This was due to the much longer pumping times and large volumes of water involved.

The samples were introduced into the 1 litre aluminosilicate glass storage ampoules after isolating the vacuum section from the pumping manifold. After the sample was drained into the flask, the isolation valve below the cylinder was closed so that the cylinder could be removed for cleaning and drying while the degassing proceeded. The capillary valve was turned to restrict water vapour loss, and the sample was initially pumped to remove the bulk of head space gases released by ex-solution during introduction into the flask.

Degassing of water samples for ^{3}He in-growth measurement of tritium required that at least 99.9995% of the normally dissolved helium was removed from the water sample. This was accomplished by repeated cycles of shaking (15 minutes) and pumping (2 minutes). Pumping was accomplished in the first three cycles with the mechanical vacuum pump, and by using a diffusion pump in the last two cycles. The pressure surges associated with pumping was measured via computer using convection and ion gauges to monitor degassing progress, and to alert the operator to leaks. Experiments indicated that 97–98% of the dissolved He was released into the head-space during the shaking cycle, and that the efficiency of its removal (from the head space) during pumping was much greater. Thus five shake and pump cycles, not including the initial degassing accomplished during introduction, in principle resulted in a minimum of 99.9999% degassing.

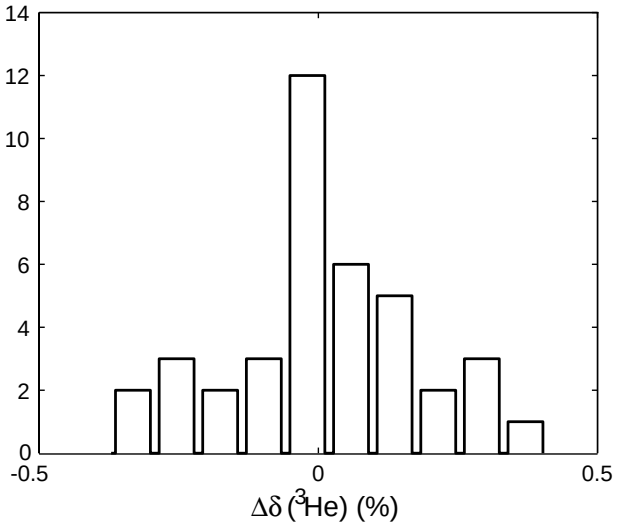

Figure 3. Histogram of helium isotope ratio anomaly differences between replicate samples.

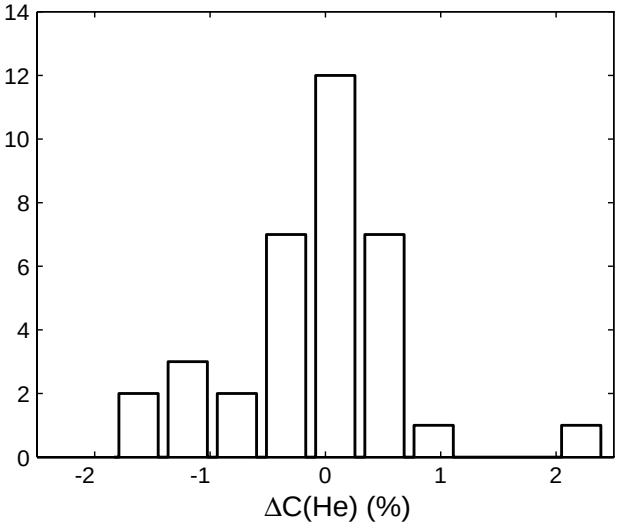

Figure 4. Histogram of helium concentration differences between replicate samples.

Mass spectrometry

Helium isotope ratios were measured in a statically operated, π/2 magnetic sector, dual-collecting mass spectrometer with cryogenic processing (e.g., see Lott and Jenkins, 1984) against a reference air standard. A slight dependence of measured isotopic ratio size was monitored using isotopically identical standards of varying size, and the results corrected for this effect. The corrections were generally no more than about one s (i.e., within measurement error). Measurement precision, as determined by reproducibility of secondary vs. running standards, and reproducibility of running standards ranged from 0.10 to 0.13% in $\delta(^3\mathrm{He})$, depending on the cruise. Systematic errors in the running air standard, as deduced by repeated comparisons with independent air standards, is less than 0.05%. Measurement reproducibility, based on replicate pairs of samples, as determined by the RMS difference between replicates (see Fig. 3) divided by $\sqrt{2}$, is 0.12%. The replicate $\delta(^3\mathrm{He})$ differences are not statistically correlated with concentration differences, suggesting that bubble trapping during sampling and that any artefacts due to sample extraction are not significant contributors to isotope ratio anomaly errors. In addition, we obtained 3 groups of quadruplicate samples (helium samples drawn in quadruplicate from the same Niskin bottle). Measurement standard deviations for these three experiments averaged to 0.08%. In summary, measurement precision for the helium isotopic ratio was better than the stipulated WOCE requirement of 0.15% of analysis.

Helium concentrations were determined by ion current manometer, referenced to accurately determined aliquots of the reference air. The air standards were compared to multiple secondary gas standards at regular intervals and some adjustments made to bring the two into agreement. Replicate water sample reproducibility indicates an uncertainty in the dissolved gas concentrations of order 0.54% (Fig. 4), significantly larger than mass spectrometric analytical errors, but close to the WOCE target specifications for those measurements (0.5%). Mass spectrometric measurement uncertainties were of order 0.1%, with systematic uncertainties around 0.1% associated with

running standard calibration. We attribute the larger errors to sample handling, in particular the probable inclusion of trapped small air bubbles during sampling. The reproducibility is identical for *both* helium and neon, despite the fact that the gases are measured on two separate mass spectrometers: the He is measured on the branch-tube, magnetic sector instrument, while the Ne is measured using a quadrupole mass spectrometer. In addition, the ΔHe and ΔNe differences were highly correlated, with a slope statistically indistinguishable from air addition. Thus the variability is clearly due to the inadvertent addition of air (in the form of trapped bubbles either in the barrel of the sample cylinders or swept in from the tygon tubing). This additional air is automatically corrected for in the computation of the excess ^{3}He so that it does not add any significant error to the excess ^{3}He results.

Tritium was measured using the standard ^{3}He regrowth technique (e.g., Clarke et al., 1976; Jenkins, 1981; Jenkins et al., 1983). On return from sea, the degassed samples were stored in a shielded area (under 4 m of concrete) for at least one year, and the tritiugenic ^{3}He harvested for mass spectrometric analysis. During storage, a significant amount of ^{3}He can be generated by cosmic ray spallation of oxygen nuclei in the sample. In an unshielded sample stored at sea level, 43°N latitude, this production of ^{3}He results in an *apparent* tritium concentration of approximately 0.020 T.U. It should be noted that this is an apparent concentration, not an actual tritium contamination. Because of the shielding the production rate experienced by our samples is much smaller, generally around 0.002 T.U. However, because our at-sea degassed samples spend part of their time in a less-sheltered environment, some additional contribution due to cosmogenic ^{3}He production will "inflate" the blank level tritium measurements. The effect, which presents itself as a non-zero blank tritium determination, varies with the *ratio* of time spent in the exposed state to the total storage time. We monitored this cosmogenic interference by obtaining, processing and analysing almost 200 tritium samples that were "known" from hydrographic and radiocarbon measurements to be tritium-free. The mean cosmogenic blank effect is 2.1 ±0.3 mTU (1 mTU = 0.001 TU) for all but one of the WOCE Pacific cruises (P21), which had an observed blank of 6.1 ±0.6 mTU due to extended exposure during shipboard storage and surface shipping. We can correct the data for the cosmogenic interference blank to an accuracy better than 1 mTU (0.001 TU).

On the mass spectrometer, running-standards were cross-compared with external standards to an accuracy of order 0.1%, with systematic uncertainties of the same order. Measurement uncertainties were dominated by ion counting statistics, and vary with sample size, tritium concentration, incubation time, and other extraneous factors. Whereas for very small tritium concentrations the measurement uncertainty was close to the detection limit (1–2 mTU), the uncertainty increases with tritium concentration to as much as 7–10 mTU for the largest tritium concentrations (1–3 TU), which corresponds to an uncertainty of 0.5%. These are calculated on an individual basis, and reported with the tritium data.

References

Clarke, W. B., W. J. Jenkins, and Z. Top, 1976: Determination of tritium by mass spectrometric measurement of ^{3}He. Int. J. Applied Radioisotopes, 27, 515.

Jenkins, W. J., 1981: Mass spectrometric measurement of tritium and ^{3}He. In: Low Level Tritium Measurement. Proc. Consult. Group Meeting on Low-Level Tritium Measurement. Organised by International Atomic Energy Agency, Vienna, 24–28 September, 1979.

Jenkins, W. J., D. E. Lott, M. W. Pratt, and R. D. Boudreau, 1983: Anthropogenic tritium in South Atlantic bottom water. Nature, 305, 45–46.

Jenkins, W.J., 1996: Tritium and 3He in the WOCE Pacific Programme. International WOCE Newsletter 23, 6–8.

Lott, D.E., and W.J. Jenkins, 1984: An automated cryogenic charcoal trap system for helium isotope mass spectrometry. Rev. Scientific Instruments, 55(12), 1982–1988.

Satellite Datasets for Ocean Research

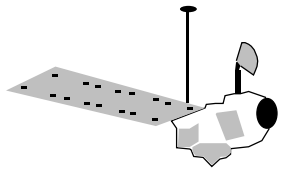

Victor Zlotnicki, Jet Propulsion Laboratory, Pasadena, CA 91109, USA.
vz@pacific.jpl.nasa.gov

The purpose of this overview is to make the reader aware of various satellite datasets currently available for ocean research. If you had a WOCE drifter in the water, knowing the surface temperature field, or the surface geostrophic current field through which it moved, or actual observations of the wind field (as opposed to atmospheric model output, especially in the southern oceans), and knowing the accuracy of these auxiliary observations, all would enhance the analysis and allow you to ask different classes of questions from the combined dataset. Satellite datasets exist, they are reasonably accurate, quite accessible, and relatively easy to use; their great advantage is global, fast coverage. The main ones are explained below. Although many future satellite missions are in various stages of preparation, they are barely mentioned here: the emphasis is on existing, reasonably well understood datasets that can be used together with already collected WOCE in-situ observations. The author's opinion as to their usability and accuracy are also included.

Sea level

Sea level is being measured by altimeters on board TOPEX/POSEIDON and ERS-2.

TOPEX/POSEIDON, a joint effort between the US space agency, NASA, and the French space agency, CNES, has been sampling the global oceans once every 10 days since October 1992, and proven to be the most accurate global sea level observing system ever deployed (Fu et al., 1994; see also http://ibis.grdl.noaa.gov/SAT/hist/tp_gauge/index.html). Even so, G. Mitchum's careful analyses of the difference between T/P sea level and selected tide gauge observations (Mitchum, 1997, J. Atm. Oceanic Tech, under review; Nerem et al., 1997), as well as a discrepancy between the two altimeters on board the satellite, pinpointed an error of the order of 6 mm/yr in an onboard algorithm to correct for clock drift, and more recently, a 1.5 mm/yr drift caused by the passive radiometer (used to measure water vapour, needed for a path correction). This was a powerful reminder of the need to combine satellite and in-situ observations knowledgeably, as well as an indication of the level of accuracy (mm/yr!) achieved, despite the nominal 130 mm single-pass accuracy NASA and CNES had promised the T/P Science Team.

Data from T/P come in three flavours: MGDR (Merged Geophysical Data Records), alongtrack residuals, and uniform space-time grids. MGDRs are the official deliverables of NASA and CNES; they contain observations, approximately once per second along the satellite track, of time, satellite horizontal position, height, altimeter range, a host of altimeter path corrections, tidal models, geoid model, and various flags. They are available at no charge from CNES's AVISO, http://alti.cnes.fr (192.134.216.41), or from NASA's PO.DAAC, http://podaac.jpl.nasa.gov. The volume is approximately 600 MB/month. Although these data contain everything needed to do oceanography, experience shows that many oceanographers prefer to use the alongtrack residuals, a smaller, more manageable dataset (about 3 MB/month), produced by a trusted colleague. Various groups share their alongtrack residuals, but two such products are widely available: the residuals produced by P.Y. leTraon and colleagues at CLS-Argos, in Toulouse, France, and distributed by AVISO (http://www-aviso.cls.cnes.fr), and those produced by C. Koblinsky and colleagues at Goddard Space Flight Center (http://neptune.gsfc.nasa.gov/ocean.html). Space-time gridded products are usually tailored for a particular use, hence many oceanographers shun them, but they provide an excellent quick look at the data to decide on the next steps of analysis. D. Chambers, at U. of Texas-Austin has produced an especially popular set (http://ftp.csr.utexas.edu), as has R. Cheney and colleagues at NOAA (http://ibis.grdl.noaa.gov/SAT/SAT.html). Cheney's team also produces a near-real time product; they have shown that the use of a short-arc GPS orbits computed at Jet Propulsion Laboratory, the IGDRs (Interim GDRs) generated by the T/P project, and a residual orbit adjustment technique by C.-K. Tai, can yield sea level with around 5 cm accuracy level, not as good as the final GDR's accuracy, but very useful nonetheless. NOAA's model to forecast seasonal to interannual climate variations used it as a key dataset to correctly forecast the 1997 ENSO event last April.

The accuracy of the T/P MGDR-derived sea level is around 3 cm for a one second (about 6 km) average; efforts to ascertain whether the slope of a time series of 10-day averages can be determined to better than 1 mm/yr are underway (Nerem et al., 1997).

ERS-2 is a mission of the European Space Agency, ESA. ERS-2 has been measuring sea level globally once every 35 days since mid May 1995. Its predecessor, ERS-1, had collected sea level since late December 1991 (it is still 'alive' but not transmitting data). In both cases, the satellite was launched earlier, but the date given here is the beginning of the usable sea level record. In the case of ERS-1, however, the orbit was changed several times, each called a 'phase'. For altimetric use, the phase changes mean that data from two different phases cannot be used in the familiar colinear analysis, whereby sea level along a groundtrack today is subtracted from sea level along the same groundtrack at some past time, yielding the change in sea level between the two times all along the groundtrack, and cancelling out the much larger geoid signal present in the data. One is forced to use crossover differences to study a long time series, the crossover points being relatively few and far between. ERS-1 has undergone several algorithm changes with time, so the usability of its data is more restricted, and apparent changes in sea level with time need to be carefully separated from algorithm changes and from orbit error (the ERS-1 main tracking device, PRARE, failed shortly after its launch). Both ERS satellites are in sun-synchronous orbit.

A separate issue related to data from ERS-2 and 1 is ESA's data policy. In principle, only ESA-approved investigators can receive ERS data free of charge, and they are not to redistribute the data (http://earthnet.esrin.esa.it/). In practice, for altimetry this has not been much of an obstacle, as the data have very limited commercial value. The ERS-1 and ERS-2 data have been carefully processed by IFREMER (http://www.ifremer.fr/cersat/english) and GDR data are available from them; IFREMER may help requesters satisfy ESA's data policy. At this writing, ESA has issued a new Announcement of Opportunity for the Exploitation of ERS data, with a 1 February 1998 deadline for submissions (http://esa-ao.org). Successful respondents would have access to needed data. Two groups share their alongtrack residuals from ERS: CLS-Argos, in Toulouse, France, distributed by CNES's AVISO, and C. Koblinsky and colleagues at Goddard Space Flight Center, at the addresses listed above in relation to similar TOPEX/POSEIDON datasets. However, because of the different phases of ERS-1, 2, only a subset of the ERS altimetry data is available in 'alongtrack residual' form.

Space-time gridded products from ERS-2 altimetry are available from ESA's Operations Center, in Darmstadt, Germany, in image form (http://nng.esoc.esa.de/ers/

alti.html).

The altimeters that measure sea level also measure significant wave height over their 6–12 km footprint and wind speed (but not direction). In addition, both T/P and ERS-2 measure water vapour to perform an altimetric correction. These data, especially the wave height, although not as widely used as the primary sea level measurement, can be useful in some investigations.

Sea surface temperature

SST has been measured operationally with the AVHRR instrument (Advanced Very High Resolution Radiometer) on board the NOAA-N series of satellites since 1981 (Kidwell, 1991). There are three main global SST products: MCSST, Reynolds, and Pathfinder SST.

The MCSST product (Multichannel Sea Surface Temperature) is named after the algorithm (McClain et al., 1985) used to derive temperature from the four infrared and one visible channel; it is produced operationally by NOAA. The coefficients of this algorithm are changed from time to time to adapt to changing atmospheric conditions and instruments, by re-fitting the observed brightness temperatures to in-situ data (Kidwell, 1991). Because AVHRR is a passive instrument which senses radiation naturally emitted by the environment, radiation transmitted to it by clouds generally preclude the computation of sea surface temperature (radar altimeters and scatterometers are active instruments: they transmit electromagnetic energy and receive it back after it interacts with the environment). In a typical week, a large fraction of the ocean surface does not have a usable MCSST retrieval. The basic MCSST and a version that fills all gaps by interpolation, both in weekly, 8 km composites, are available from http://podaac.jpl.nasa.gov.

The Reynolds product (Reynolds and Smith, 1994, 1995) uses an objective mapping algorithm to combine the MCSST retrievals with in-situ sea surface temperature observations, to produce a highly-regarded, well-calibrated, weekly, 1 degree product. It is available at ftp://nic.fb4.noaa.gov/pub/ocean/clim1/oisst.

AVHRR Pathfinder is named after an early 1990s NASA program that funded the reprocessing of certain satellite datasets of interest in climate (there is also a Land AVHRR Pathfinder product). With improvements to the MCSST algorithms based on the work of Brown et al. (1993), a large database of in-situ observations, and work by R. Evans and colleagues, the Pathfinder SST increased both the accuracy in the recovery of SST and the number of valid values; it also provides a uniform time series, with a single algorithm and a single scheme to estimate the coefficients for data from 1985 to the present. The current scheme recomputes a different set of coefficients to relate the observables to SST once per month, from 5 months worth of data. This product is available as two global daily grids, one for local daytime samples and one for local nighttime samples, on an approximately 8 km grid as well as coarser grids, from http://podaac.jpl.nasa.gov. This site allows the user to subset the data geographically and by time, view images and ftp digital data.

None of the MCSST, Reynolds, or Pathfinder SST products models the effects of aerosols, or departures of atmospheric profiles from the averages assumed in algorithms (R. Evans, 1997, pers. comm.) nor do they use independent estimates of water vapour to correct for its attenuation (Emery et al., 1994). As a consequence, the real accuracy of the retrieval depends on local atmospheric conditions.

AVHRR data are transmitted from the satellite to the ground in two modes: (1) HRPT (or LAC) is a 1 km high-resolution mode, which is not buffered onboard but transmitted continuously and can be captured by any specialised antenna within 'view' of the satellite transmitter; (2) GAC (Global Area Coverage) is a 4 km low resolution mode recorded onboard, and the global recording transmitted to NOAA ground stations. The three global products just described all derive from the GAC transmission. In addition to those global products, there are many local SST products derived from the HRPT transmission, held by various academic and other groups (e.g., Scripps Satellite Facility) all over the world, and processed with possibly different software.

The ERS-2 satellite, and its predecessor, ERS-1, also carry a passive, infrared radiometer, ATSR (AlongTrack Scanning Radiometer). These data have not yet been widely used, so their accuracy is less well understood. A special session of the American Geophysical Union Meeting of December 1997 is devoted to an intercomparison of sea surface temperature products and a discussion of their accuracies.

Winds

The ERS-1 and 2 satellites carry a radar scatterometer, an active microwave instrument designed to measure wind speed and direction; they have provided an almost continuous, global, record of wind data since 1992. NSCAT, also a scatterometer, measured wind vectors over the global oceans between October 1996 and June 1997. A third observation of wind between 1987 and now is obtained by combining the wind speed data from the SSM/I instrument with a direction from an atmospheric model.

The NSCAT instrument, a K-band (14 GHz) NASA scatterometer, was flown on the ADEOS satellite of the Japanese space agency, NASDA. NSCAT sampled 95% of the ice-free global oceans once every 3 days with 25 or 50 km 'wind vector cell' resolution. The mission terminated 30 June 1997, when the satellite's solar panel failed. The accuracy of the data was the greater of 2 m/s or 10% in speed, and 20° in direction. NASA's PO-DAAC (http://podaac.jpl.nasa.gov) distributes the data. The main product is a GDR-type of product, with alongtrack samples of wind, radar cross-section, and other variables, at about 1 GB/week. A reduced GDR, with only time, position, and wind is also available.

The ERS-2 scatterometer, operating in C-band (5.3 GHz) shares the same basic electronics with the Synthetic Aperture Radar (SAR; the combined instrument is called AMI); as a consequence when the SAR is turned on (over ice, land and occasionally over oceans) there are no wind measurements. In addition, AMI-wind has antennas to only one side of the satellite. These issues combine so a global sample of winds is measured in 4 or 5 days. The ERS scatterometer's nominal accuracy is similar to NSCAT's (see also, Beaudoin et al., 1996). IFREMER (http://www.ifremer.fr/cersat/english) distributes both a GDR-like product, and a set of space-time gridded estimates of wind speed and direction, divergence, stress and curl, on a 1 degree by 1 week grid; the volume is about 10 MB/month. The issues of data policy discussed for the ERS altimeter data also apply here.

The passive radiometer SSM/I (Special Sensor Microwave Imager) aboard the US Air Force's DMSP (Defense Meteorological Satellite Program) satellite series measures water vapour, wind speed, and more crudely sea surface temperature and rain. The data have been carefully processed and calibrated by F. Wentz (Wentz, 1997) into 25 km samples of wind speed without wind direction. R. Atlas and colleagues take the Wentz SSM/I wind speeds, and combine them with a background wind vector field from an atmospheric model plus scattered ship and buoy observation, and minimisation constraints on the smoothness in space and time of the resulting field, using a Variational Analysis scheme (VAM). The resulting datasets include the alongtrack, 25 km samples with their assigned directions, as well uniformly gridded 2°-latitude, 2.5° longitude, and 6 hrs or 5 day or 30 day averages. The data exist between July 1987 and December 1996, over the global oceans within ±78 degrees latitude. They are available from PO-DAAC (http://podaac.jpl.nasa.gov).

Water vapour

Although typically oceanographers have not used water vapour data much, it is a very useful quantity, especially at low latitudes. ENSO (El Niño-Southern Oscillation) events always show strong correlations between anomalies in sea surface temperature, sea level, wind and water vapour (e.g., Liu et al., 1996). The same DMSP SSM/I series of instruments mentioned in the context of winds, has measured vertically integrated water vapour since 1987. Again, the best data products come from F. Wentz (Wentz, 1997) and are available from his company (http://www.ssmi.com). Various NASA centres also distribute parts of Wentz's product.

Ocean colour

Ocean 'colour', the amount of energy radiated in various visible bands, is due to the concentration of chlorophyll and other plant pigments, and can be used to infer the abundance of plankton and 'primary productivity' (e.g., Hood, 1995; Frouin and Pinker, 1995). It is especially useful in coastal and equatorial regions, where upwelling brings nutrients to the surface. NASA's SeaWiFS (Sea-viewing Wide Field-of-view Sensor) has been collecting data since August 1997. NASDA's ADEOS satellite also measured colour with its OCTS instrument between October 1996 and June 1997. SeaWIFS is a NASA instrument on a commercial satellite. SeaWIFS, like the AVHRR instruments, measures in a higher resolution mode, LAC, which is broadcast continuously and can be captured for local data by HRPT stations around the globe, and a lower resolution global model, GAC, whose data are saved onboard and downloaded over selected NASA stations for processing at Goddard Space Flight Center. HRPT access to LAC data must be purchased from the satellite operator, except for select stations which NASA already contracted for. If the oceans were cloud-free, SeaWIFS would sample each square kilometre of ocean every 48 hours. The processed GAC data are available from the SeaWIFS project and the Goddard SFC DAAC, at http://seawifs.gsfc.nasa.gov/SEAWIFS.html, where one can see abundant information about the SeaWIFS project, find, view and download images or hdf-formatted digital data, as well as 'explore the world with SeaWiFS at 4 kilometre resolution'.

Future satellites

While the emphasis of this review has been on existing satellite data that can be used in conjunction with WOCE in-situ ocean observations, a few words about future satellite missions is worth adding. The series of infrared AVHRR observations and microwave SSM/I observations will continue for the foreseeable future, as they are operationally useful. Future altimeters: planned for launch in November 1997 is the US Navy's Geosat Follow-on (GFO, see http://gfo.bmpcoe.org/) and for launch in 2000 is Jason, the NASA-CNES follow-on to TOPEX/Poseidon. NASA is scrambling to put a scatterometer in orbit (temporarily dubbed 'Quickscat') over the next 15 months to replace NSCAT; placing a mission in orbit less than 2 years after conceiving it is a very ambitious undertaking. NASA's Seawinds will carry a scatterometer into orbit probably in 2000. Also approved for a 2001 launch is GRACE, a NASA mission to measure the global gravity field to some 200 km resolution, at least once per month; simulations show that it will retrieve ocean bottom pressure, averaged over several hundred kilometres, at least once per month, an intriguing and unprecedented prospect. CHAMP is a European mission to measure earth's gravity and magnetic fields, gravity with lower accuracy than GRACE. Research to measure surface salinity from space is ongoing, but no mission has been approved yet.

Footnote

GFO was successfully launched on 10 February 1998. See: http://www.orbit.com/OSC/Press_Releases/pr26.html

References

Beaudoin, P. T., Legler, D. M., Obrien, J. J., 1996: Information-content in the ERS-1 3-day repeat orbit scatterometer winds over the North Pacific from January through March 1992. M. Weath. Rev., v124 (4): pp583–601.

Brown J. W., O. B. Brown, and R. H. Evans, 1993: Calibration of AVHRR infrared channels: A new approach to non-linear correction. J. Geo. Res. O., 98 (nc10), 18257–18268.

Emery, W., Y. Yu, and G. Wick, 1994: Correcting infrared satellite estimates of sea surface temperature for atmospheric water vapor attenuation. J. Geo. Res. O., 99 (c3), 5219–5236.

Frouin, R., and R. T. Pinker, 1995: Estimating photosynthetically active radiation (PAR) at the earth's surface from satellite-observations. Remote Sen. E., V51 (1): pp98–107.

Fu, L.-L., E. J. Christensen, C. Yamarone, M. Lefebvre, Y. Menard, M. Dorrer, and P. Escudier, 1994: TOPEX/POSEIDON mission overview. J. Geo. Res. O., 99 (c12), 24369–24381.

Hood, R. R., 1995: Light response of phytoplankton in the South-Atlantic Ocean: Interpretation of observations and application to remote-sensing. J. Geo. Res. O., v100 (c6): pp10927–10942.

Kidwell, K., 1991: NOAA Polar Orbiter User's Guide. NCDC/NESDIS, Tech. Report, available from National Climatic Data Center, Washington, DC.

Liu, W. T., W.Q. Tang, and R. Atlas, 1996: Responses of the Tropical Pacific to wind forcing as o bserved by spaceborne sensors and simulated by an Ocean General-Circulation Model. J. Geo. Res. O., v101 (c7): pp16345–16359.

McClain, E. P., W. G. Pichel, and C. C. Walton, 1985: Comparative performance of AVHRR-based multichannel sea surface temperatures. J. Geo. Res. O., 90, c6, 11587–11601.

McMillin, L. M., and D. S. Crosby, 1984: Theory and validation of the multiple window sea surface temperature technique. J. Geo. Res. O., 89(c3), 3655–3661.

Nerem, R.S., B. J. Haines, J. Hendricks, J-F. Minster, G. Mitchum et al., 1997: Improved determination of global mean sea-level variations using TOPEX/POSEIDON altimeter data. Geophys. Res. L., v24 (11): pp1331–1334.

Reynolds, R. W., and T. S. Smith, 1994: Improved global sea surface temperature analyses. J. Climate, 7, 929–948.

Reynolds, R. W., and T. M. Smith, 1995: A high resolution global sea surface temperature climatology. J. Climate, 8, 1571–1583.

Wentz, F.J., 1997: A well-calibrated ocean algorithm for special sensor microwaver/imager. J. Geo. Res. O., 102 (c4), pp8703-8718.

Subsurface Float Tracking and Processing Using the ARTOA and ARPRO Packages

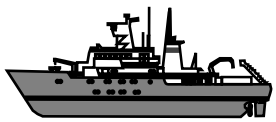

Michael Sparrow, AINCO-Interocean, Spain; Martin Menzel, Laboratoire de Physique des Océans, France; Vassilis Zervakis, National Centre for Marine Research, Greece; and Alán Cantos-Figuerola, AINCO-Interocean, Spain.
Martin.Menzel@ifremer.fr

One only has to visit the float data archive at Woods Hole (http://wfdac.whoi.edu) to appreciate how much the use of subsurface floats has increased over the last few years. The large number of ongoing float projects and amount of unreleased data assures that the data available will increase hugely over the next years. Much of this data now consists of RAFOS (e.g. Rossby et al., 1986) and its French cousin Marvor (e.g. Ollitraut et al., 1994) floats which have now replaced the older and more bulkier SOFAR floats. This article presents two new software packages, which are freely available to the scientific community, for the tracking and processing of subsurface float data. The first section deals with the tracking software and the second with the software developed to process the data.

Float tracking

Marvor and RAFOS floats are tracked by triangulation of distances between the floats and moored sound sources (SoSo's). At regular intervals (e.g. once every 24 hours) each SoSo emits a characteristic signal. The float records the time taken for particular sound signals to travel from the SoSo's to the float (the Time of Arrival – TOA). Knowing the speed of sound in the area the TOA can be converted into a distance between the SoSo and the float. Depending on the float type, additional information such as temperature, pressure and salinity are also recorded.

Tracking the floats is no easy task. This is due to several factors: variations in the speed of sound between the SoSo's; clock drift of the SoSo's, and the floats and problems with background noise and deviations of the SoSo signals (e.g. because of reflections due to topography). To facilitate the tracking procedure, Matlab4 routines were developed by Martin Menzel at the Institut für Meereskunde Kiel supervised by Walter Zenk, Olaf Boebel and Claudia Schmid. The first version of the tracking software supported RAFOS floats only and consisted of two separate programmes, ARTOA and ARTRK. (Both names were taken with the permission of Tom Rossby from float tracking programmes used by the University of Rhode Island). This version of the software was updated by Claudia Schmid and is currently the version compatible with the ARPRO processing software (see Part 2). Heather Hunt from the WHOI has also updated ARTOA and ARTRK to Matlab5.

ARTOA II is a more advanced Matlab5 based float tracking programme combining graphical data selection and tracking into one programme. This development aims

to ease the tracking process by assisting the user from the initial data selection to the production of a final trajectory. The programme can process floats with an unlimited number of listening windows, TOA's per window and SoSo's.

The programme consists of two main modules. A selection module assists the user in assigning the TOA's to the most likely SoSo's and examining other available data such as pressure and temperature. TOA data may be selected graphically using different selection criteria such as single value (selecting each TOA individually and assigning it to a SoSo), polygon region (as before, but for a group of TOA's) or semi-automatic selection (where an algorithm selects the data automatically based on different boundary conditions). The programme gives visual assistance in two ways. Firstly, at the beginning and end of each float cycle or mission, the known TOA's associated with each SoSo are plotted. Additionally, all TOA's recorded by the float are colour coded according to the correlation height (a measurement for the reception quality) of the respective TOA.

Once the TOA's have been assigned to SoSo's, one can calculate the trajectory in the tracking module. The programme supports, amongst others, a least square tracking algorithm allowing the use of an unlimited number of SoSo's to calculate the trajectory. Due to the aforementioned uncertainties some alterations may be necessary. The programme allows the user to alter the sound speed or offsets for each SoSo and float to obtain a more accurate trajectory. Once calculated, the trajectory is plotted over previously calculated trajectories in order to compare different combinations of parameters. By comparing the float trajectories obtained by the combination of different parameters, one can obtain the most accurate estimate of the float's path.

ARTOA II is still under development. One of the next steps will be to update the code to include features of the new Matlab5 in order to have a common base for further programming. Further information concerning ARTOA II can be found at the Eurofloat Web Site listed at the end of this article.

Processing the float data

ARPRO consists of a series of Matlab4 subroutines originally developed at AINCO-Interocean by Vassilis Zervakis and updated by Mike Sparrow. The software allows the visualisation and analysis of float data as well as calculating a variety of statistical parameters. The software was designed to process float data from the EUROFLOAT project, and therefore to be run in conjunction with the ARTRK and ARTOA programmes described in Part 1. ARPRO is currently being modified to read data from the Woods Hole float data archive and will be updated to run with the new ARTOA II programme.

ARPRO allows the processing of float data in two ways, either by examining individual floats or by analysing a group of floats.

Examining individual floats

The number of position fixes per day of the float can be specified in the initial options before a float is loaded (the default is one position fix per day). Once loaded, the data can be low-passed (in order, for example, to minimise tidal influences). Three types of filters are provided – Boxcar, Triangle and Hanning with filter lengths of 3–7 points, though these options can easily be changed.

The programme allows the examination of temperature and pressure records of the float (low-passed or raw). This is helpful in ascertaining whether, for example, a particular float crosses a water mass boundary or changes depth. The user can zoom into particularly interesting sections of the temperature or pressure plots by using the left and right mouse buttons.

It is sometimes useful to consider the ratio between the non-linear and Coriolis terms, known as the Rossby Number. In ARPRO the Rossby number can be plotted on polar or Cartesian co-ordinates. Additionally, a summary of individual floats may be obtained. This option plots the track of the current float and the temperature and pressure along the float's path (including bathymetry if required).

Analysing a group of floats

The utility for examining a group of floats plots the float trajectories on a map. Options for bathymetry, and colour or black and white maps are included in the programme. Being able to watch a movie of float trajectories is useful in demonstrations, or for ascertaining a more accurate flow pattern. As with the map plotting option, colour or black and white figures are produced.

The data can be processed using several types of statistical analyses. One of these is an examination of the Kinetic Energy Spectra in which both log-log and energy conserving spectra can be plotted, with the option of producing rotary spectra. ARPRO allows the user to calculate Eulerian velocities (mean, perturbation and r.m.s) and simple Taylor (Lagrangian) statistics (Taylor, 1921), such as Integral Time (T) and Length Scales and eddy diffusivities as well as their associated errors (see, for example Davis (1991) and Kraus and Böning (1987) for a full description of the statistics).

In this programme, the desired map limits, grid size etc. are specified. If Eulerian velocities are required (and the data density is reasonably high) a small grid size may be used. If Lagrangian statistics are required then a larger grid size should be used as the statistics need a large number of observations in each grid box. Vectors are drawn from the centre of each grid box representing the mean Eulerian velocity.

In ARPRO, T can be calculated by the method of "autocorrelation" (e.g. Spall et al., 1993) or by "structure function" (e.g. Kraus and Böning, 1987). Alternatively, the user may 'force' a value of T (this can be useful if, for example, you wish to find the error of the velocities of one float but using a previously calculated value). The statistical results and their associated errors are then calculated

automatically and the results written to a file.

During processing it is straightforward to return to the Matlab command window and continue processing. This allows the user to modify the data interactively whilst running ARPRO. For the moment ARPRO has coastline and bathymetry files for the Mediterranean, North East and North West Atlantic and the South Atlantic, though additional data can quite easily be included.

Both the ARTOA programmes and ARPRO are freely available. Any feedback, comments or ideas for further developments are welcome. When you think you've added a feature that might be of interest to the rest of the float community let us know in order to integrate it into one of the updated versions.

Contact Addresses

ARTRK and ARTOA (Matlab4.2):
cschmid@ifm.uni-kiel.de
ARTOA II (Matlab5.0):
mmenzel@ifremer.fr
http://www.ifremer.fr/lpo/eurofloat
ARPRO (Matlab4.2):
mike.sparrow@ainco.es
http://www.ainco.es/ainco

Acknowledgements

We would like to thank the following people who have all made contributions to this work: Walter Zenk, Olaf Boebel, Claudia Schmid, Chris Wooding, Breck Owens, Roger Goldschmith, Heather Hunt, Tom Rossby, Sandy Fontana, Yves Auffret and Loïc Gourmelen. This work was funded under the MAST II programme EUROFLOAT (contract MAS2CT940103) coordinated by John Gould.

References

Davis, R.E., 1991: Observing the general circulation with floats. Deep-Sea Res., 38, 531–571.
Krauss, W., and C. W. Böning, 1987: Lagrangian properties of eddy fields in the northern North Atlantic as deduced from satellite-tracked buoys. J. Marine. Res., 45, 259–291.
Ollitraut, M., G. Loaëc and D. Dumortier, 1994: MARVOR: a multicycle RAFOS float. Sea Technology Vol. 35, No. 2, 39–44.
Rossby, T., D. Dorson and J. Fontaine, 1986: The RAFOS system. J. Atmospheric and Oceanic Tech., 3, 672–679.
Spall, M. A., P. L. Richardson and J. Price, 1993: Advection and eddy mixing in the Mediterranean salt tongue. J. Marine. Res., 51, 797–818.
Taylor, G. T., 1921: Diffusion by continuous movement. Proc. London Math. Soc. Ser. A, 20, 196–221.

An Assimilation of Historical Observations of Temperature Profiles into an Ocean Model

M. J. Bell and L. S. Gregorious, Ocean Applications, Meteorological Office, Bracknell, UK. mjbell@meto.gov.uk

The FOAM (Forecasting Ocean Atmosphere Model) group at the Met. Office has developed a system for assimilating observations of temperature profiles of the upper 1000 m of the ocean into the ocean component of the Unified Model (Alves et al., 1995). This system interleaves analysis steps, which nudge the model towards the observations, with the forward timesteps of the ocean model and can be used to assimilate very large numbers of observations. A climatology has been produced by assimilating all the 6,000,000 observations of temperature profiles made available by Levitus et al. (1994).

Data and methods used

The FOAM $1° \times 1°$ global ocean model used has the same vertical levels as the ocean component of the Hadley Centre Coupled Climate Model, described in an earlier WOCE newsletter (Gordon et al., 1997), and the same physics, except that the Redi scheme and weak horizontal diffusion of tracers is still employed rather than the Gent-McWilliams scheme.

The initial conditions for the integrations were the averages of the December and January potential temperature and salinity fields of Levitus et al. (1994). The integrations were driven as by the monthly climatological surface stresses of Hellerman and Rosenstein (1983) and heat fluxes of Esbensen and Kushnir (1981). The surface temperature was relaxed, with relaxation coefficient of $35\,\mathrm{W\,m^{-2}\,K^{-1}}$, to a version of GISST (the Global Ice and Sea Surface Temperature dataset of Parker et al. 1995). The surface salinity and sea ice depth were also relaxed to climatologies as in Alves et al. (1995).

The observations were taken from the CD ROM distributed by Levitus et al. (1994). Data on standard levels were chosen and re-organised into "pentad" data sets containing all observations made in each 5 day period regardless of the year in which they were made. The depths of observations judged to be XBTs were multiplied by 1.05 and the Levitus gridded mean and root mean square climatologies interpolated in space and time to each observation. Only observations less than 2 standard deviations from the mean which had also passed Levitus' quality control checks were assimilated. The observed differences from the climatology were averaged to the

FOAM model levels and the differences and weights given to these differences extrapolated vertically to fill gaps in the profiles and extend the depth of the profiles (Alves et al., 1995).

The observations were assimilated as in Alves et al. (1995) using the filtered increment scheme of Lorenc (1992). Each observation is used over a 10 day period with the weight decreasing linearly with the absolute difference between the observation and model time to zero when the difference is 5 or more days. The model background and observation are given equal weight so that, in the absence of other observations, the difference between the model and observation at the observation point would be reduced by half after the observation had been used for 10 days. Observation increments are interpolated ("spread") using a forecast error correlation scale of 300 km, except close to the equator where the east-west correlation scale is doubled. In order to avoid disruption to the barotropic streamfunction, observations are only assimilated above 1000 m depth (Bell, 1994).

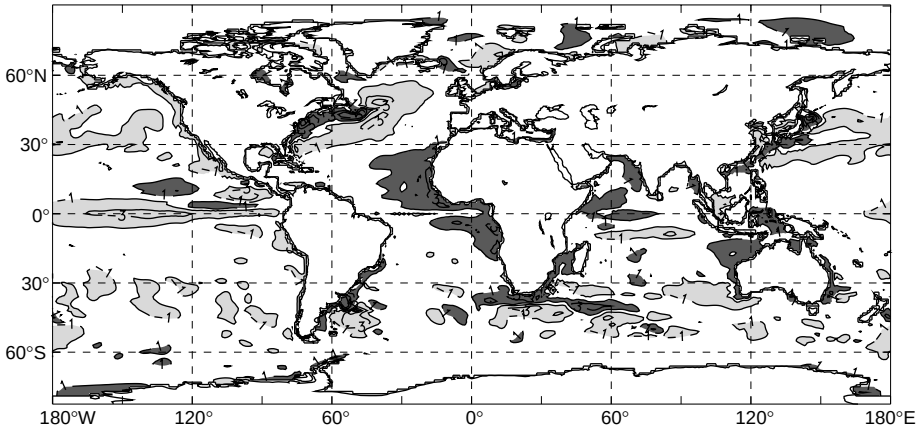

Figure 1. Annual mean global potential temperature (q) at 50 m of control run (year 2) minus Levitus climatology. Contour interval is 2K. Light (dark) shadow indicates q less (greater) than -0.5 (+0.5)K.

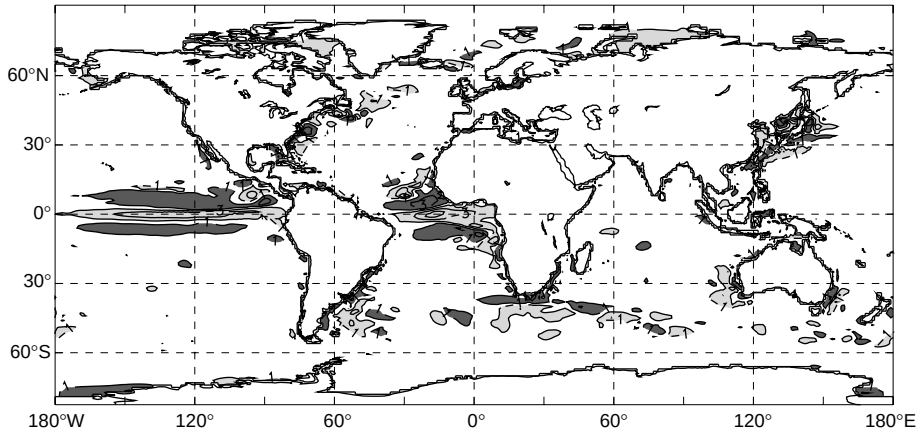

Figure 2. Same as Fig. 1, for assimilation run minus Levitus climatology.

Preliminary results

Two two-year integrations have been performed: an assimilation and a control integration (which did not assimilate thermal profiles). Figs. 1 and 2 display annual mean global fields from the second year of integration at 50 metres depth. Fig. 1 displays the potential temperature q of the control run minus that of the Levitus climatology and Fig. 2 the q field of the assimilation run minus that of the Levitus climatology. The contour interval in both cases is 2 K. Areas where the field is less (greater) than -0.5 (+0.5) K are lightly (darkly) shaded. These fields have been lightly smoothed to aid legibility. Fig. 3 displays the increments made by the analysis system at the same depth during the second year of integration. The contour interval is 1 K per month.

The control run, Fig. 1, has large differences from the Levitus climatology in the Northern Atlantic. The model is warmer along the east coast of the USA, particularly just north of 35°N where the model Gulf Stream does not separate properly from the coast, and colder on the warm side of the Gulf Stream, particularly to the east of the Flemish Cap (47°N, 43°W). Differences between the assimilation and climate in these regions (Fig. 2) are much smaller in magnitude and scale. Fig. 3 shows that the analysis is making increments averaging 3 K per month where the Gulf Stream is failing to separate. Similarly large increments are being made on the Brazilian coast at about 40°S and just north of the Kuroshio separation point.

The assimilation and control runs have large differences from the climatology near the equator in both the east Pacific and Atlantic Oceans (Figs. 1 and 2). On the equator in both the east Pacific and Atlantic the analysis steps are making increments in excess of 3 K per month (Fig. 3). Fig. 4 displays the annual mean meridional structure of the potential temperature field at 155°W for (a) the Levitus climatology, (b) the second year of the control integration and (c) the second year of the assimilation. The meridional variation is clearly weakest in field (a) from Levitus and strongest in field (c) from the assimilation. The variation in the assimilated field is greater than that in the section for April 1979–March 1980 compiled by Wyrtki and Kilonsky (1984). This is unexpected and needs detailed investigation.

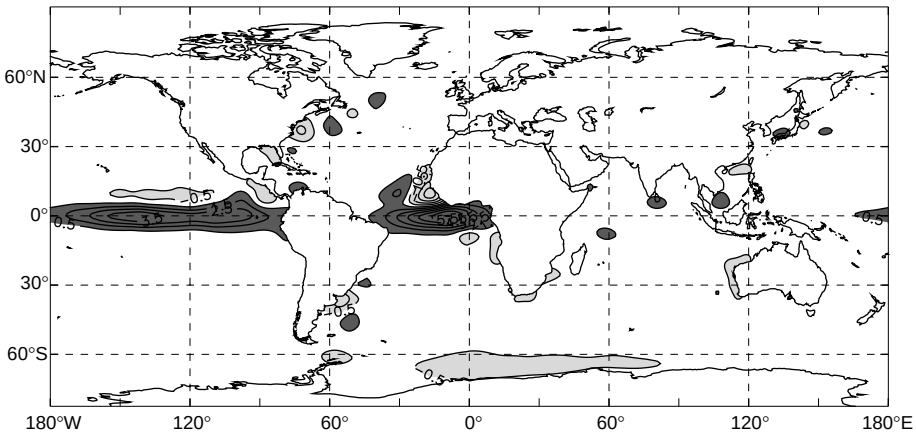

Figure 3. Assimilation increments at 50 m. Contours show K per month.

Discussion

The main aims of the integrations just discussed were to demonstrate their feasibility and to assess their value. The integrations themselves could clearly be improved. In addition to the thermal profiles it would be instructive to assimilate the historical salinity observations. Future integrations could use a coupled atmosphere-ocean model or alternative surface flux climatologies (e.g. those derived by da Silva et al. 1994) to drive the ocean model and include various improvements to the model formulation and the parameters used by the assimilation.

The "climatologies" resulting from assimilation runs could have several advantages over that developed by Levitus. They should have greater temporal consistency (particularly in the southern hemisphere) than Levitus' climatology. They may also have better resolution in the western boundary currents. Finally the model's surface temperature is nudged towards the GISST climatology which is based on far more observations than the Levitus climatology.

There were several other reasons for assimilating these data. The ocean model driven by the available fluxes has significant systematic errors; the discussion of Fig. 3 shows that the thermal increments made during the analysis steps can provide valuable insight into these. The assimilation of the complete historical data set will also serve as a platform for the assimilation of data from particular decades (e.g. the IGY and WOCE datasets).

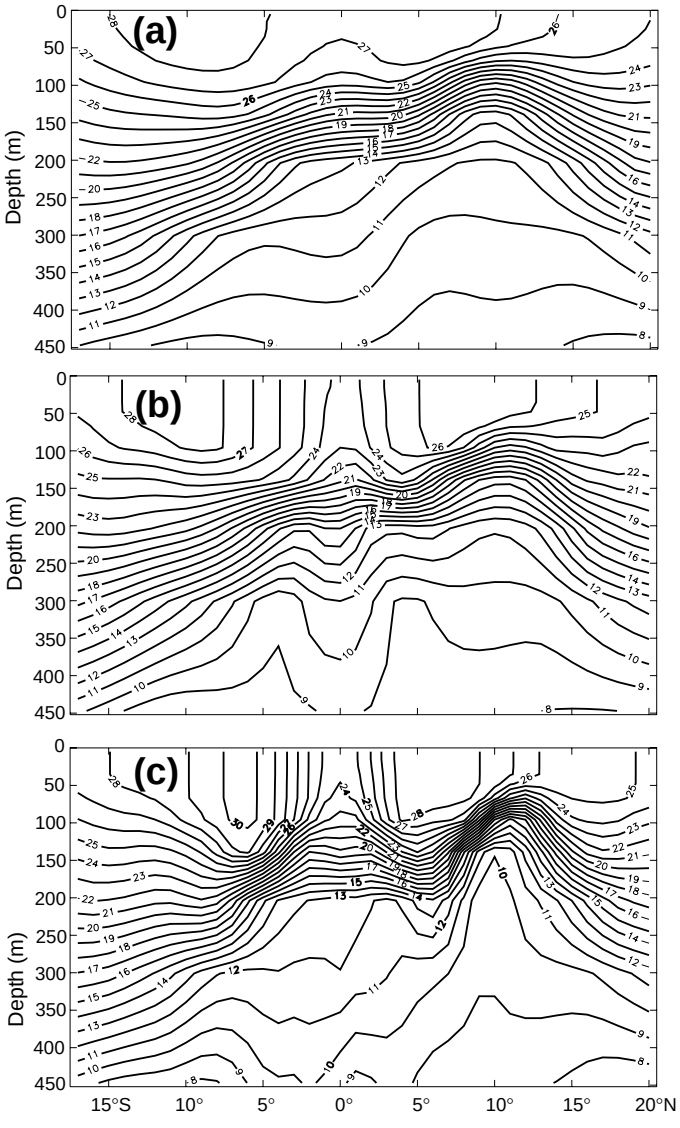

Figure 4. Annual mean meridional cross section of q at 155°W. (a) Levitus climatology, (b) year 2 of control run, (c) year 2 of assimilation run.

References

Alves, J. O. S., M. J. Bell, N. P. J. Brooks, A. L. Cooper, S. J. Foreman, R. M. Forbes, and C. G. Sherlock, 1995: Performance review of the prototype FOAM system. Met. Office Report: FR Tech. Note 159.

Bell, M. J., 1994: Experiments with the assimilation of thermal profiles into a dynamical model of the Atlantic Ocean. Met. Office Report: FR Tech Rep 134.

da Silva, A., C. C. Young, and Levitus, S. 1994: Atlas of surface marine data volumes 1–5. NOAH Atlas Series.

Esbensen, S. K., and Y. Kushnir, 1981: The heat budget of the global ocean: an atlas based on estimates from surface marine observations. Climate Research Institute, Oregon State Univ, Corvallis, Report No. 69.

Gordon, C., C. Cooper, R. Wood, and H. Banks, 1997: The ocean simulation in the Hadley Centre Coupled Climate Model. International WOCE Newsletter, 26, 9–11.
Hellerman, S., and M. Rosenstein, 1983: Normal monthly wind stress over the world ocean with error estimates. J. Phys. Oceanogr. 13, 1093–1104.
Levitus, S., R. Burgett, and T. Boyer, 1994: World ocean atlas 1994. Volume 3: Salinity, and Volume 4: Temperature. NOAH Atlas NESDIS 3 and 4.
Lorenc, A. C., 1992: Iterative analysis using covariance functions and filters. Quart. J. Roy. Met. Soc., 118, 569-591.
Parker, D. E., M. Jackson, and E. B. Horton, 1995: The GISST2.2 sea surface temperature and sea-ice climatology. Met. Office Report: CR Tech Note 63.
Wyrtki, K., and B. Kilonsky, 1984: Mean water and current structure during the Hawaii-to-Tahiti shuttle experiment. J. Phys. Oceanogr., 14, 242–254.

WOCE Floats in the South Atlantic

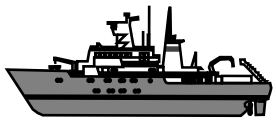

Walter Zenk and Claudia Schmid, Institut für Meereskunde, Kiel, Germany; and Olaf Boebel, University of Cape Town, RSA. wzenk@ifm.uni-kiel.de.

Here we want to summarise the diversity of WOCE float experiments in the South Atlantic. The material for this note was compiled for and presented at the South Atlantic Workshop in Brest (Zenk, 1997a)[1]. Together with a previous overview of ongoing deep Lagrangian observations in the North Atlantic (Zenk, 1997b) we demonstrate the increasing importance of this modern technique in observational oceanography for the exploration of intermediate and deep circulation in the whole Atlantic Ocean.

Lagrangian work in the South Atlantic was initiated by pre-WOCE SOFAR[2] float experiments (Richardson and Schmitz, 1993). Today, aside from their scientific results, SOFAR floats are of historical interest[2]. They have been replaced by RAFOS floats, which utilise the reverse principle of drifting receivers and moored sound sources. In principle, former SOFAR floats continue to exist as moored sound sources within the RAFOS system. In the following years, the South Atlantic was seeded with a diversity of modern float techniques: RAFOS-, MARVOR-, and ALACE-floats have been launched by various institutions.

RAFOS floats, especially if made isopycnal, are currently the instruments that follow their associated water parcels the best. They are designed as single-mission instruments (Rossby et al., 1986), allowing for an eddy resolving tracking by acoustic underwater navigation. Fig. 1 displays the large-scale array of RAFOS sound sources in the South Atlantic, initially co-ordinated by the WOCE float implementation group. The western side is part of the Deep Basin Experiment (DBE) in the Brazil Basin where 19 sound sources served as the base for all seeded RAFOS and MARVOR floats. By the end of 1997 ten sources will insonify the south-eastern part of the subtropical South Atlantic and the neighbouring Agulhas current region.

In contrast to the RAFOS technology, the ALACE float (Davis et al., 1992) features no underwater navigation facilities and hence needs no sound source array. It surfaces at fixed intervals and transmits its data collected during its submersion. Its position is observed by Systeme ARGOS. In addition, the more recently developed PALACE floats

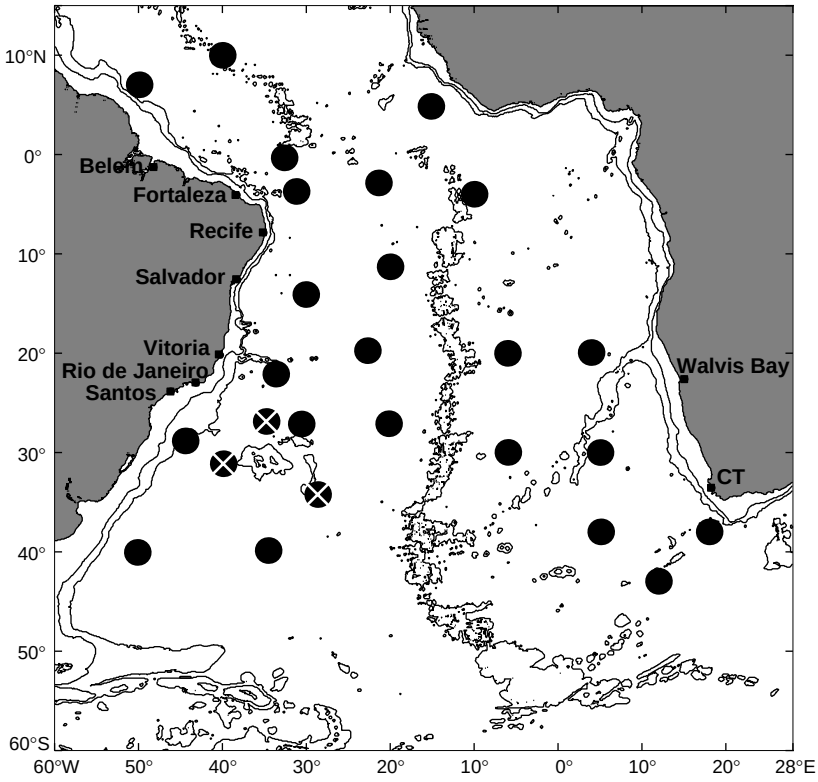

Figure 1. Distribution of WOCE sound sources in the South Atlantic. The array consists of 25 moorings, contributed by WHOI (12), IfM Kiel (9) and IFREMER (4). In the meantime the Kiel array in the south-west has been partially recovered (X) and was redeployed in the Cape Basin as the base for KAPEX (according to Hogg et al., 1996; Boebel et al., 1997b). Status: November 1997.

1. Scientific results of the meeting will be published in a special volume of the J. Geophys. Res. edited by A. Gordon, see web page <http://www.ldeo.columbia.edu/physocean/woce_sai/>.

2. A very informative compendium of the neutrally buoyant float technology by W. J. Gould can be found on the world-wide web under <http:wfdac.whoi.edu/Gould.html>.

Table 1. Compilation of float missions in the South Atlantic. All given quantities originate from the answers of principal investigators. In most cases cited float years are underestimates of the actual results. Mission lengths are based on rather conservative life time estimates according to Table 2. Thick (thin) lines represent approx. 10 (5) floats.

Project Intermediate Water	1989 1990 1991 1992 1993 1994 1995 1996 1997 1998 1999	Region No.	Expected Fl.y
WHOI			
21 SOFAR,800 m nominal		Equatorial band **1**	63
IFREMER			
20 MARVOR 800 m, SAMBA 1	T(z) 60d	Western Brazil Basin **2**	> 60
29 MARVOR 800 m, SAMBA 2	T(z) 90d	Equator Brazil Basin **1,2**	> 87
51 MARVOR 800 m, SAMBA 3 (planned)	T(z) 90d	Equator eastern Brazil Basin **1,2**	> 153
100 MARVOR			> **300**
IfM Kiel			
23 RAFOS AAIW core layer		Rio Grande Rise **3**	6
29 RAFOS AAIW core layer	S(x,y)	Rio Grande Rise **2,3**	> 45
42 RAFOS AAIW core layer	S(x,y)	Equatorial Arg. Basin → **1-4**	> 63
42 RAFOS AAIW core layer	S(x,y)	Southern Cape Basin **6**	> 53
KAPEX			
129 RAFOS			> **167**
WHOI			
30 RAFOS 700 m, (planned)		northern Cape + Angola Basin **6,7**	> 45
SIO			
10 ALACE 750 m	14d	Drake Passage **5**	20
6 ALACE 700 m	T(z) 11d	Drake Passage **5**	> 12
8 ALACE 750 + 1000 m	T(z) 9d	SW Arg. Basin **4**	> 16
10 ALACE 800 + 1000 m	T(z) / S(z) 9d	Central Arg. Basin **4**	> 20
6 ALACE 1000 m	T(z) 10d	SW Arg. Basin **4**	> 12
8 ALACE 1000 m	T(z) / S(z) 10d	S Arg. Basin **4**	> 16
12 ALACE 1000 m, from Pacific.	T(z) / S(z) 26d	Drake Passage **5**	24
60 ALACE			> **120**
Project Deep and Bottom Water			
WHOI			
27 SOFAR 1800 - 3600 m		Equatorial band **1**	81
42 RAFOS 2500 + 4000 m		Eastern Brazil Basin **2**	> 63
53 RAFOS 2500 + 4000 m			> 80
48 RAFOS 2500 + 4000 m			> 72
26 RAFOS 2500 + 4000 m			> 39
169 RAFOS			> **335**
196 RAFOS/SOFAR			
536 Floats		**>> 1030**	

collect temperature profiles. The most advanced version features complete CTD facilities. Due to the ascending and descending period, the original water parcel may be lost, and each cycle can be regarded as an independent velocity measurement.

The MARVOR (Ollitrault et al., 1994) is a hybrid system unifying acoustical tracking of RAFOS floats with cycling properties of the ALACE. It actively controls its mission depth, a property that may or may not be desirable, depending on the specific scientific question to be addressed.

Fig. 2 and Table 1 contain the logistical results from the questionnaires returned. The majority of floats was used or will be sent on missions in intermediate waters (800–1000 m depth) of the tropical and subtropical South Atlantic. Initially these experiments were concentrated in the Brazil Basin where also the only deep RAFOS float (>2500 m) experiment in the South Atlantic took place (see last group in Table 1). In addition to the equatorial SOFAR measurements in the early 1990s, during WOCE primarily RAFOS and MARVOR floats were used roughly between the equator and the Confluence Zone at about 40°S. The region farther south was well sampled by ALACE floats, with the initial batch launched in January 1990 during the first official WHP cruise across Drake Passage from the FS Meteor.

In Table 1 on the left side we find the number of commissioned floats together with their providing laboratories, target depths and other specific details. Launch regions (also reproduced in Fig. 2) and expected float years (Fl.y) are given on the right side of Table 1. In case of cycling floats we also included mission intervals by double

Figure 2. Schematic distribution of regional float experiments in the South Atlantic originally prepared for the WOCE South Atlantic Workshop in Brest, June 1997.

Table 2. Expected minimum life times of South Atlantic float types. In Table 1 we assumed 1.5 y for the averaged mission of RAFOS floats.

ALACE	> 2 y	WOCE
MARVOR	> 3 y	WOCE
RAFOS	> 1 y	WOCE
SOFAR	> 3 y	pre-WOCE

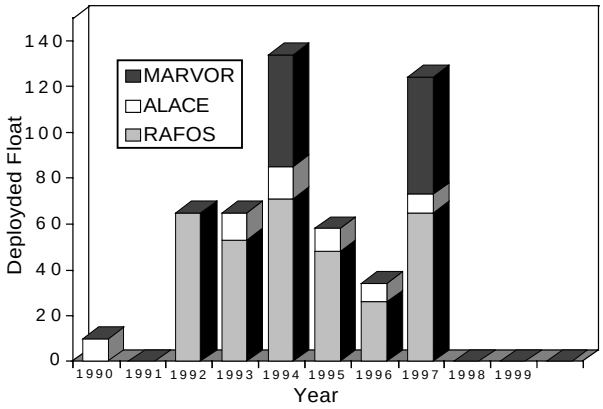

Figure 3. WOCE floats in Intermediate Waters were launched in the South Atlantic irregularly since 1990. Peaks in 1994 and 1997 contain seedings in privileged regions in the western and the eastern South Atlantic, respectively. The diagram represents 536 float launches at intermediate and at greater depths. Status: May 1997.

arrows interrupting the beams. Float seedings in the South Atlantic happened irregular, 1994 and 1997 being peak years (Fig. 3). We expect an overall return rate of at least 85%. By 1999 over 1000 float years collected by at least 536 floats will help to further reveal the internal circulation of the South Atlantic.

The three basic float types are complementary rather than competitive future technologies. Their relative contributions to the intermediate level in the South Atlantic are shown in Fig. 4. We expect the SOFAR technique to be replaced totally by its RAFOS successor. The need for spatially highly resolved trajectories will influence future choices between acoustically supported methods or the low-cost bottle post types with repeat cycles like ALACE. The MARVOR float covers both needs though at a

substantially higher price.

This note was written as a technical memorandum of the diversity of floats used during WOCE in the South Atlantic. It demonstrates increasing interest in the float technology. Nevertheless, we do not expect that moored current meters or convential hydrography will be replaced by roving instruments. The latter simply have enlarged our means of observations and provide access to formerly inaccessible areas. Intentionally we have shown no scientific result. Instead, we refer to first WOCE float papers from this area by Davis et al. (1996), Peterson et al. (1996) and Boebel et al. (1997a). More details about all WOCE float deployment and surface positions as far as available can be obtained from the DIU web page

http://www.cms.udel.edu/woce/

The float data inventory is accessible at the WOCE subsurface float data assembly centre in Woods Hole

http://wfdac.whoi.edu

Latest information of the ongoing KAPEX experiment is available from

http://triton.sea.uct.ac.za

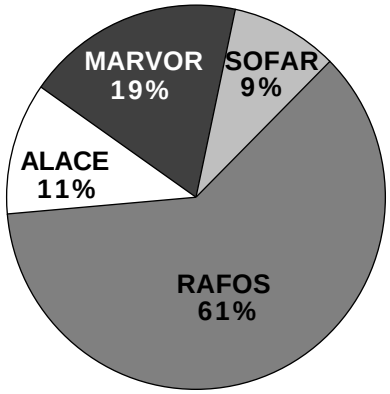

Figure 4. Relative contributions of three modern float types to Lagrangian current observation in the South Atlantic during WOCE 1989–1999. The diagram is based on 536 seedings covering layers of Intermediate and Deep Waters. Status: May 1997.

Acknowledgements

We would like to point out the excellent international co-operation we had with all float groups working in the South Atlantic. We explicitly acknowledge the prompt replies to our questionnaires returned by A. Colin de Verdière, R. Davis, N. Hogg, B. Owens, R. Peterson, P. Richardson and R. Schopp.

In Germany the WOCE float programme is funded by the Deutsche Forschungsgemeinschaft (Ze 145/6-1) and the Bundesministerium für Bildung, Wissenschaft, Forschung und Technologie (03F0157A). The well organised workshop in Brest helped to further develop existing relationships between float laboratories and to inform the whole WOCE community about the already available potential of float data sets for the starting synthesis phase.

References

Boebel, O., C. Schmid, and W. Zenk, 1997a: Flow and recirculation of Antarctic Intermediate Water across the Rio Grande Rise. J. Geophys. Res., 102 (C9), 20,967–20,986.

Boebel, O., C. Schmid, and W. Zenk, 1997b: KAPEX: observing the intermediate flow at the tip of Africa. EOS, Transactions of the American Geophysical Union. (submitted).

List of acronyms and abbreviations

ALACE	Autonomous Lagrangian Circulation Explorer (Davis et al., 1992)
PALACE	Profiling ALACE
MARVOR	Bretonean name for sea horse (Ollitrault et al., 1994)
RAFOS	Ranging And Fixing Of Sound or SOFAR spelled backwards (Rossby et al., 1986)
SOFAR	SOund Fixing And Ranging (Webb, 1977)
IfM	Institut für Meereskunde an der Universität Kiel
IFREMER	Institut Français de Recherche pour l'Exploitation de la Mer, Brest
SIO	Scripps Institution of Oceanography, San Diego
WHOI	Woods Hole Oceanographic Institution, Woods Hole
Fl y	float year
T(z)	device that measures temperature profiles
S(z)	device that measures salinity profiles
S(x,y)	device that enables the calculation of interred salinity along the underwater track (Boebel et al., 1995)
DBE	Deep Basin Experiment (Hogg et al., 1996)
KAPEX	Kap der Guten Hoffnung Experiment (Boebel et al., 1997b) http://triton.sea.uct.ac.za
DIU	Data Information Unit, U. Delaware
WHP	WOCE Hydrographic Programme
SAMBA	Subantarctic Motions in the Brazil Basin

Boebel, O., K. Schultz Tokos, and W. Zenk, 1995: Calculation of Salinity from neutrally buoyant RAFOS floats. J. Atm. Oc. Technology, 12 (4), 923–934.
Davis, R. E., P. D. Killworth, and J. R. Blundell, 1996: Comparison of Autonomous Lagrangian Circulation Explorer and fine resolution Antarctic model results in the South Atlantic. J. Geophys. Res., 101 (C1), 855–884.
Davis, R. E., D. C. Webb, L. A. Regier, and J. Dufour, 1992: The autonomous Lagrangian Circulation Explorer (ALACE). J. Atm. Oceanic Techn., 9, 264–285.
Hogg, N. G., W. Brechner Owens, G. Siedler, and W. Zenk, 1996: Circulation in the Deep Brazil Basin. In: Wefer, G., W. H. Berger, G. Siedler and D. J. Webb (Eds.): The South Atlantic: Present and Past Circulation. Springer Verlag, Berlin, Heidelberg, 249–260.
Ollitrault, M., N. Cortès, G. Loaëc, and J.-P. Rannou, 1994: MARVOR float present results from the SAMBA experiment. OCEANS 94 proceedings, Vol. III, 17–22.
Peterson, R. G., C. S. Johnson, W. Krauss, and R. E. Davis, 1996: Lagrangian measurements in the Malvinas Current. In: Wefer, G., W.H. Berger, G. Siedler and D. J. Webb (Eds.): The South Atlantic: Present and Past Circulation. Springer Verlag, Berlin, Heidelberg, 239–247.
Richardson, P. L., and W. J. Schmitz Jr., 1993: Deep cross-equatorial flow in the Atlantic measured with SOFAR floats. J. Geophys. Res., 98 (C5), 8371–8387.
Rossby, T., D. Dorson, and J. Fontain, 1986: The RAFOS system. J. Atmos. Oceanic Technol., 3, 672–679.
Webb, C. D., 1977: SOFAR floats for POLYMODE. OCEANS 77 proceedings, MTS-IEEE, 44B-1–5.
Zenk, W., 1997a: The new float data set as a complement to our understanding of the South Atlantic circulation. In: WOCE South Atlantic Workshop, Brest, France, 16–20 June 1997, Scientific Programme and Abstracts.
Zenk, W., 1997b: North Atlantic anticipates biggest float fleet ever. Intern. WOCE Newsletter, 27, 32–34.

Water Mass Analysis as a Tool for Climate Research, a Workshop held at the IAMAS/IAPSO General Assembly in Melbourne, July 1997

Matthias Tomczak, FIAMS, Flinders University, Adelaide, Australia.
matthias.tomczak@flinders.edu.aus.edu.au

Water mass analysis has been a tool of oceanographers for decades. The rising interest in the ocean's role in climate variability and climate change has given water mass studies a new prominence. The One-time Hydrographic Survey of WOCE, for example, offers an unparalleled opportunity to advance our understanding of water mass formation, movement and decay and their relevance for the heat and freshwater budgets.

The foundations of water mass analysis were laid nearly a century ago with the introduction of the temperature-salinity (TS) diagram. It dominated the methodology of water mass studies until two or three decades ago, when major new developments combined to create a challenging new situation.

On the observational side, the introduction of chemical compounds into the ocean through human activity and the development of techniques for measuring their presence in minute quantities has opened the field of tracer oceanography. In the area of analysis, numerical modelling became a powerful tool in oceanography and is now capable of identifying formation regions and pathways of water masses. Inverse methods can be adapted to extract the maximum amount of information on water masses from the new hydrographic data set which includes nutrients and tracers.

These examples show that water mass analysis is on the threshold of a new era. It will evolve from a tool for the qualitative description of the oceanic circulation into a tool for the quantitative determination of water mass formation rates, water mass mixing and ageing, and storage capacity for heat, freshwater, carbon and other components of the climate system.

Physical oceanographers, tracer chemists and numerical modellers are rediscovering the art of water mass analysis and developing it further, unfortunately without much contact between them. To change this situation and encourage dialogue between these groups, I convened a workshop on "water mass analysis as a tool for climate research" at the IAMAS/IAPSO General Assembly in Melbourne in July 1997. Lynne Talley and Arnold Gordon acted as co-convenors and were instrumental for getting the workshop together but were unfortunately not able to attend.

Presentations at the workshop were by invitation only and were designed to initiate vivid discussion. Invited speakers were selected to represent the three major groups (physical oceanography, tracer oceanography and numerical modelling) in about equal strength. A working paper was sent out to registered participants two months before the workshop.

The workshop was structured into three sessions, each with three invited papers and a discussion period at the end. The first session was entitled "Traditional water mass description and analysis" and opened by an extended version of the working paper, "The theoretical framework for the study of water masses" (M. Tomczak). S. Wijffels ("Water masses of the deep ocean") presented her innovative work of quantitative water mass assessment in the Bottom and Deep Waters. This was followed by a summary of processes responsible for the formation and consolidation of the Central and Intermediate Waters (M. Tomczak: "Water masses of the thermocline and the intermediate ocean circulation").

The second session, "Information on water mass

structure and pathways from tracers", concentrated on the impact of tracer observations on our understanding of water masses and its consequences. M. Warner reviewed the history of CFC in the atmosphere and ocean and gave a thorough account of the available data, their distribution and their use for determining water mass movement and estimating water mass age ("The use of CFCs and other tracers in water mass studies").

Tracers with a time-dependent source function have given us the means to identify processes which were invisible to the classical methods of analysis. An obvious example is the situation of a water mass residing in its formation region and receiving volumes of newly formed water every winter. Classical TS-analysis cannot distinguish contributions from different years unless changes in the atmospheric conditions in the region produce variations in the TS-properties. A time-dependent tracer signal allows us to quantify the annual formation rate even if there is no change in the heat and freshwater fluxes. This theme was developed by A. Putzka ("Observations of water mass consolidation in tracer data") with a discussion of observations and related theoretical ideas.

In the ensuing discussion it became clear that our increased understanding of water mass processes requires more refined definitions. Some tentative ideas were sketched out in the working paper and are very briefly summarised here.

The first process to occur after a water mass is formed is further homogenisation through mixing. This process, properly called water mass consolidation, is active even in the absence of any mixing with other water masses; in other words, it occurs also in situations where the water mass has exclusive occupancy of a certain depth range as it spreads through the ocean. It can take various forms. It may, for example, eliminate layers of large vertical property change. By mixing contributions from the source region formed during several winters it may reduce the degree of interannual variability in the water mass properties.

A second process, active as soon as a water mass leaves its formation region, is water mass ageing which might also be called water mass modification. It occurs irrespective of any mixing with other water masses. It has no effect on the conservative properties but changes non-conservative properties in line with their bio- or physico-chemical behaviour. As a result, a water mass undergoes change even if it continues to be the only occupant of a well defined region of the ocean.

The next process to occur is mixing between water masses. Mixing does not result in a change of water mass properties but it produces new combinations of water properties not found in the water masses themselves. The mixing process defines a mixing sub-space of the n-dimensional parameter space (the mixing line in the TS-diagram between two water types, the mixing triangle between three water types etc.). It is always possible in principle to identify the contributing water masses and determine their relative contribution to the new mixture.

The sequence of water mass consolidation, modification (ageing) and mixing can be described as the period of water mass evolution. Eventually, every water mass is mixed with others to such a degree that it can no longer be seen. In some situations, the water mass disappears without trace; this end to a water mass might appropriately be called water mass absorption. In other situations, water masses disappear to be transformed into new water masses; this is appropriately called water mass transformation. Water mass absorption and transformation are two possible forms of the final phase in the history of a water mass; they can be classed together as water mass decay.

M. England, the last speaker in this session, reviewed the impact of tracer observations on numerical models ("Using tracers to assess water-mass formation in ocean models"). This then lead into the third session "Using tracers to assess water-mass formation in ocean models". A. Hirst gave an overview of the capability of various models to represent the water masses of the world ocean ("Water masses in ocean climate models"), quoting extensively from his now well known manuscript which seems to be destined to go down in the history of oceanography as "under revision". E. Guilyardi presented some very recent work of his group ("The parameterisation of mixing in coupled GCMs and the effect of lateral ocean physics on water mass formation"), and R. Wood summarised methods to trace water masses in models with artificial numerical tracing techniques ("Using idealised 'age' and 'dye' tracers to diagnose water mass formation in ocean models").

Modellers find it relatively easy to determine water mass age by using appropriate artificial tracers. The challenge for physical oceanographers is to derive corresponding quantities from observations. The workshop provided a clear demonstration that the combination of new tracers with new modelling methods can lead to new insight. As an example I show here the results from a recent Optimum Multiparameter study which includes the effects of biochemical processes (Poole and Tomczak, submitted).

Fig. 1 (page 26) shows the distribution of Central Water in the Atlantic Ocean at 300 m and 500 m depth. Western South Atlantic Central Water (WSACW) is formed in the Brazil Current extension region, while Eastern South Atlantic Central Water (ESACW) is Indian Central Water imported with Agulhas Current rings. The two water masses have nearly identical TS-properties but differ in nutrient content and age. Their vertical layering is quite striking and implies a low rate of mixing between them. Their age distribution shows features which agree with the concept of the ventilated thermocline, such as "shadow zones" in the eastern equatorial regions which are not reached by the ventilated subtropical gyre circulation, and equatorial ventilation through the equatorial undercurrent.

The study does not use tracers with a time-dependent input function and therefore cannot produce absolute ages. Karstensen and Tomczak (in press) have shown that by combining the technique with CFC measurements it is not only possible to determine absolute water age but also the

ages of individual components in a mixture of water masses, which can than be traced and "timed" through entire ocean basins.

Several invited speakers returned from the workshop with the promise to turn their contributions into papers for publication. In the meantime interested colleagues are welcome to approach me for copies of the working paper and ask for mail and e-mail addresses of invited speakers to obtain more information.

References

Karstensen, J., and M. Tomczak, 1997: Age determination of mixed water masses with CFC and oxygen data. J. Geophys. Res. (in press)

Poole, R., and M. Tomczak, 1998: Optimum multiparameter analysis of the water mass structure in the Atlantic Ocean thermocline. Deep-Sea Res. (sub.)

WOCE-GODAE Workshop on Global-Scale Ocean State Estimation

Many of the existing large-scale field programmes (WOCE, JGOFS, etc.) have come to recognise that numerous important scientific issues can be resolved only with a complete, time-evolving three dimensional estimate of the ocean either globally or over entire basins. This workshop is intended to bring together the communities around the world which already begun the process of learning how to carry out such estimation.

By focusing on sharing the existing experience and understanding the extent to which goals are common or complementary – whether cooperative efforts (e.g., data flow) might render the combined efforts more efficient – we hope to move the international discussion away from future possibilities to present realities.

All participants of the workshop have been invited and the emphasis will be on practical experience and the overall goal is to speed up progress from the present experimental stage towards something more operational by sharing understanding of specific problems and their possible solutions. Moreover, it is intended that the group will produce a strategic plan for steps necessary to improve ocean state estimation as well as discussions of progress toward inter-institutional or centre-like activities.

Meeting Convenors: Detlef Stammer, Carl Wunsch and Ichiro Fukumori.

Meeting Committee: Philippe Courtier, Bill Large, Christian Le Provost and Neville Smith.

Venue: Johns Hopkins University (JHU), Baltimore.

Date: 9–11 March 1998.

Bifurcations and Pattern Formation in Atmospheric and Ocean Dynamics

The Italian-French summer school on "Fundamental Problems in Geophysical and Astrophysical Fluid Dynamics" organizes its VI Course.

- Description: This intensive nine-days course centres on giving mathematical and physical tools for the study of geophysical flows, and on their application to the study of the oceans, atmosphere, and coupled ocean-atmosphere system.
- Date and location: 22–30 June 1998.
  Conference Center of St. Oyen, Aosta, Italy.
- Directors: Michael Ghil (UCLA),
  Eli Tziperman (Weizmann Institute).
- Partial support for a few highly qualified graduate students and post-doc will be available. For information and applications please visit the school homepage at
  http://www.unito.it/unito/dipart/dfg/grandcombin/main.html
  or contact the Scientific Secretary:
  Dr Claudia Pasquero
  Istituto di Cosmogeofisica - CNR
  Corso Fiume, 4
  Torino I-10133 ITALY
  fax: +39 11 6604056
  e-mail: grandcombin@icg.to.infn.it
- Deadline for applications: 27 March 1998.

Ocean Data Symposium Review

Anthony W. Isenor, Ocean Circulation Section, Bedford Institute of Oceanography, Dartmouth, Canada. isenora@mar.dfo-mpo.gc.ca

The proper management of collected data is important to any research effort, from the single cruise to the large international experiment such as WOCE. Proper management helps ensure that the data contribute to current and future research efforts. To help continue dialogue between the data management and scientific community, an international Ocean Data Symposium was held in Dublin, Ireland on 15–18 October 1997. The Symposium was sponsored by the IOC, NOAA, EU MAST and the Irish Marine Data Centre.

The 128 scientists, data managers and industry people from 28 countries came together to discuss their common need for marine data.

The four main themes of the Symposium were:

A. the data and metadata requirements of scientists in order to support ocean research,
B. the benefits of statistical techniques and numerical modelling for analysis and prediction,
C. development of advanced technology for data collection, analysis and exchange,
D. advances in information and data management tools for policy and decision makers.

Theme A presentations dealt with science data requirements. Lectures focused on topics such as the allocation of resources for meeting coastal and deep ocean data management needs. The complementary sea level data management activities at the University of Hawaii Sea Level Centre and the British Oceanographic Data Centre were described. The theory, implementation and evolution of the US JGOFS data management system was also presented. A report card presentation evaluated how well GTSPP objectives were met and the experience gained during the project.

The obvious need for high quality ocean data in an understandable and transferable form was identified. Current formats for ocean data were highlighted as a continuous source of problems for most, if not all, participants. A pilot study involving the Australian Oceanographic Data Centre and the National Oceanographic Data Centre is testing and evaluating technology to create Internet linkages between different database products. Such linkages may reduce the need for format conversions while providing the user with seamless access to all products.

Other presentations described current research involving ocean datasets. A presentation of the 1982-83 El Niño event used a combination of in-situ and remote sensed data to show how the spatial-temporal time scales of the two data sources compliment each other. The need for improved ocean data, management and research in developing countries was also identified.

Presentations during **Theme B** focused on statistical techniques and modelling. The World Ocean Database 1997 and World Ocean Atlas 1997 were identified as important products for the oceanographic, meteorological and climate research communities. The use of neural networks and statistical methods to predict upwelling was presented as an efficient alternative to physical models. An Irish wave model nested inside the global ECMWF model was discussed. Finally, an evaluation of the XBT depth equations for the Indian Ocean showed agreement with international fall rate equations and stressed the need for intelligent quality control that accounts for the collection area oceanography.

Theme C dealt with data collection, analysis and exchange technology. Experience gained during the OceanPC Project was presented with emphasis on the need for international data format coordination. The Web-based distribution of data was noted to increase data sharing (as opposed to collaboration) with associated data integrity problems. However, it was noted that Web distribution only serves approximately one-third of the global community, with many developing countries not having access.

The recent establishment of the Marine Information Research Centre (Japan) was discussed. Its objectives include assisting the Japan Oceanographic Data Centre produce high quality data products for the public, industry and researchers. New developments in integrated marine data management using subject oriented applications and GIS were presented.

Theme D concentrated on management tools. Presentations dealt with the data requirements of environmental impact assessment of offshore discharges from drill rigs. A software package was demonstrated that provides time window information for offshore operational planners. A data inventory for finding oceanographic datasets was discussed. Lastly, a software package that combined commercial GIS databases, environmental data and numerical models to study hydrodynamic and pollutant transport issues was presented.

Numerous issues raised at the Symposium are important to large-scale programmes such as WOCE. Among the notable issues was the need to supply users with tools as well as data. The tools discussed at the Symposium focused on data distribution. However, the extension can easily go beyond distribution to include all programme aspects including data collection, processing and delivery to the data centres.

A second issue involves programme methods. There is a need to harmonise formats, collection and processing procedures, data dictionaries, etc. between programmes to minimise the number of individual standards. This would reduce complexity for the user community and enhance inter-programme cooperation, both in terms of data and software.

The final Symposium recommendations will be made available through the Irish Marine Data Centre.

Meeting TIMETABLE 1998/1999

March 9-11	**WOCE/GODAE Data Assimilation Workshop**	**Baltimore, MD, USA**
March 10–13	Oceanology International '98	Brighton, UK
March 16–21	WCRP JSC 19th Session	Cape Town, South Africa
April 20–24	EGS XXIII General Assembly	Nice, France
April 27–30	CLIVAR SSG 7th Session	Santiago, Chile
May 11–14	EuroCLIVAR Workshop on "The role of the Atlantic in climate variability"	Florence, Italy
May 25–29	**WOCE Conference "Ocean Circulation and Climate"**	**Halifax, NS, Canada**
May 26–29	AGU Spring Meeting	Boston, MA, USA
August 10–13	**WOCE/CLIVAR Workshop on Ocean Modelling for Climate Studies**	**Boulder, CO, USA**
August 17–21	International Conference on Satellites, Oceanography & Society at Expo'98	Lisbon, Portugal
September 22–25	**WOCE Indian Ocean Workshop**	**New Orleans, LA, USA**
October 12–16	**WOCE-25**	**Brest, France**
October 19–24	JSC/CLIVAR Working Group on Coupled Modelling, 2nd Session	Melbourne, Australia
December 1–3	International CLIVAR Conference	Paris, France
January 1999	**WOCE Tracer Workshop**	**Bremen, Germany**
April 1999	**WOCE DPC-12**	**Bidston, UK**
July 19–30 1999	IUGG XXII General Assembly	Birmingham, UK
August 23–28 1999	**WOCE North Atlantic Workshop**	**Kiel, Germany**

For more information on the above meetings contact the IPO. If you are aware of any conferences or workshops which are suitable for the presentation of WOCE results and are not mentioned in the above list please let the IPO know.

Note on Copyright

WOCE is a component of the World Climate Research Programme (WCRP), which was established by WMO and ICSU, and is carried out in association with IOC and SCOR. The scientific planning and development of WOCE is under the guidance of the Scientific Steering Group for WOCE, assisted by the WOCE International Project Office.

The International WOCE Newsletter is edited by Roberta Boscolo (roberta.boscolo@soc.soton.ac.uk) at the WOCE IPO at Southampton Oceanography Centre, Empress Dock, Southampton, SO14 3ZH, UK, Tel: 44-1703-596789, Fax: 44-1703-596204, e-mail: woceipo@soc.soton.ac.uk,

http://www.soc.soton.ac.uk/OTHERS/woceipo/ipo.html

We hope that colleagues will see this Newsletter as a means of reporting work in progress related to the Goals of WOCE as described in the Scientific Plan.

The editor will be pleased to send copies of the Newsletter to institutes and research scientists with an interest in WOCE or related research.

Printed by Technart Ltd., Southern Road, Southampton SO15 1HG.